



**A comparative analysis of cowpox virus (CPV WT)  
and a deletion mutant lacking the gene encoding the  
inflammation modulatory protein (CPV IMP<sup>-</sup>)**

**By Janis Paulsen**

Submitted in fulfilment of the degree of Master of Science in Medicine in the  
Division of Medical Virology, Department of Clinical Laboratory Sciences, Institute  
of Infectious Disease and Molecular Medicine



**UNIVERSITY OF CAPE TOWN**  
IYUNIVESITHI YASEKAPA • UNIVERSITEIT VAN KAAPSTAD

The copyright of this thesis vests in the author. No quotation from it or information derived from it is to be published without full acknowledgement of the source. The thesis is to be used for private study or non-commercial research purposes only.

Published by the University of Cape Town (UCT) in terms of the non-exclusive license granted to UCT by the author.

## DECLARATION

I, Janis Paulsen, hereby declare that the work on which this thesis is based is my original work (except where acknowledgements indicate otherwise), and that neither the whole work nor any part of it has been, is being, or is to be submitted for another degree in this or any other university.

I empower the University of Cape Town to reproduce for the purpose of research either the whole or any portion of the contents in any manner whatsoever.

signature removed

---

Signature

12 November 2007

---

Date

# **CONTENTS**

<b>Acknowledgements</b>	<b>i</b>
<b>List of abbreviations</b>	<b>ii</b>
<b>List of figures</b>	<b>v</b>
<b>List of tables</b>	<b>vii</b>
<b>Abstract</b>	<b>ix</b>
<b><u>Chapter 1: Literature Review</u></b>	<b>1</b>
1. The <i>Poxviridae</i> family: phylogenetic analysis and genome organization	2
2. The orthopoxvirus lifecycle	5
3. Interactions between poxviruses and the innate immune response	6
4. The complement system	9
4.1. Complement control proteins	12
5. Complement control proteins encoded by poxviruses	12
6. Cowpox virus	14
<b><u>Chapter 2: Computer modelling of the inflammation modulatory protein of cowpox virus</u></b>	<b>18</b>
2.1. Introduction	19
2.2. Materials and methods	21
2.3. Results	22
2.3.1. Amino acid differences between VCP and IMP in beta sheets	23
2.3.2. Analysis of amino acids important in binding complement components and cofactor activity	24
2.3.3. Intramolecular hydrogen bonding in VCP and IMP	25
2.3.4. Comparison of Ramachandran plots for VCP and IMP	27
2.4. Discussion	29

<b>Chapter 3: Large-scale preparation of cowpox virus, titration of stocks, comparison of pock and plaque morphology and PCR amplification of the gene encoding IMP</b>	<b>31</b>
<b>3.1. Introduction</b>	<b>32</b>
<b>3.2. Materials and methods</b>	<b>35</b>
3.2.1. Growth of virus on the chorioallantoic membrane of 9-11 day old embryonated hens' eggs	35
3.2.2. Comparison of pock morphology of CPV WT and CPV IMP <sup>-</sup> on the chorioallantoic membrane	36
3.2.3. Cell culture	36
3.2.3.1. Maintenance of CV-1 cells	36
3.2.3.2. Titration of virus stocks	37
3.2.3.3. Comparison of plaque morphology of CPV WT and CPV IMP <sup>-</sup> on CV-1 monolayers	38
3.2.4. PCR analysis of CPV WT and CPV IMP <sup>-</sup> to confirm the presence of absence, respectively, of the gene encoding IMP	38
3.2.4.1. Virus culture in CV-1 monolayers for DNA isolation	38
3.2.4.2. DNA isolation	39
3.2.4.3. PCR to confirm the presence or deletion of the gene encoding IMP in CPV WT or CPV IMP <sup>-</sup> , respectively	40
3.2.4.4. Agarose gel electrophoresis	41
<b>3.3. Results</b>	<b>45</b>
3.3.1. Growth of virus on the chorioallantoic membranes of 9-11 day old embryonated hens' eggs	45
3.3.2. Comparison of pock morphology of CPV WT and CPV IMP <sup>-</sup> on CV-1 monolayers	45
3.3.3. Titration of virus stocks	46
3.3.4. Comparison of plaque morphology of CPV WT and CPV IMP <sup>-</sup> on CV-1 monolayers	47
3.3.5. PCR analysis of CPV WT and CPV IMP <sup>-</sup> to confirm the presence or absence, respectively, of the gene encoding IMP	48
<b>3.4. Discussion</b>	<b>50</b>

<b>Chapter 4: Comparison of growth characteristics of CPV ET and CPV IMP<sup>+</sup> on CV-1 monolayers and embryonated hens' eggs</b>	<b>52</b>
4.1. Introduction	53
4.2. Materials and methods	55
4.2.1. Quantitation of CV-1 cells on a 25 cm <sup>3</sup> surface area	55
4.2.2. Viral growth curves generated by growth of CVP WT and CPV IMP <sup>+</sup> in CV-1 monolayers using multiplicities of infection of either 2.9 x 10 <sup>-5</sup> or 2.9 x 10 <sup>-3</sup> pfu	55
4.2.3. Viral growth curves generated by growth of CPV WT and CPV IMP <sup>+</sup> on chick chorioallantoic membranes using either 1 x 10 <sup>2</sup> or 1 x 10 <sup>4</sup> pfu per egg membrane	57
4.3. Results	59
4.3.1. Quantitation of CV-1 cells on a 25 cm <sup>3</sup> surface area	59
4.3.2. Viral growth curves generated by growth of CPV WT and CPV IMP <sup>+</sup> in CV-1 monolayers	59
4.3.2.1. Viral growth curve generated using a multiplicity of infection of 2.9 x 10 <sup>-5</sup> pfu on CV-1 monolayers (1 x 10 <sup>2</sup> pfu/flask)	59
4.3.2.2. Viral growth curve generated using a multiplicity of infection of 2.9 x 10 <sup>-3</sup> pfu on CV-1 monolayers (1 x 10 <sup>4</sup> )	61
4.3.3. Viral growth curves generated by growth of CPV WT and CPV IMP <sup>+</sup> on chick chorioallantoic membranes	65
4.3.3.1. Viral growth curve generated using 1 x 10 <sup>2</sup> pfu/egg membrane	65
4.3.3.2. Viral growth curve generated using 1 x 10 <sup>4</sup> pfu/egg membrane	66
4.4. Discussion	71

<b>Chapter 5: Comparison of growth characteristics of CPV WT and CPV IMP<sup>+</sup> using the air pouch model in BALB/c mice</b>	<b>75</b>
5.1. Introduction	76
5.2. Materials and methods	78
5.2.1. Evaluation of viral titres using the connective tissue air pouch Method	78
5.2.2. Extraction of DNA from connective tissue samples	79

5.2.3.	PCR to confirm the presence of BALB/c mouse DNA in the connective tissue samples	80
5.2.4.	PCR to confirm the presence of viral DNA in the connective tissue samples	80
5.2.5.	PCR to confirm the presence of the <i>gpt</i> insert in the connective tissue samples infected with CPV IMP	81
<b>5.3.</b>	<b>Results</b>	<b>83</b>
5.3.1.	Evaluation of viral titres using the connective tissue air pouch method	83
5.3.2.	PCR to confirm the presence of viral and cellular DNA in the connective tissue samples	83
5.3.2.1.	PCR to detect BALB/c mouse DNA	83
5.3.2.2.	PCR to detect viral DNA	83
5.3.3.	PCR to confirm the presence of the <i>gpt</i> insert in the connective tissue samples infected with CPV IMP	88
5.4.	Discussion	90
	<b>Concluding remarks</b>	<b>92</b>
	<b>Appendix</b>	<b>95</b>
	<b>References</b>	<b>96</b>

## Acknowledgments

I thank Dr. Nicola Douglass for her supervision of this project and for her patient assistance and guidance in the laboratory, and Prof. Anna-Lise Williamson for co-supervision of this project and for thorough review of the thesis.

Thanks go to A/Prof. Ed Sturrock and Jean Watermeyer for supervision and guidance of the computed protein modelling.

Thanks to Dr. Ros Chapman for providing the purified plasmid DNA containing the *gpt* insert and to Dr. Tayo Odunuga for providing the VCP primer sequences. Thanks also go to Prof. Brombacher's research group for providing the IL-4R $\alpha$  primers and PCR reagents.

I also thank Rodney Lucas for assistance with animal work, Jolanda Truter for assistance with photographing the membranes in the pox laboratory, and Bruce Allan for helpful discussion on DNA extraction and PCR.

I thank Dr. Gerald Chege and Dr. Darren Martin for assistance and helpful discussion on statistical analysis.

Most of all I thank my parents for constant love and understanding. Thank you for being patient, caring, supportive and encouraging, especially during the last few years. I would not have been able to complete this degree had I not had your guidance.

I acknowledge Prof. Girish Kotwal for initiating this project, for design of the mouse model experiment and supervision of the mouse work and analysis of mouse tissue.

I acknowledge the MRC, PRF and UCT for funding.

### List of abbreviations

°C	degrees Celsius
A	adenine
bp	base pair
BP	binding protein
C3	complement protein 3
C3b	complement protein 3b
C4	complement protein 4
C4b	complement protein 4b
C4BP	C4b binding protein
CAM	chorioallantoic membrane
CCP	complement control protein
CMPV	camelpox virus
CO <sub>2</sub>	carbon dioxide
CPV	cowpox virus
CPV IMP <sup>-</sup>	cowpox virus lacking IMP
CPV WT	wild type cowpox virus
CR1	complement receptor 1
CrmA	cytokine response modifier A
DAF	decay accelerating factor
DMEM	Dulbecco's minimal essential medium
DNA	deoxyribonucleic acid
dNTP	deoxyribonucleic acid triphosphate
ECTV	ectromelia virus
EDTA	ethylenediaminetetraacetic acid
EGF	epidermal growth factor
FCS	fetal calf serum
fH	factor H
fI	factor I
GMP	guanine monophosphate
<i>gpt</i>	gene encoding xanthine-guanine phosphoribosyltransferase
h	hour

Ig	immunoglobulin
IL	interleukin
IMP	inflammation modulatory protein
INF	interferon
ITR	inverted terminal repeat
kb	kilobase
kDa	kiloDalton
MAC	membrane attack complex
MASP	mannan-binding lectin associated serine protease
MBL	mannan-binding lectin
MCP	membrane cofactor protein
MgCl <sub>2</sub>	magnesium chloride
MHC	major histocompatibility complex
min	minutes
ml	millilitre
mM	millimolar
MOIPICE	monkeypox inhibitor of complement enzymes
MPV	monkeypox virus
mRNA	messenger ribonucleic acid
NFκB	nuclear factor κB
NK	natural killer cells
ORF	open reading frame
PBS	phosphate buffered saline
RCA	regulator of complement activation
rpm	revolutions per minute
RPV	rabbitpox virus
s	seconds
SCR	short consensus repeat
SFV	Shope fibroma virus
SPICE	smallpox inhibitor of complement enzymes
T	thymine
TAE	tris, acetic acid and EDTA buffer
TGF	transforming growth factor
TLR	toll-like receptor

TNF	tumour necrosis factor
TNFR	tumour necrosis factor receptor
U	units
V	volts
VAR	variola virus
VCP	vaccinia virus complement control protein
VV	vaccinia virus
XGPRT	xanthine-guanine phosphoribosyltransferase
XMP	xanthine monophosphate
µg	microgram
µl	microlitre
µM	micromolar

University of Cape Town

## List of figures

Figure 1: The complement system	10
Figure 2.1: VCP and IMP amino acid sequence alignment	22
Figure 2.2: Computed three-dimensional structure of IMP	23
Figure 2.3: VCP and IMP three-dimensional structure alignment	26
Figure 2.4: IMP Ramachandran plot	28
Figure 2.5: VCP Ramachandran plot	28
Figure 3.1: Segment of CPV genome, showing the IMP PCR FWD and IMP PCR REV binding sites	42
Figure 3.2: Schematic diagram of IMP PCR FWD and IMP PCR REV binding sites within the CPV WT genome	43
Figure 3.3: Schematic diagram of IMP PCR FWD and IMP PCR REV binding sites within the CPV IMP <sup>-</sup> genome	43
Figure 3.4: VCP gene sequence showing the VCP PCR FWD and VCP PCR REV binding sites	44
Figure 3.5: Chorioallantoic membranes of 12-14 day old chick embryos infected with CPV WT or CPV IMP <sup>-</sup>	46
Figure 3.6: 24-well plates seeded with CV-1 monolayers and infected with CPV WT or CPV IMP <sup>-</sup>	47
Figure 3.7: CV-1 monolayers infected with CPV WT or CPV IMP <sup>-</sup> and stained with carbol fuchsin	48
Figure 3.8: Image of PCR products following amplification from purified CPV WT and CPV IMP <sup>-</sup> DNA, using IMP PCR FWD and IMP PCR REV primers	49
Figure 4.1: Growth curve of CPV WT and CPV IMP <sup>-</sup> in CV-1 monolayers infected with $1 \times 10^2$ pfu of virus	68
Figure 4.2: Growth curve of CPV WT and CPV IMP <sup>-</sup> in CV-1 monolayers infected with $1 \times 10^4$ pfu of virus	68
Figure 4.3: Growth curve of CPV WT and CPV IMP <sup>-</sup> in embryonated hens' eggs infected with $1 \times 10^2$ pfu of virus	69
Figure 4.4: Growth curve of CPV WT and CPV IMP <sup>-</sup> in embryonated hens' eggs infected with $1 \times 10^4$ pfu of virus	69
Figure 5.1: The coding sequence of <i>gpt</i>	82

Figure 5.2: Image of PCR products following amplification from connective tissue samples harvested 2 and 10 days post infection, using IL-4R $\alpha$ primers	84
Figure 5.3: Image of PCR products following amplification from connective tissue samples harvested 4 and 6 days post infection, using IL-4R $\alpha$ primers	84
Figure 5.4: Image of PCR products following amplification from connective tissue samples harvested 8 days post infection, using IL-4R $\alpha$ primers	85
Figure 5.5: Image of PCR products following amplification from connective tissue samples harvested 2 days post infection, using IMP PCR FWD and IMP PCR REV primers	86
Figure 5.6: Image of PCR products following amplification from connective tissue samples harvested 4 and 6 days post infection, using IMP PCR FWD and IMP PCR REV primers	87
Figure 5.7: Image of PCR products following amplification from connective tissue samples harvested 8 and 10 days post infection, using IMP PCR FWD and IMP PCR REV primers	87
Figure 5.8: Image of PCR products following amplification from connective tissue samples infected with CPV IMP <sup>r</sup> using GP FWD and GPT REV primers	88
Figure 5.9: Image of PCR products following amplification from connective tissue samples harvested 8 days post infection, infected with CPV WT or mock-infected using GP FWD and GPT REV primers	89

## List of tables

Table 1: Table showing examples of immune evasion proteins encoded by poxviruses and their cellular functions	8
Table 2: Table showing the amino acid residues at various positions in VCP and IMP, and the number of hydrogen bonds formed by each	26
Table 3: Table showing number of plaques counted and calculated titre for each virus	47
Table 4.1: Table showing average titres obtained at various time points following infection of CV-1 monolayers with CPV WT at an MOI of $2.87 \times 10^{-5}$ ( $1 \times 10^2$ pfu/flask)	60
Table 4.2: Table showing average titres obtained at various time points following infection of CV-1 monolayers with CPV IMP <sup>-</sup> at an MOI of $2.87 \times 10^{-5}$ ( $1 \times 10^2$ pfu/flask)	61
Table 4.3: Table showing average titres obtained at various time points following infection of CV-1 monolayers with CPV WT at an MOI of $2.87 \times 10^{-3}$ ( $1 \times 10^4$ pfu/flask)	62
Table 4.4: Table showing average titres obtained at various time points following infection of CV-1 monolayers with CPV IMP at an MOI of $2.87 \times 10^{-3}$ ( $1 \times 10^4$ pfu/flask)	64
Table 4.5: Table showing average titres obtained at 0, 24, 48 and 72 h following infection of embryonated hens' eggs with $1 \times 10^2$ pfu of CPV WT	65
Table 4.6: Table showing average titres obtained at 0, 24, 48 and 72 h following infection of embryonated hens' eggs with $1 \times 10^2$ pfu of CPV IMP <sup>-</sup>	66
Table 4.7: Table showing average titres obtained at 0, 24, 48 and 72 h following infection of embryonated hens' eggs with $1 \times 10^4$ pfu of CPV WT	67
Table 4.8: Table showing average titres obtained at 0, 24, 48 and 72 h following infection of embryonated hens' eggs with $1 \times 10^4$ pfu of CPV IMP <sup>-</sup>	67

Table 4.9: Table summarizing the average titres obtained at each time point when CPV WT and CPV IMP <sup>r</sup> were propagated in CV-1 monolayers or in choriollantoic membranes, using $1 \times 10^2$ and $1 \times 10^4$ pfu of virus to infect	70
Table 5: Table showing the number of samples out of a total of 3 in each test group that yielded a positive PCR result using the primers IMP PCR FWD and IMP PCR REV	86

University of Cape Town

## Abstract

Cowpox virus has been found to encode the inflammation modulatory protein (IMP) (Miller, C.G., 1997), a homologue of vaccinia virus complement control protein (VCP). VCP belongs to the regulation of complement activation (RCA) protein superfamily. It has been shown to inhibit both the alternative and classical pathways of complement activation by binding to the proteins C3 and C4, thereby preventing complement-mediated opsonisation of virus, antibody-mediated lysis of infected cells and migration of inflammatory cells into the site of infection. VCP also possesses heparin binding sites.

VCP and IMP were shown to have 92% amino acid sequence identity. The structure of VCP has been elucidated and was used to produce a model of IMP. The IMP model was found to be very similar to VCP, with only a few changes in hydrogen bonding.

A deletion mutant of cowpox virus, lacking IMP (CPV IMP<sup>-</sup>) has been generated (Miller, C.G., *et al*, 1997). CPV IMP<sup>-</sup> and the wild type cowpox virus (CPV WT) were cultured on the chick chorioallantoic membranes. The deletion of IMP in CPV IMP<sup>-</sup> was confirmed by PCR. CPV WT and CPV IMP<sup>-</sup> were compared with respect to pock morphology on chick chorioallantoic membranes (CAMs) and plaque morphology on CV-1 monolayers. The 2 viruses were found to be indistinguishable with respect to size and appearance of both pocks and plaques.

The growth of CPV IMP<sup>-</sup> was compared to that of CPV WT in cell culture and on the chick chorioallantoic membrane. Growth curves were generated for both viruses using 2 different multiplicities of infection. The growth rates of CPV WT and CPV IMP<sup>-</sup> in cell culture and on the chick membranes were found to be statistically similar.

A mouse model was used to investigate the role of IMP *in vivo*. Unfortunately, virus could not be detected by plaque assay. However, viral DNA was detected by PCR both for CPV WT and CPV IMP<sup>-</sup>. The PCR assay was not quantitative

and so no conclusions could be drawn with respect to the effect of IMP on the growth of CPV *in vivo*.

University of Cape Town

# **CHAPTER 1**

## **LITERATURE REVIEW**

1.	The <i>Poxviridae</i> family: phylogenetic analysis and genome organization	2
2.	The orthopoxvirus lifecycle	5
3.	Interaction between poxviruses and the innate immune	6
4.	The complement system	9
4.1.	Complement control proteins	12
5.	Complement control proteins encoded by poxviruses	12
6.	Cowpox virus	14

University of Cape Town

to each other at each end of the genome (Garon, C.F., *et al*, 1978). The ITRs contain a hairpin loop which is purine-rich (Baroudy, B.M., *et al*, 1982), sets of short tandem repeats (Witteck, R. and Moss, B., 1980), ORFs, and a short conserved region (DeLange, A.M. and McFadden, G., 1987; Merchlinsky, M., 1990).

Phylogenetic analysis of chordopoxviral genomes has been performed (Gubser, C. *et al*, 2004; McLysaght, A., 2003). This has shown that the central 100 kb of DNA is highly conserved amongst all of the chordopoxviruses (except for gene inversions and insertions in *Avipoxvirus* and *Molluscipoxvirus*, respectively) (Gubser, C., *et al*, 2004). Within this 100 kb of DNA, 90 genes are conserved. In addition to the high level of conservation seen, the order and spacing of these genes is also highly conserved (McLysaght, A., *et al*, 2003).

On the other hand, the terminal regions of the chordopoxviral genomes are highly divergent, and this divergence is seen even amongst different strains of the same species (Gubser, C., *et al*, 2004).

In spite of this conservation of DNA sequence, there is variation in the length of the chordopoxviral genomes (139 kb in Orf virus [Delhon, G., *et al*, 2004] to 365 kb in canarypox virus [Tulman, E.R., *et al*, 2004]), as well as in the A+T (adenine + thymine) content (36% in *Parapoxvirus* to 75% in *Capripoxvirus*).

Phylogenetic analysis splits the *Chordopoxvirinae* into four groups (Gubser, C. *et al*, 2004). The first group consists entirely of the *Molluscipoxvirus* genus, and the second group of the *Avipoxvirus* genus. Molluscipoxviruses and Avipoxviruses have diverged from the other chordopoxviruses a long time ago, and strictly infect only humans or birds, respectively. Thus, they have evolved unique countermeasures to deal with the immune systems of their hosts. The third and largest group consists of the *Yatapoxvirus*, *Capripoxvirus*, *Suipoxvirus* and *Leporipoxvirus* genera. The fourth group consists solely of the *Orthopoxvirus* genus. This group has diverged most recently, as the members in this group show greater similarity to each other than members within other groups do to each other in the same group.

Within the orthopoxviral group, variola virus (VAR) and camelpox virus (CMPV) group most closely together, and within the central conserved DNA region, these two genomes differ in length by only 82 nucleotides. Cowpox virus (CPV) Brighton strain, monkeypox virus (MPV) and ectromelia virus (ECTV) do not show close grouping with any of the other orthopoxviruses. VV groups closely to CPV GRI-90 strain.

Interestingly, the two strains of CPV analyzed by Gubser, *et al* (2004), Brighton and GRI-90, did not group closely together at all, which indicates that perhaps they should be reclassified as two separate Orthopoxvirus species. In addition, Shchelkunov, S.N., *et al*, (1998), suggest that CPV is the common ancestor virus for all orthopoxviruses, as the terminal region of its genome is intact, compared to other orthopoxviruses that have fragmented genes in this region. Both the Brighton and GRI-90 strains have these “complete” terminal genome regions, so both are candidates for the ancestral orthopoxvirus.

The notion of CPV being the ancestral strain of orthopoxviruses is reiterated by the fact that of the complement protein 4 (C4) binding proteins, the inflammation modulatory protein (IMP) of CPV is the oldest of the homologues among the orthopoxviruses, by studies of the evolutionary relationships between the different complement-binding proteins and human C4b binding protein (Howard, J., *et al*, 1998). Indeed, it may be considered to be the ancestor of the VV and VAR homologues (Kotwal, G.J., 1997).

There are a large number of genes occurring uniquely in the genomes of particular Chordopoxviruses and not in others. This indicates that evolution of poxvirus genome content has occurred and that poxviruses are continuously evolving independently of each other. Furthermore, analysis done by McLysaght *et al* (2003) show that both gene loss and gene gain have occurred during poxviral evolution, and that most of the gain of genes occurs by horizontal transfer events. Hughes and Friedman (2005) report that genes obtained by horizontal transfer are derived from the host and that this “stealing” of genes is fundamental to the virus’s ability to counteract the host immune defense system.

## 2. The orthopoxviral lifecycle

The life cycle of VV, the prototypal orthopoxvirus has been elucidated. It is extensively reviewed by Moss, B. (2001). It begins when VV virions attach to the cell membrane, penetrating it (Chang, A. and Metz, D.H., 1976; Doms, R.W., *et al*, 1990). The virion core is released, which includes the double stranded DNA genome, enzymes and transcription factors. The early messenger ribonucleic acid (mRNA) molecules are synthesized within the core and then translated into various proteins, such as growth factors, immune defense molecules, enzymes, DNA replication factors and intermediate transcription factors (Sans, P. and Moss, B., 1999; Sanz, P. and Moss, B., 1998; Harris, N., *et al*, 1993; Vos, J.C., *et al*, 1991).

Following translation of the early mRNAs, uncoating of the core occurs, followed by replication of the released DNA. The intermediate genes are then transcribed from the DNA in the cytoplasm and the mRNAs are translated. The proteins synthesized here are late transcription factors (McCraith, S., *et al*, 2000; Wright, C.F., *et al*, 1991; Keck, J.G., *et al*, 1993a; Keck, J.G., *et al*, 1993b; Wright, C.F. and Corneios, A.M., 1993; Hubbs, A.E. and Wright, C.F., 1996; Passarelli, A.L., *et al*, 1996; Kovacs, G.R. and Moss, B., 1996). Next, the transcription of late genes and the translation of the mRNAs occur. The proteins synthesized here are virion structural proteins, enzymes and early transcription factors (Broyles, S.S., *et al*, 1991; Broyles, S.S. and Moss, B., 1988; Broyles, S.S., *et al*, 1988; Broyles, S.S. and Fesler, B.S., 1990; Broyles, S.S. and Li, J., 1993; Gershon, P.D. and Moss, B., 1990; Li, J., *et al*, 1994; Ahn, B.Y., *et al*, 1994; Ahn, B.Y. and Moss, B., 1992).

The membrane structures are then assembled and the DNA is packaged into immature virions (Hollinshead, M., *et al*, 1999; Salmons, T., *et al*, 1997; Sodeik, B., *et al*, 1993; Rodriguez, J.R., *et al*, 1997; Wolffe, E.J., *et al*, 1996; Rodriguez, J.R., *et al*, 1998; Traktman, P., *et al*, 2000). The immature virions then mature to form infectious intracellular mature virions. These virions are wrapped by Golgi membranes and moved to the cell periphery. Actin tails are attached to each virion (Sanderson, C.M., *et al*, 2000), and these then fuse with the plasma

membrane and the extracellular enveloped virion is released from the cell (Moss, B., 2001).

### 3. Interaction between poxviruses and the innate immune response

Poxvirus infections result in either a localized infection, where there is a benign, self-limiting skin lesion e.g., infection with molluscum contagiosum (MCV) and Shope fibroma virus (SFV), or a systemic infection, where there is viral dissemination and possibly death e.g. infection of mice with ECTV and humans with VAR.

The innate immune response plays an important role in combating poxvirus infections before an acquired immune response can be successfully mounted. In order to counteract this response the viruses encode a number of proteins which interact with the innate immune response. For example, this was shown by Froggatt, G.C., *et al* (2007), when the product of the vaccinia virus F3L gene was shown to down regulate the number of natural killer (NK) cells at the site of infection. The absence of this protein allows the NK cells to quicken the immune response to infection.

Many different arms of the immune system are activated during poxvirus infection. In addition, there are many examples of poxvirus encoded homologues of immune proteins. These proteins are thought to have been acquired by the virus from the host during the co-evolution of the two species (Hughes, A.L. and Friedman, R., 2005). Thus, there is a fair amount of interplay between the host immune response and these viral encoded proteins, and this interplay determines to a large extent the outcome of disease in the infected host.

For example, Interleukin (IL)-12 and IL-18 have been shown to act in synergy, activating NK cells and upregulating CD8<sup>+</sup> T cells and Th1 activated immune responses against vaccinia virus (Gherardi, M.M., *et al*, 2003). Bowie, A., *et al* (2000) have shown that the A52R gene product of vaccinia virus blocks activation of nuclear factor (NF)  $\kappa$ B by more than one toll-like receptor, by disrupting signalling processes. The A46R gene product of vaccinia virus has a domain with

homology to the toll-like-IL-1-resistance domains (Stack, J., *et al*, 2005), and is able to inhibit the signalling pathways that are toll-like receptor (TLR)-dependant. The TLRs are able to recognize pathogen molecular patterns that are conserved and in this way bring about recognition of particular pathogens (Medzhitov, R., *et al*, 1997; Zarembek, K.A. and Godowski, P.J., 2002). Thus, interference of this system allows the virus to avoid the antiviral action of the TLRs.

Sakala, I.G., *et al* (2007) investigated the role of the ECTV interferon (INF)- $\gamma$  binding protein, and found that it was necessary to evade the development of a successful host immune response in mice. Furthermore, NK cells were found to be vital for mouse survival and control of viral replication following infection with ECTV (Parker, A.K., *et al*, 2007). Thus, though the immune system is able to mount a response to a poxvirus infection, many poxviruses have evolved to counteract very specific aspects of the immune system. Table 1 gives a few more examples of these proteins and the host function that the proteins inhibit.

MCV, ECTV, VV and CPV all encode proteins which, although they have no sequence similarity to IL-18 receptors, are able to inhibit IL-18 activity (Smith, V.P., *et al*, 2000). IL-18 is pro-inflammatory, activates NK cells, and induces the T-helper 1 response and the production of IFN- $\gamma$ . The viral-encoded IL-18 binding proteins would bind endogenous IL-18, thus dampening the effects of this interleukin.

In addition to encoding virokines, poxviruses also encode viroreceptors. These are a subset of virokines and homologs of receptors of cytokines. For example, viral homologs of tumour necrosis factor receptor (TNFR) are encoded by myxoma virus, VV, CPV and SFV (Shchelkunov, S.N., *et al*, 1993; Upton, C., *et al*, 1991). Tumour necrosis factor (TNF) is pro-inflammatory and activates many processes in the immune system (Fiers, W., 1991). The large amounts of viral TNFR secreted during infection by these viruses bind TNF, thus blocking its effects.

Table 1: Table showing examples of immune evasion proteins encoded by poxviruses and their cellular functions

Poxvirus	Pox protein	Cellular function	Reference
MCV ECTV VV CPV	IL-18BP	Binds IL-18 which: Is pro-inflammatory; activates NK cells; induces T-helper 1 response; induces IFN- $\gamma$	Smith, V.P., <i>et al</i> , 2000 Viac, J. and Chardonnet, Y., 1990
Myxoma virus VV CPV SFV	TNFR	Binds TNF which: Is pro-inflammatory; activates many immune system processes	Shchelkunov, S.N., <i>et al</i> , 1993
VAR VV CPV CMPV	IFN- $\gamma$ BP	Binds IFN- $\gamma$ which: Inhibits viral replication; prevents lysis of infected cells; protects surrounding cells from infection	Shchelkunov, S.N., <i>et al</i> , 1993 Mossman, K., <i>et al</i> , 1995 Alcami, A. and Smith, G.L., 1995
VV CPV	IL-1BP	Binds IL-1 which stimulates lymphocytes	Spriggs, M.K., <i>et al</i> , 1992 Alcami, A. and Smith, G.L., 1992
Orf virus	IL-10	Inhibits production of IFN- $\gamma$ , IL-1, IL-6, and TNF- $\alpha$ . Important in B cell activation.	Haig, D.M., 1998
VV SFV CPV VAR	35 kDa binding protein	Binds CC chemokines	Patel, A.H., <i>et al</i> , 1990 Martinez-Pomares, L., <i>et al</i> , 1995 Smith, C.A., <i>et al</i> , 1997 Alcami, A., <i>et al</i> , 1998
VV Myxoma virus SFV	EGF-like proteins	Promotes cell growth and differentiation	Blomquist, M.C., <i>et al</i> , 1984 Brown, J.P., <i>et al</i> , 1985 Chang, W., <i>et al</i> , 1990

VAR, VV, CPV and CMPV encode INF- $\gamma$  receptor homologs (Shchelkunov, S.N., *et al*, 1993; Mossman, K., *et al*, 1995; Alcami, A. and Smith, G.L., 1995). This viral receptor binds INF- $\gamma$ , thus blocking its effects (which are to protect surrounding cells from infection, inhibit viral replication and prevent lysis of the infected cell (Farrar, M.A. and Schreiber, R.D., 1993)). VV and CPV also encode an IL-1 binding protein (Spriggs, M.K., *et al*, 1992; Alcami, A. and Smith, G.L., 1992). Binding of endogenous IL-1 by viral IL-1 receptor inhibits the stimulation of lymphocytes by IL-1 (Dinarello, C.A., 1989).

The MCV proteins mc053R and mc054R share homology with the host IL-18/IL-1 $\alpha$  receptor (Viac, J. and Chardonnet, Y., 1990). Orf virus produces a homolog of IL-10, which is most closely related to the IL10 of sheep, its host. The orf IL-10 may play a role in orf viral replication (Haig, D.M., 1998). VV, SFV, CPV and VAR all encode a 35 kDa (Patel, A.H., *et al*, 1990; Martinez-Pomares, L., *et al*, 1995) protein that binds CC chemokines and is thus a chemokine binding protein

(Smith, C.A., *et al*, 1997; Alcamí, A., *et al*, 1998). The vaccinia virus C11R gene product is a protein that shares sequence identity with epidermal growth factor (EGF) and transforming growth factor- $\alpha$  (TGF $\alpha$ ) (Blomquist, M.C., *et al*, 1984; Brown, J.P., *et al*, 1985). It competes for binding to the EGF receptor with EGF. It is also a strong mitogen (Stroobant, P., *et al*, 1985; King, C.S., *et al*, 1986).

In this review, however, only the complement system will be given attention in detail, since the focus of the project is on a CPV protein postulated to mimic the complement control proteins.

#### 4. The complement system

The complement system consists of more than 30 proteins that form a proteolytic cascade system. The complement system operates in an exact sequence to eliminate invading micro-organisms from the body. Once the complement cascade is initiated, proteins in the pathway are activated sequentially. Activation of each successive protein occurs by the cleavage and/or association of two or more proteins that are activated at earlier stages in the cascade.

There are three pathways whereby the complement system can be activated: the classical pathway (Müller-Eberhard, H.J. *et al*, 1967), the alternative pathway (Götze and Müller-Eberhard, 1971; Marcus *et al*, 1971), and the mannan-binding lectin (MBL) pathway (Thiel, S., 1997). The proteins in the three pathways share structural and functional homology, and the same end-product is produced by them (namely, the membrane attack complex [MAC]). Complement protein 3 (C3) is central to each pathway. However, activation of the different pathways occurs by different mechanisms. The classical pathway is triggered by binding of antibody (Immunoglobulin (Ig) M or IgG) to foreign antigen, whereas in the alternative pathway there is continuous degradation of C3 (Pangburn, M.K. and Müller-Eberhard, H.J., 1980; Pangburn, M.K., *et al*, 1981) allowing for activation when there is a pathogen or infected cell in the vicinity. The mannan-binding lectin pathway is activated when C3 is in complex with MBL associated serine protease (MASP)-1, -2 and -3, and binds to carbohydrates, especially mannose, on the surface of microbial or virus-infected host cells (Lee, S-H, *et al*, 2003;

Favoreel, H.W., *et al*, 2003). Figure 1 shows an overview of the complement cascade.

Following activation of the complement system, C3 is continuously cleaved to yield the products C3a and C3b. The enzymes catalyzing this reaction are called C3 convertases. C3b binds to the protein Bb, which is generated by the enzymatic cleavage of Factor B. This new protein, C3bBb, catalyzes the breakdown of still more C3 to C3a and C3b, and thus it is the alternative pathway C3 convertase.

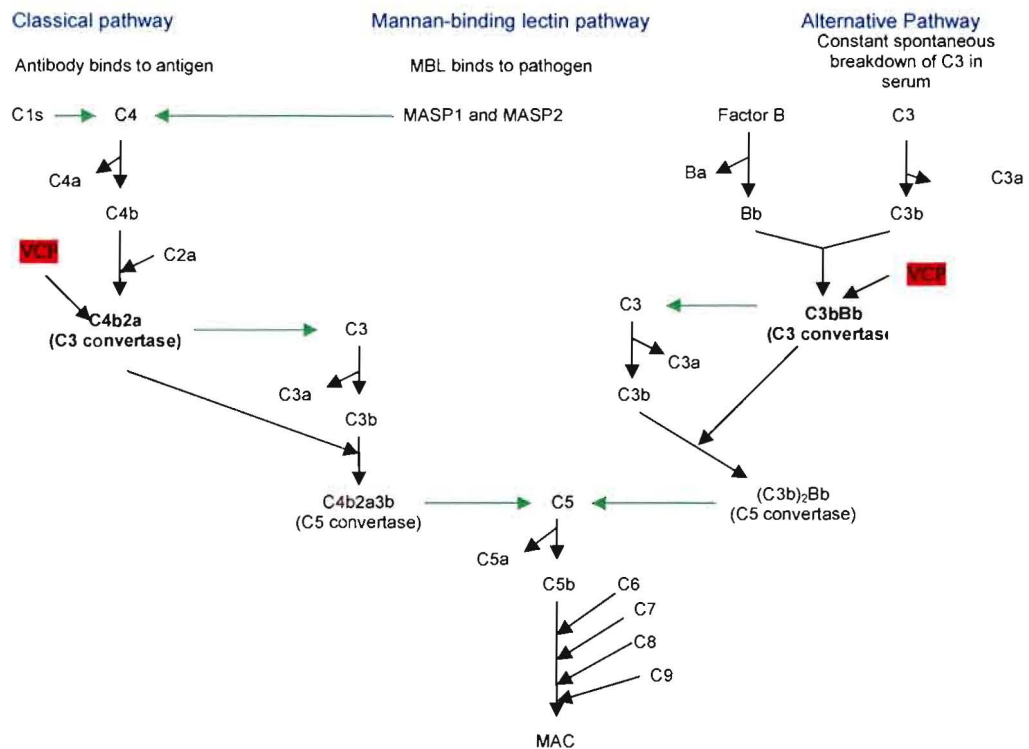


Fig. 1: Flow diagram outlining the sequence of events in the classical, alternative and MBL pathways of complement activation, leading to the formation of the MAC. Green arrows indicate enzymatic cleavage.

The classical pathway C3 convertase is the protein C4b2a, formed by the binding of complement proteins C4b and C2a. It forms in the following way: antigen-bound antibodies bind to the complement protein C1. This C1-antibody-antigen complex then catalyzes the cleavage of C4 and C2 into C4b and C2a, respectively. C4b and C2a then bind and cleave C3 into C3a and C3b.

The C3b produced through the enzymatic cleavage of C3 by the C3 convertases has one of two fates. Firstly, the C3b can attach to the surface of pathogens or pathogen infected cells, acting as opsonins. Complement receptor 1 (CR1), which is expressed in the membranes of macrophages and polymorphonuclear leukocytes, then binds to this C3b, activating the phagocytosis of the C3b-coated pathogen/infected cell (Parham, P., 2005). This opsonisation is one of the main goals of the complement system.

Secondly, the C3b produced can form a complex with the C3 convertases to form the C5 convertases. (Alternative pathway C5convertase: C3bBb3b; classical pathway C5 convertase: C4b2a3b). Both convertases, although distinct enzymes, catalyze the cleavage of C5 into C5a and C5b.

Once C5b is formed, C6 and C7 bind to it to form the C5b67 complex, which then binds to a cell membrane (e.g. that of a virus-infected cell). C8 and C9 then join the membrane-bound complex to form C5b6789, the MAC (Parham, P., 2005). The MAC functions to insert into the membranes of infected cells, forming pores and this results in lysis of the cell (Kolb, W.P. and Müller-Eberhard, H.J., 1973). This is the second function of the complement system: to lyse and thus kill pathogen-infected cells, resulting in the destruction of the pathogen as well.

C3a, C4a and C5a are small chemoattractant peptides produced during the activation of the complement system that are anaphylatoxins (Parham, P., 2005). They bind to receptors on mast cells and basophils, resulting in the release of vasoactive compounds, such as histamine, causing increased blood flow and permeability in the region of infection (Hugli, T.E., 1984, Structure and function of the anaphylatoxins, *Springer Seminars in Immunopathology*, 7:193-220; taken from Tosi, M.F., 2005). In doing so, these peptides implicate the complement system in the inflammatory response. In addition, C5a attracts monocytes and neutrophils to the site of infection by acting as a chemoattractant. This is the third function of the complement system: to increase blood flow and influx of immune cells to the site of infection.

#### 4.1. Complement control proteins

Control of the complement system centres on the C3 convertase of the classical and MBL pathways (C4b2a) and that of the alternative pathway (C3bBb). This is not surprising, since the C3 convertases form the central point of the complement cascade. Two plasma proteins involved in C3 convertase regulation are C4b binding protein (C4BP) and factor H (fH) (Parham, P., 2005). C4BP binds to the C4b moiety of C4b2a, making the convertase vulnerable to cleavage by factor I (fI). fH binds to the C3b moiety of C3bBb, also making it vulnerable to cleavage by fI. This binding of C4BP and fH to the C3 convertase in order to facilitate its cleavage by another protein is known as cofactor activity.

Two membrane-bound proteins involved in complement regulation are decay acceleration factor (DAF) and membrane cofactor protein (MCP) (Parham, P., 2005). DAF binds to both the C4b and C3b moieties of the classical/MBL and alternative pathways, respectively, causing their dissociation from the 2a and Bb moieties. In this way the convertase is inactivated. This activity of DAF is known as decay acceleration. MCP also bind to C4b and C3b, resulting in dissociation of the convertase. However, by binding to the convertase MCP also makes it vulnerable to cleavage by fI. Thus MCP has both decay acceleration activity and cofactor activity.

These regulatory proteins all belong to the regulators of complement activation (RCA) family. All contain between 2 and 30 copies of repeat unit, known as a short consensus repeat (SCR) or a complement control protein module. Each SCR is made up of roughly 60 amino acids, with a consensus sequence of four cysteine residues, in which residues 1 and 3, and 2 and 4, are linked by disulphide bonds. In addition, a tryptophan residue is situated between residues 3 and 4 (Herbert, A., *et al*, 2002).

#### 5. Complement control proteins encoded by poxviruses

Since the complement system forms part of defence against viral infections, it is not surprising that many viruses have evolved to specifically counteract this

proteolytic cascade. Many viruses have been found to encode complement control protein (CCP) homologues. These too form part of the RCA family. One viral genus with multiple species encoding CCP homologues is *Orthopoxvirus*. In fact, the first CCP homologue to be discovered was that of VV, called vaccinia virus complement control protein (VCP) (Kotwal, G.J., and Moss, B., 1988). Other orthopoxviruses with CCPs are VAR, which encodes the smallpox inhibitor of complement enzymes (SPICE) (Massung, R.F., *et al*, 1996), CPV, encoding IMP (Miller, C.G., *et al*, 1997) and MPV, encoding the monkeypox inhibitor of complement enzymes (MOPICE) (Chen, N., *et al*, 2005).

VCP has greatest homology to C4BP (Kotwal, G.J. and Moss, B, 1988), and in binding C4b it causes accelerated decay of the classical pathway C3 convertase (Miller, C.G., *et al*, 1997). It is also able to bind to C3b, causing decay acceleration of the alternative pathway C3 convertase (McKenzie, R., *et al*, 1992) (see fig. 1). As a result of this decay acceleration, the complement system is inhibited. Opsonization of the infected cell does not occur; the membrane attack complex is not formed and thus lysis of the infected cell is avoided; and inflammation does not occur in the infected region of the body. All this means that VV is able to regulate its environment, making it a favourable one for infection and replication.

The role VCP plays in downregulating the complement system is thought to be of potential therapeutic use. There are certain pathophysiological processes in which the resulting damage is due to the consequences of activating the complement system. Examples of these are spinal cord injury and ischaemia-reperfusion injury (Fleming, S.D., *et al*, 2003), as well as in the diseases Alzheimer's (Tuppo, E.E. and Arias, H.R., 2005) and multiple sclerosis (Tran, G.T., *et al*, 2002).

All of these poxviral CCPs consist of four RCAs, with the exception of MOPICE which has a truncated fourth CCP, and also a single base deletion that results in a premature stop codon in the fourth CCP (Uvarova, E.A. and Shchelkunov, S.N., 2001). Furthermore, the poxviral proteins all share more than 90% sequence identity with each other and approximately 35% identity with their human homologues (Liszewski, M.K., *et al*, 2006).

Each poxviral protein is derived from its particular host homolog (Shchelkunov, S.N., *et al*, 1996). For example, SPICE is derived from the human protein C4bp, and thus it is more specific for human C4b than is VCP (Rosengard, A.M., *et al*, 2002). The proteins act as virulence factors. There are two strains of MPV, the Congo Basin strain, encoding an intact MOPICE, and the West Africa strain, which lacks MOPICE. The West African strain is less virulent, whereas the Congo Basin strain is virulent (Chen, N., *et al*, 2005). Human-to-human transmission has also been described for the Congo Basin strain and this strain has a fatality rate of 4-25% (Hutin, Y.J.F., *et al*, 2001). It is not known whether MOPICE contributes directly to the virulence of the Congo Basin strain or not, however one could speculate that it does. VCP prevents antibody-dependent complement-enhanced neutralization of vaccinia virus, and in addition rabbits inoculated with a VCP-knockout virus caused skin lesions that were smaller in size than those seen in animals infected with wild type virus (Isaacs, S.N., *et al*, 1992).

## 6. Cowpox virus

Cowpox virus is thought to be the most likely ancestor of all the other orthopoxviruses (Shchelkunov, S.N. *et al*, 1998). This is due to the fact that it has a somewhat “complete” genome, whereas the other genera of orthopoxvirus have a larger number of fragmented genes whose cowpox virus counterparts are intact. The CPV has been sequenced and deposited in Genbank (AF482758).

Cowpox virus has been isolated in western Eurasia, with Norway, Northern Russia, Turkmenia, Northern Italy, France and Great Britain forming the boundary around the region (Baxby, D., *et al*, 1994). Despite its name, cows are not the natural reservoir for CPV, and Chantrey *et al* (1999) have shown that the natural reservoir in Great Britain is both the bank and field vole. These two species are also endemic in the geographic range of CPV. In addition, other rodents may act as reservoirs, such as suslicks, gerbils and wood mice, but it is likely that these species of rodent need the virus to be re-introduced from time to time by the voles.

CPV infection in humans represents a zoonosis, and more often than not the source of virus infection is the domestic cat (Baxby, D., *et al*, 1994). Acquisition of virus occurs when the virus comes into contact with broken skin. Lesions are found most commonly on the fingers and hands, and also on the face of infected individuals.

Cowpox virus has an array of proteins which allow it to actively evade attack from the immune system. These will be discussed individually below.

- Cytokine response modifier A (CrmA) (Pickup, D.J., *et al*, 1986) was first predicted to be an inhibitor of one or more of the serine proteases involved in the blood coagulation cascade. Later it was shown to bind the IL-1 $\beta$  converting enzyme (Ray *et al*, 1992), thus blocking the effects of IL-1 $\beta$ , a pro-inflammatory cytokine. Other cytokine response modifiers include CrmB (Hu, F.-Q., *et al*, 1994); CrmC (Smith, C.A., *et al*, 1996); CrmD (Loparev, V.N., *et al*, 1998); and CrmE (Saraiva, M. and Alcami, A., 2001). CrmB, CrmC, CrmD and CrmE all have the ability to bind TNF. Thus they are TNFR homologues. They differ in size, time of production post-infection, and also in their binding specificity for TNF. For example, CrmB is expressed early in infection and binds both TNF $\alpha$  and TNF $\beta$ . CrmC is expressed late and only binds TNF $\alpha$ . CrmD is also expressed late, but like CrmB, binds TNF $\alpha$  and TNF $\beta$ . CrmE binds only TNF $\alpha$ . Thus cowpox virus is able to modulate the cytokine response at practically all times post-infection. CrmA has also been found to inhibit apoptosis in infected cells (Tewari, M. and Dixit, V.M., 1995)
- An IFN- $\gamma$ -binding protein (Mossman, K., *et al*, 1995; Alcami, A. and Smith, G.L., 1995) of CPV displays a wide range of species specificity. It can bind human, bovine and rat IFN- $\gamma$ , which is a critical antiviral component of the immune system. This is indicative of the wide host range displayed by the virus. It may also be an indication of the different species used by the virus as a natural host during its evolution.

- CPV expresses an IL-18 binding protein (Smith, V.P., *et al*, 2000). IL-18 is also involved in inducing an antiviral state and thus secretion of a protein that binds it would be advantageous to CPV. It is notable that the viral IL-18 binding protein does not have homology to the host IL-18 receptor (Smith, V.P., *et al*, 2000).
- A chemokine binding protein (Smith, C.A., *et al*, 1997; Graham, K.A., *et al*, 1997) binds proinflammatory chemokines and acts as a competitive inhibitor of chemokine receptors. Like the IL-18 binding protein encoded by CPV, this chemokine binding protein also does not show sequence homology to known host chemokine receptors (Graham, K.A., *et al*, 1997).
- An IL-1 binding protein (Spriggs, M.K., *et al*, 1992) binds IL-1 $\beta$ . Thus, CPV encodes two proteins which are structurally unrelated yet have the same function, i.e. to inhibit the effects of host-derived IL-1 $\beta$ . These are CrmA, which binds IL-1 $\beta$  converting enzyme, and the viral IL-1 $\beta$  binding protein, which binds IL-1 $\beta$ .
- An as yet unidentified protein which allows the virus to bypass identification by CPV-specific T cells (Dasgupta, A., *et al*, 2007) is encoded by CPV. This is thought to be mediated by interference with the major histocompatibility complex (MHC) processing and transport within the infected cell, thus preventing MHC I antigen presentation. Furthermore, CPV has been shown to inhibit expression of genes under the regulation of NF- $\kappa$ B, interfere with NF- $\kappa$ B activation, and to disrupt processes leading to the degradation of I $\kappa$ B $\alpha$  (Oie, K.L. and Pickup, D.J., 2001)
- CPV complement control protein (Miller, C.G., *et al*, 1997) will be discussed in more detail below.

The CPV IMP is a homologue of VCP (Miller, C.G., *et al*, 1997). Previous work has also shown that CPV is able to regulate its habitat via C5 (Miller, C.G., *et al*, 1995). C5-deficient mice show a considerably greater swelling response than do

C5-sufficient mice following injection in the footpads with CPV. Also, reinfection in the footpads following complete recovery elicited only slight swelling, indicating that the secondary response to infection is not regulated by the complement system.

Studies in C3-sufficient and C3-deficient mice indicated that the IMP also interacts with C3 (Kotwal, G.J., *et al*, 1998), since footpad infections elicited greater swelling responses in the C3-deficient mice than in C3-sufficient mice. Furthermore, swelling in C3-deficient mice injected with either CPV or CPV lacking IMP was relatively equal.

A recombinant virus lacking IMP has been generated (Miller, C.G., *et al*, 1997). The aim of this project was to determine the effect of IMP on viral growth *in vitro*, *in ovo* and in an *in vivo* mammalian model. Although the role of VCP has been established in VV, the effect of VCP on viral growth has not been determined. I have compared the putative structure of CPV IMP to that of the known structure of VV VCP. To determine the effect of this complement modulating protein on growth, wild type and recombinant CPV were compared with respect to growth in cell culture, on chick chorioallantoic membranes (CAMs) and in mice (since rodents are the natural host of CPV [Chantrey, J., *et al*, 1999]).

## **CHAPTER 2**

### **COMPUTER MODELLING OF THE INFLAMMATION MODULATORY PROTEIN OF COWPOX VIRUS**

<b>2.1.</b>	<b>Introduction</b>	<b>19</b>
<b>2.2.</b>	<b>Materials and methods</b>	<b>21</b>
<b>2.3.</b>	<b>Results</b>	<b>22</b>
2.3.1.	Amino acid differences between VCP and IMP in beta sheets	23
2.3.2.	Analysis of amino acids important in binding complement components and cofactor activity	24
2.3.3.	Intramolecular hydrogen bonding in VCP and IMP	25
2.3.4.	Comparison of Ramachandran plots for VCP and IMP	27
<b>2.4.</b>	<b>Discussion</b>	<b>29</b>

## 2.1. Introduction

The complement modulatory protein sequences that have been analysed thus far include those for membrane cofactor protein (MCP) (Cervoni, F., *et al*, 1993), C4b binding protein (C4BP) (Lintin, S.J., *et al*, 1988), smallpox inhibitor of complement enzymes (SPICE) (Zhang, L. and Morikis, D., 2006) and vaccinia virus complement control protein (VCP) (Ganesh, V.K., *et al*, 2004; Murthy, K., *et al*, 2001). The sequence of the inflammation modulatory protein (IMP) of cowpox virus (CPV), a homolog of VCP, is also known, but to date its three-dimensional structure has not been determined.

The IMP of CPV has 92% amino acid identity to VCP of VV (Miller, C.G., *et al*, 1997). This high sequence similarity, together with the availability of crystal structures of VCP (Ganesh, V.K., *et al*, 2004; Murthy, K., *et al*, 2001), makes IMP a good candidate for homology modelling, since the accuracy of predicted protein structures increases with an increase in homology between the target and template sequences ([www.expasy.org](http://www.expasy.org)).

To date, the only poxviral complement control protein structure available is that of VCP. Thus, the aim of this experiment was to generate a three-dimensional structure of IMP, based on the known structure of VCP, using computer modelling.

The SWISS-MODEL server (Guex, N. and Peitsch, M.C., 1997; Arnold, K., *et al*, 2006; Kopp, J., and Schwede, T., 2006) is a tool for homology modelling. This server has three different modes, which can be used depending on the modelling requirements (Schwede, T., *et al*, 2003):

1. First approach mode – this requires only the amino acid sequence of the protein to be modelled. Suitable templates are automatically chosen from the protein database by SWISS-MODEL. At least one template with more than 25% sequence identity with the target amino acid sequence is required.

2. Alignment interface mode – a sequence alignment is submitted to the SWISS-MODEL server. The model of the target sequence is then built using the structure of the protein to which it is aligned.
3. Project mode – in this mode a manually optimized model is submitted to the server. The model consists of superimposed structures as well as an alignment between the target amino acid sequence and the template sequences. Unlike the first two modes, in this one the user decides on the templates to be used, and in addition it can be used to improve the result of the first approach mode.

The alignment interface mode is suitable for cases such as IMP, where a single template sequence has been identified. This mode was used to determine the structure of cowpox virus IMP. The vaccinia virus VCP structure was used as a template.

University of Cape Town

## 2.2. Materials and Methods

The amino acid sequences of IMP and VCP were obtained from [www.ncbi.nlm.nih.gov](http://www.ncbi.nlm.nih.gov) (accession numbers AAM13481 and P68638, respectively). The two sequences were aligned using DNA MAN version 4.0 (Lynnon BioSoft). The alignment was submitted to the SWISS MODEL server at <http://swissmodel.expasy.org> in fasta format using the Alignment Interface mode. The protein structure of VCP has already been determined (Ganesh, V.K., *et al*, 2005, Ganesh, V.K., *et al*, 2004, and Murthy, K.H.M., *et al*, 2001) and the structures are available the protein databank. The template structure used to generate the IMP protein model was that produced by Murthy, K.H.M., *et al*, 2001, (PDB ID 1g40). The output structure was visualized and analyzed using Swiss-PdbViewer. The template and model coordinates were submitted to MolProbity ([www.molprobity.biochem.duke.edu/](http://www.molprobity.biochem.duke.edu/); Davis, I.W., *et al*, 2004), a programme which calculates the Ramachandran plots for protein structures and identifies errors in stereochemistry.

The template and model structures were then compared, using the following criteria:

- 2.2.1. Amino acid differences between VCP and IMP.
- 2.2.2. Analysis of amino acids important in binding complement components and cofactor activity.
- 2.3.3. Intramolecular hydrogen bonding in VCP and IMP. The hydrogen bond detection threshold was set at 2.4 – 3.6 Å.
- 2.3.4. Comparison of Ramachandran plots for VCP and IMP. The co-ordinates for each structure obtained were submitted to the MolProbity website



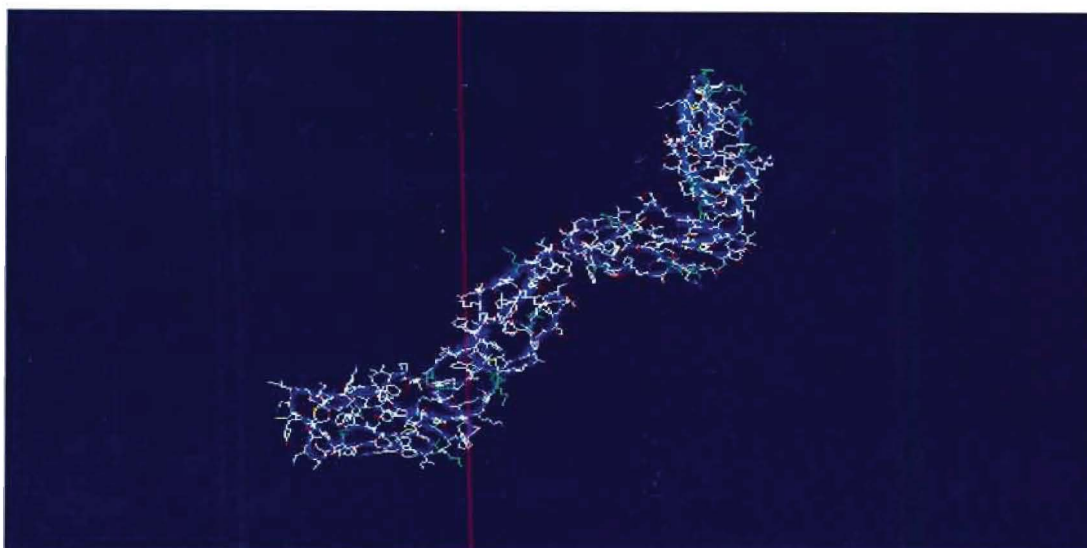


Fig 2.2: Computed three-dimensional structure of IMP based on a VCP template structure from the protein data bank (1g40.pdb; Murthy, K.H.M., *et al*, 2001), shown as a ribbon diagram (blue) with white line representation of the atomic structure. Amino acids shown in green are those that are mutated with respect to VCP.

### 2.3.1. AMINO ACID DIFFERENCES BETWEEN VCP AND IMP IN BETA SHEETS

Figure 2.1 shows the amino acid sequence alignment between VCP and IMP. Horizontal dashes indicate identical residues between the two sequences. As shown in figure 3, there are 17 amino acid differences in IMP with respect to the VCP sequence. The majority of these differences are not likely to result in any major changes in protein conformation or function. VCP residues which are postulated to form points of contact with C3b are R7, K12, K14, R40, K41, K43, K50, K64, R65, R66, E102, K186 and H189. In IMP all these residues are conserved, except R66 which is substituted by K in IMP. However, this is the replacement of one positive residue with another, and so the positively charged patch formed by these residues at the junction between modules 1 and 2 would be conserved (Ganesh, V.K., *et al*, 2004). Furthermore, residues postulated to contact C4b in VCP are N94, H98 and E102. In IMP, residue 98 is Q, which is a change from a positively charged amino acid (histidine) in VCP to an uncharged

amino acid (glutamine) in IMP. Two other differences occur in the beta sheets and these are Gln98, which is a His in VCP, and Gln236, which is a Lys in VCP.

There are 4 potentially significant amino acid differences between VCP and IMP. Firstly, <sup>VCP</sup>E-18-G<sup>IMP</sup> is a change from a polar, charged amino acid (glutamate) to a non-polar, uncharged amino acid (glycine). Furthermore, glutamate has a high helix-forming propensity, whereas glycine does not promote helix formation, since it is highly flexible and thus it is energetically unfavourable for it to adopt the restrained alpha-helix conformation.

<sup>VCP</sup>S-111-Y<sup>IMP</sup> is a change from an amino acid with a short side chain that is inclined to interrupt alpha helices (serine), to one with an aromatic ring (tyrosine). In VCP, S111 forms part of module 2 and lies within a 5-residue insertion that forms a loop close to the interface between modules 1 and 2 (Murthy, K.H.M., *et al*, 2001).

<sup>VCP</sup>Q-130-P<sup>IMP</sup> is a change from a polar amino acid with a chain structure (glutamine) to a hydrophobic, cyclic amino acid (proline). Furthermore, proline is not usually found in  $\alpha$  helices and has the propensity for forming  $\beta$  turns.

<sup>VCP</sup>K-236-Q<sup>IMP</sup> is a change from a long chain amino acid (lysine) to a short chain one (glutamine).

### **2.3.2. ANALYSIS OF AMINO ACIDS IMPORTANT IN BINDING COMPLEMENT COMPONENTS AND COFACTOR ACTIVITY**

R7, K12, K14, R40, K41, K43, K50, K64, R65 and R66 are residues in the VCP molecule shown to be important in binding C3b and/or C4b (Murthy, K.H.M., *et al*, 2001). Except for R66 (a conservative change from arginine to lysine), all these residues are conserved in IMP.

As mentioned previously, of particular importance in C4b binding are the residues 94, 98 and 102 (Liszewski, M.K., *et al*, 2000; Murthy, K.H.M., *et al*, 2001). Residues 94 and 102 are conserved in IMP, however residue 98 is not. Figure 2.3

shows an alignment of IMP and VCP, with residue 98 highlighted in each molecule. This alignment was kindly provided by Prof. Krishna Murthy. In VCP this residue is histidine, while in IMP it is glutamine.

The conservation of the heparin binding sites in IMP is also of biological importance. In VCP, binding of heparin results in a conformational change in the protein that changes the orientation of K186, H189, F201 and R203, relative to N94, H98, E102 and E108 (Ganesh, V.K., *et al*, 2004). This conformational change is thought to be important in VCP binding to C3b and C4b, because, with the exception of F201, the residues affected are thought to be points of contact between VCP and C3b or C4b.

### **2.3.3. INTRAMOLECULAR HYDROGEN BONDING IN VCP AND IMP**

There are some changes regarding hydrogen bonding of residues that are mutated in IMP with respect to VCP (Table 2). However, the overall number of hydrogen bonds in the whole molecule is fairly similar in VCP and IMP. VCP has 144 hydrogen bonds while IMP has 139. Hydrogen bonds play an important role in holding the molecule together. Here there is a 5 hydrogen bond difference between the two molecules. This suggests that IMP may be less stable than VCP. However, the intramolecular hydrogen bonds are formed between atoms in the side chains of the amino acids. In a model, the side chain atoms do not necessarily occupy the same positions in space as they do in reality. Thus, caution needs to be exercised when making predictions regarding protein structure and stability based on the intramolecular hydrogen bonding from a model.

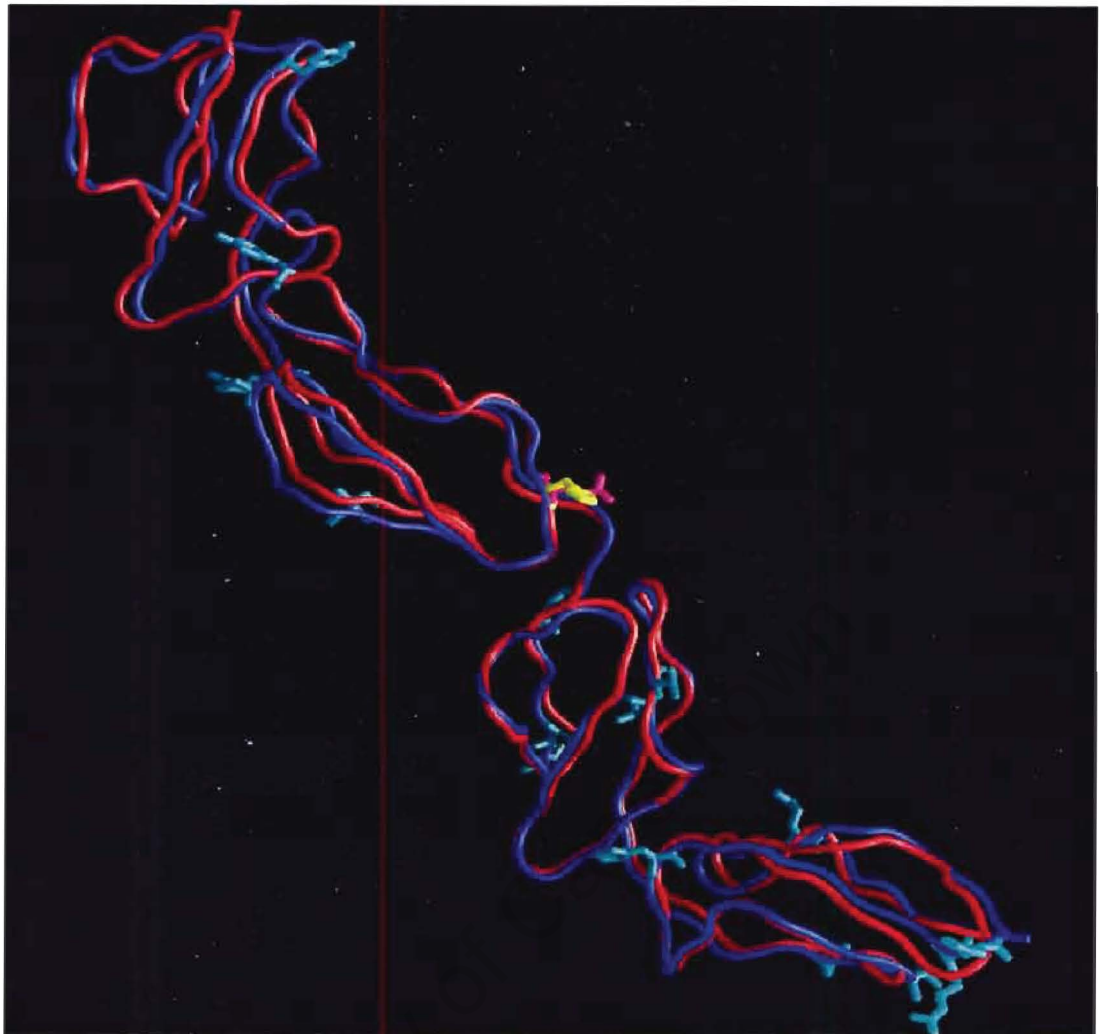


Fig 2.3: Alignment of three-dimensional structures of VCP and IMP. VCP is shown in red and IMP is shown in blue. Residue 98 in each molecule is highlighted. In IMP this is a glutamine, shown in magenta, and in VCP it is a histidine, shown in yellow.

Table 2: Table showing the amino acid residues at various positions in VCP and IMP, and the number of hydrogen bonds formed by each

Residue Number	VCP		IMP	
	Residue	# H bonds	Residue	# H bonds
18	E	2	G	0
84	D	2	E	1
111	S	3	Y	1
130	Q	3	P	1
135	I	0	V	2
191	T	1	S	0
207	Y	0	H	2
236	K	1	Q	2

#### **2.3.4. Comparison of Ramachandran plots for VCP and IMP**

A Ramachandran plot is a two-dimensional plot of psi vs phi torsion angles of the protein backbone for each amino acid in a protein structure. Favoured regions of the plot have been determined by analysing databases of known protein structures of high quality (Struyer, L., 1995).

The Ramachandran plots obtained are shown in figures 2.4 and 2.5. In a Ramachandran plot, it is preferable that most of the residues lie in favoured regions (98%) or at least allowed regions (>99.8%). For IMP (Fig. 2.4), 69.3% and 89.6% of the residues were found to be in favoured and allowed regions, respectively. For VCP (Fig. 2.5), 70.1% and 88.8% were found to be in favoured and allowed regions, respectively.

The percentage of residues found in allowed regions for IMP appears to be low. However, the template used (VCP) yielded a Ramachandran plot with an even lower percentage of residues in allowed regions. Thus this is probably the reason the low percentage for IMP was obtained and one could say that these two structures (VCP and IMP) are similar.

Ramachandran plots were generated for the 1y8e and 1rid VCP templates. For 1y8e, 73.1% and 90.5% of residues were found in favoured and allowed regions, respectively. For 1rid, 74.8% and 90.9% of residues were found in favoured and allowed regions, respectively. These values are slightly higher than those for the 1g40 VCP template (70.1% and 88.8%). However, the resolutions for each template (2.1, 2.2 and 2.1 for 1g40, 1y8e and 1rid, respectively) were close in value, so that modelling IMP on a template other than 1g40 is not warranted.

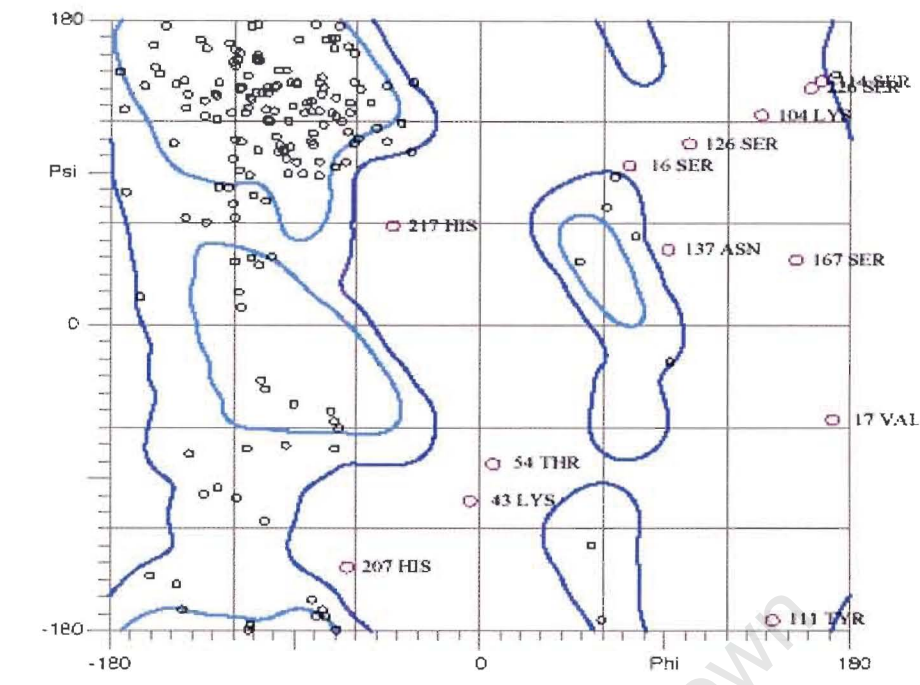


Figure 2.4: Ramachandran plot for IMP. Circles/squares that fall within the dark blue regions represent amino acids in allowed positions. Circles/squares that fall within the light blue regions represent amino acids in favoured regions. Purple circles represent amino acids in disallowed regions.

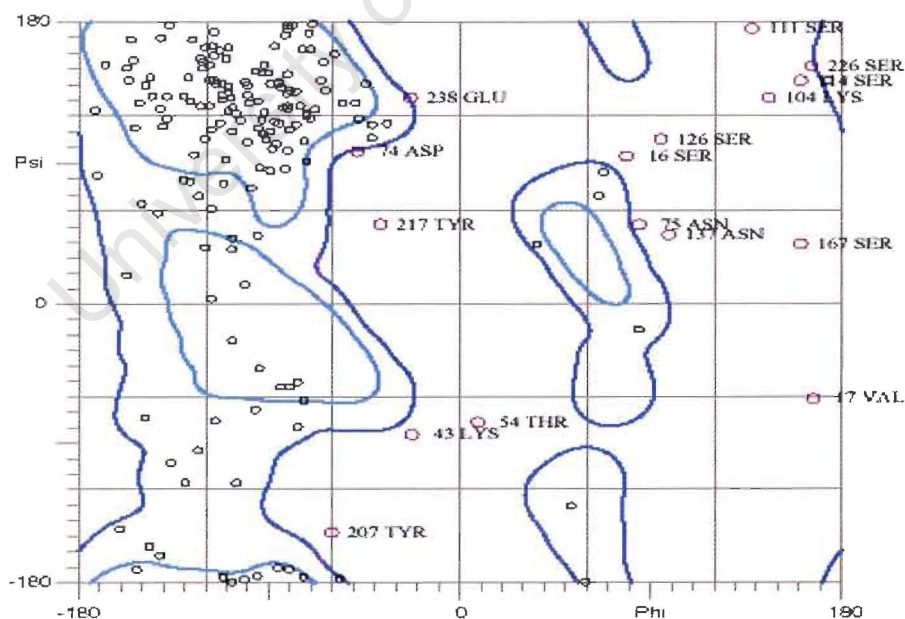


Figure 2.5: Ramachandran plot for VCP. Circles/squares that fall within the dark blue regions represent amino acids in allowed positions. Circles/squares that fall within the light blue regions represent amino acids in favoured regions. Purple circles represent amino acids in disallowed regions.

## 2.4. Discussion

The inflammation modulatory protein of CPV has 92% amino acid identity to the complement modulatory protein of VV, vaccinia virus complement control protein (VCP). The high level of homology suggests that these two proteins have analogous functions. Indeed, vaccinia virus VCP is the inflammation modulating protein homolog of IMP in VV.

Extensive research has been done on the structure and function of VCP, as VV is the most studied orthopoxvirus. It has been found that VCP is able to bind heparin on the surface of human endothelial cells (Smith, S.A., *et al*, 2000). This is analogous to the presence of heparin binding sites in fH and C4BP (Pangburn, M.K., *et al*, 1991; Blackmore, T.K., *et al*, 1998; Hessing, M., *et al*, 1990). For fH, the ability to bind heparin is crucial in differentiating between complement activator surfaces and host cell surfaces (Pangburn, M.K., *et al*, 2000) as the alternative pathway does not make use of antibodies to distinguish between target and host cells (Meri, S. and Pangburn, M.K., 1990).

These heparin binding sites in VCP are conserved in IMP, as shown in figure 2B. Thus it would be expected that IMP retains the properties conferred on VCP through its heparin binding ability. These include binding to the surface of host cells, thus protecting them from complement mediated lysis; entry into mast cells, allowing for persistence in host tissue, thus contributing to preservation of the viral habitat (Smith, S.A., *et al*, 2000); reduction of chemotactic migration of leukocytes to the site of infection (Smith, S.A., *et al*, 2000); and the ability to prevent binding of antibodies to surface MHC class I molecules, by binding heparin-like molecules on the surface of endothelial cells (Smith, S.A., *et al*, 2000).

Murthy, K.H.M., *et al*, (2001) highlighted a few important regions within the VCP molecule. The first of these consist of the amino acid residues R7, K12, K14, R40, K41, K43, K50, K64, R65, and R66. These residues are postulated to form points of contact between VCP and either C3b or C4b, thus accounting for VCP's ability to regulate both the alternative and classical pathways, respectively.

All of these residues are conserved in IMP. Thus it retains the ability to bind C3b or C4b via this region.

Liszewski, M.K., *et al* (2000) showed that in membrane cofactor protein (MCP), the principle cofactor for fI which binds both C3b and C4b, residues Y97, Y98, L99, and E103 are important in cofactor activity of C4b, while mutations of residues E95, G96 and E102 decrease binding of C4b and cofactor activity.

In VCP, this stretch of residues is homologous to MCP, and Murthy, K.H.M., *et al*, (2001) have shown that of particular importance are the residues 94, 98 and 102. In VCP these are N94, H98 and E102. However, in IMP there is a H98Q mutation, relative to VCP. While histidine is aromatic and positively charged, glutamine remains uncharged and polar. This may affect the binding affinity of IMP for C4b if the interaction between the proteins is an electrostatic one. SPICE is the homolog of VCP and IMP in variola virus (Massung, R.F., *et al*, 1993) and analysis of its sequence shows that this residue is a tyrosine (Y98) (Rosengard, A.M., *et al*, 2002), making it more similar to H98 of MCP, and therefore perhaps accounting for the greater efficiency of SPICE in C4b binding than VCP. The amino acid difference between IMP and SPICE at residue 98 most likely has implications in the efficiency of IMP in binding C4b. The natural host of CPV is the rodent. However, mouse C4b is 95% homologous to that of humans (Blangchong, C.A., *et al*, 2001). Thus one would expect that IMP is likely to have the ability to bind human C4b with as high efficiency as it binds mouse C4b.

Overall, this experiment has shown that the computed putative structure of IMP is very similar to that of VCP. It is highly likely that the function of this protein is conserved in the two viruses, vaccinia virus and cowpox virus.

# **CHAPTER 3**

## **LARGE-SCALE PREPARATION OF COWPOX VIRUS, TITRATION OF STOCKS, COMPARISON OF POCK AND PLAQUE MORPHOLOGY AND PCR AMPLIFICATION OF THE GENE ENCODING IMP**

<b>3.1.</b>	Introduction	<b>32</b>
<b>3.2.</b>	Materials and methods	<b>35</b>
3.2.1.	Growth of virus on the chorioallantoic membrane of 9-11 day old embryonated hens' eggs	<b>35</b>
3.2.2.	Comparison of pock morphology of CPV WT and CPV IMP <sup>-</sup> on the chorioallantoic membrane	<b>36</b>
3.2.3.	Cell culture	<b>36</b>
3.2.3.1.	Maintenance of CV-1 cells	<b>36</b>
3.2.3.2.	Titration of virus stocks	<b>37</b>
3.2.3.3.	Comparison of plaque morphology of CPV WT and CPV IMP <sup>-</sup> on CV-1 monolayers	<b>38</b>
3.2.4.	PCR analysis of CPV WT and CPV IMP <sup>-</sup> to confirm the presence or absence, respectively, of the gene encoding IMP	<b>38</b>
3.2.4.1.	Virus culture in CV-1 monolayers for DNA isolation	<b>38</b>
3.2.4.2.	DNA isolation	<b>39</b>
3.2.4.3.	PCR to confirm the presence or deletion of the gene encoding IMP in CPV WT or CPV IMP <sup>-</sup> , respectively	<b>40</b>
3.2.4.4.	Agarose gel electrophoresis	<b>41</b>
<b>3.3.</b>	Results	<b>45</b>
3.3.1.	Growth of virus on the chorioallantoic membranes of 9-11 day old embryonated hens' eggs	<b>45</b>
3.3.2.	Comparison of pock morphology of CPV WT and CPV IMP <sup>-</sup> on CV-1 monolayers	<b>45</b>
3.3.3.	Titration of virus stocks	<b>46</b>
3.3.4.	Comparison of plaque morphology of CPV WT and CPV IMP <sup>-</sup> on CV-1 monolayers	<b>47</b>
3.3.5.	PCR analysis of CPV WT and CPV IMP <sup>-</sup> to confirm the presence or absence, respectively, of the gene encoding IMP	<b>48</b>
<b>3.4.</b>	Discussion	<b>50</b>

### 3.1. Introduction

The inflammation modulatory protein (IMP) of cowpox virus (CPV) is a complement control protein homolog, having greatest similarity to C4BP (Miller, C.G., *et al*, 1997). Miller, C.G., *et al* (1997) have produced a knockout cowpox virus, in which the gene encoding IMP is disrupted.

This recombinant virus was produced in the following way: The plasmid pGK10 containing the open reading frame for vaccinia virus complement control protein (VCP) was cleaved with *EcoRV*. This resulted in the deletion of 70 bp within the VCP gene (VCP is the IMP homolog in vaccinia virus). The plasmid pTK61 (Falkner, F.G. and Moss, B., 1988) containing a *gpt* cassette was cleaved with *EcoRI*, resulting in the excision of this *gpt* cassette within a 2 kb fragment. The *E. coli* gene *gpt* encodes the enzyme xanthine-guanine phosphoribosyltransferase (XGPRT), which catalyzes the synthesis of guanine monophosphate (GMP) from xanthine monophosphate (XMP), using xanthine (Mulligan, R.C. and Berg, P., 1981). The 2 kb fragment containing the *gpt* cassette was then inserted into the VCP open reading frame of plasmid pGK10. This new plasmid was called pGK12. CV-1 monolayers that were infected with CPV were transfected with this plasmid, following which the knockout virus was plaque purified in medium containing mycophenolic acid (MPA), hypoxanthine and xanthine. MPA inhibits the synthesis of XMP from inosine monophosphate (IMP) via IMP dehydrogenase. (Miller, C.G., *et al*, 1997; Falkner, F.G. and Moss, B., 1988; Mulligan, R.C. and Berg, P., 1980). Thus, production of XGPRT by cells infected with the recombinant virus will overcome the inhibition of MPA in the presence of xanthine, and so plaques formed would be due to the presence of recombinant virus, which could then be purified.

This recombinant virus thus has the VCP/IMP gene disrupted by a 2 kbp fragment. This recombinant virus was named vSIGK5 (Miller, C.G., *et al*, 1997). In this thesis it will be referred to as CPV IMP.

CPV IMP<sup>-</sup> was used in all experiments and compared to wild type CPV (CPV WT) in order to investigate the effect of IMP on plaque and pock morphology and viral growth.

Pock morphology on the chorioallantoic membranes (CAMs) of embryonated hens' eggs was once routinely used to identify poxviruses (Baxby, D., 1969). For example, the pocks formed by VV are white in colour, whereas those produced by CPV are red. The genes responsible for pock colour have been identified in CPV (Pickup, D.J., *et al*, 1986) and rabbitpox virus (RPV) (Martinez-Pomares, L., *et al*, 1993). The pocks produced by CPV are distinguishable from those produced by RPV as they are slightly more haemorrhagic. However, Baxby, D. (1969) showed the existence of white pock mutants of CPV. In addition to this he showed that this mutant strain of CPV could spontaneously revert to producing red pocks. These spontaneous revertants were macroscopically indistinguishable from wild type CPV. However, they were genetically identical to the white pock mutants. Thus pock morphology proved to be an unreliable method for distinguishing between various poxviruses.

Nevertheless, since poxviruses are able to propagate on CAMs, producing pocks of varying morphology, it was decided to look at the pock morphology of CPV WT and CPV IMP<sup>-</sup>. CPV IMP<sup>-</sup> has a disrupted IMP gene. IMP is postulated to inhibit the complement system, and thus its presence results in a decrease in production of the cleavage products C3a, C4b and C5b, which are involved in the attraction of immune cells to the site of infection (Parham, P., 2005). Fredrickson, *et al* (1992) showed that following inoculation of CPV WT onto the CAM, there is only a very small influx of inflammatory cells. In addition, Kotwal, *et al* (1998) found that infection of BALB/c mice in the dorsal connective tissue with CPV IMP<sup>-</sup> resulted in greater mononuclear cell influx at the site of infection than in mice infected with CPV WT. Thus it would be interesting to see whether the absence of IMP has any influence on pock morphology in the CAM.

This chapter describes:

- The culture of stocks of both CPV WT and CPV IMP<sup>-</sup> to a high titre for use in all experiments.
- Titration of virus stocks.
- Confirmation of the deletion of IMP in CPV IMP<sup>-</sup>.
- Comparison of pock morphology of the two viruses on chick CAMs.
- Comparison of plaque morphology of the two viruses in CV-1 cells.

University of Cape Town

### 3.2. Materials and methods

#### 3.2.1. Growth of virus on the chorioallantoic membranes of 9-11 day old embryonated hens' eggs

CPV WT and CPV IMP<sup>-</sup>, a deletion mutant lacking the inflammation modulatory protein (Miller, C.G., *et al*, 1997), provided by Prof. Girish Kotwal, were cultured using 9-11-day old embryonated hens' eggs, using a modification of the method outlined by Joklik, W.K. (1962). Eggs were viewed using an egg candler to ensure the embryos were the correct age and ascertain the positions of blood vessels. Using an egg-pricker, holes were made at the air-sac end and on the lateral side of each egg, next to, but not directly above, a large blood vessel. A drop of phosphate buffered saline containing penicillin and streptomycin (Gibco, Grand Island, New York, USA) at 100 U/ml and 100 µg/ml, respectively, was placed on the lateral hole. A pipette filler bulb was placed over the hole at the air-sac end and gentle pressure was applied using the bulb, thus causing the chorioallantoic membrane (CAM) to collapse at that region. The eggs were placed at 37°C for 1.5 h to allow the membranes to stabilize.

After removal from 37°C, 100 µl of virus at various dilutions was injected into the lateral hole on each egg using a 1 ml syringe. The hole was covered with wax to prevent contamination. Each egg was swirled gently, and then placed at 37°C for 72 h.

After 72 h, the eggs were removed from the incubator. Each egg was cut open and the section of CAM that had dropped from the egg shell was collected. The membranes were washed by swirling in physiological saline twice. The membranes were placed in autoclaved McCartney bottles containing glass beads. For each membrane in the tube, 700 µl McIlvain's buffer (0.1 M citric acid, 0.2 M disodium hydrogen orthophosphate, pH 7.4) (Stannard *et al*, 1998) and 170 µl of the organic solvent Arklone-X was added. The tubes containing the membrane-solvent mixture were shaken vigorously for 2 minutes. The tubes were centrifuged at 1 000 rpm for 10 min, in a Sigma 301K centrifuge. The

supernatants were collected and transferred to clean McCartney bottles without glass beads. McIlvain's buffer and Arklone-X were once again added to the membranes in the universal tubes with glass beads, in the same ratio, and the mixture was centrifuged at 1 000 rpm for 10 min. This supernatant was then added to the supernatant collected previously in the clean universal tubes without glass beads. The supernatants from each virus suspension were placed on ice for 1.5 h.

The supernatants were then centrifuged for 10 min at 2 000 rpm to remove cellular debris. The supernatant fluid was then transferred to sterile centrifuge tubes. To each tube 5 ml of 36% sucrose in TE buffer pH 9 (w/v) was added. The suspension was then centrifuged at 11 000 rpm for 1 hour at 4°C, in a Beckman J2-21 centrifuge, using a JA-20 rotor. The supernatant was then discarded and the pellet was resuspended in 0.5 ml TE buffer (pH 9) at 4°C overnight.

### **3.2.2. Comparison of pox morphology of CPV WT and CPV IMP<sup>r</sup> on the chorioallantoic membrane**

The viruses CPV WT and CPV IMP<sup>r</sup> were cultured in embryonated hens' eggs using a method modified from that outlined by Joklik, W.K. (1962). The protocol was followed as indicated in section 3.2.1 until the membranes were harvested and rinsed in physiological saline. Thereafter, each membrane was gently spread out on a Petri dish using a pair of forceps and then photographed (Nikon Coolpix 4500). For each egg,  $1 \times 10^2$  pfu of each virus was used to infect the CAM.

### **3.2.3. Cell culture**

#### **3.2.3.1. Maintenance of CV-1 cells**

A CV-1 cell line, derived from the African green monkey kidney (Jensen, F.C., *et al*, 1964) was maintained in cell culture flasks (Greiner Bio-One, Gloucestershire, UK) containing Dulbecco's modified Eagle's medium (DMEM) (Gibco, Grand Island, New York, USA) supplemented with 4-10% fetal calf serum (FCS)

(Gibco, Grand Island, New York, USA). The antibiotics penicillin (Gibco, Grand Island, New York, USA) and streptomycin (Gibco, Grand Island, New York, USA) and an anti-fungal agent, fungin (InvivoGen, Wiltshire, UK), were added to the medium to final concentrations of 100 U/ml, 100 µg/ml, and 10 µg/ml, respectively. The cells were incubated at 37°C and 5% CO<sub>2</sub>.

Sub-culturing of cells was performed in a biosafety level 2 cabinet. The working surface of the cabinet was wiped with 70% ethanol before and after work was done. Cell monolayers were sub-cultured once they had reached 90-100% confluency. This was done as follows: the DMEM was removed from the flask; the monolayer was washed with phosphate buffered saline (PBS); trypsin (Gibco, Grand Island, New York, USA) (0.5%) was added to the flask, which was then incubated at 37°C and 5% CO<sub>2</sub> for 5-10 min to allow for detachment of the monolayer from the flask. Once the cells had detached from the flask surface a percentage of the cells was transferred to a clean flask and to these cells fresh DMEM, supplemented with the appropriate amount of FCS, was added.

#### **3.2.3.2. Titration of virus stocks**

All virus stocks were titrated on CV-1 cell monolayers in 24-well plates (Cellstar, Greiner Bio-One, Frickenhausen, Germany). The titration was performed in triplicate. Ten-fold serial dilutions of each virus were prepared in DMEM. Dilutions of 10<sup>-3</sup> to 10<sup>-9</sup> were used for the titration. The final volume of each dilution was 1 ml. Thus, the appropriate amount of virus stock and DMEM were added to each other. Once the monolayers in each well were confluent, the medium was removed. Into 3 adjacent wells, 200 µl of a particular dilution was added. DMEM was used as a negative control. There were 7 groups of wells to which viral dilutions (10<sup>-3</sup> to 10<sup>-9</sup>) had been added as an inoculum, and 1 group to which just DMEM had been added as an inoculum. The plate was then placed at 37°C and 5% CO<sub>2</sub>, and adsorption was allowed for 1.5 h. After 1.5 h the plate was removed from the incubator and the inoculum was removed from each well. To each well, 500 µl DMEM supplemented with 4% FCS was added. The plate was then incubated at 37°C and 5% CO<sub>2</sub> for 72 h.

After 72 h the plate was removed from the incubator and the medium was removed from each well. A few drops of carbol-fuchsin (obtained from Medical Virology Diagnostic Laboratory, C22, Groote Schuur Hospital) were added to each well. After 20-30 s the stain was washed off with water, and the plate was allowed to dry in an inverted position on paper towel. The plaques in each well were then counted. The total number of plaques for each well was multiplied by 5 (since only 200µl of inoculum had been added to each well and the final titre is expressed as plaque forming units per ml) and the dilution factor was taken into account to determine the final virus titre of each well. The titres for 3 wells inoculated with the same viral dilution were added and divided by three to give a final average titre of the virus stock.

### **3.2.3.3. Comparison of plaque morphology of CPV WT and CPV IMP<sup>-</sup> on CV-1 monolayers**

Viruses were grown in CV-1 monolayers. The protocol followed was as outlined in section 3.2.3.2.; however, 6-well plates were used. Briefly, serial dilutions of each virus were prepared. Of each dilution, 500 µl was used to inoculate each well. Virus adsorption was allowed for 1.5 h at 37°C, following which the inoculums were removed and replaced with DMEM (4% FCS). After 72 h incubation at 37°C, the medium was removed from each well and cells were stained with carbol fuchsin.

### **3.2.4. PCR analysis of CPV WT and CPV IMP<sup>-</sup> to confirm the presence or absence, respectively, of the gene encoding IMP**

#### **3.2.4.1 Virus culture in CV-1 monolayers for DNA isolation**

This protocol was adapted from Kellogg, D.E. and Kwok, S. (1990). A 6-well plate (Costar, Corning Incorporated, Port Elizabeth, South Africa) was seeded with CV-1 monolayers in DMEM supplemented with 10% FCS, and placed at 37°C and 5% CO<sub>2</sub> until the cells in each well were confluent. CPV WT and CPV IMP<sup>-</sup> were diluted serially 10-fold to infect each well. The medium was then

removed and each well was inoculated with 500  $\mu$ l of DMEM containing  $10^5$  to  $10^2$  pfu/ml of either CPV WT or CPV IMP. Adsorption was allowed for 1.5 h at 37°C. Following adsorption the inoculum was removed from each well and replaced with DMEM supplemented with 4% FCS. The plates were then incubated at 37°C until cytopathic effect was evident (24-48 h). Once cytopathic effect was evident, the cells were scraped off the bottom of the well and transferred to an Eppendorf tube. The cell/medium mixture was centrifuged at 14 000 rpm (Beckman Microfuge E) for 10 min and the supernatant discarded. To the pellet, 25  $\mu$ l lysis buffer A (100 mM KCl; 10 mM Tris-HCl, pH 8.3; 2.5 mM  $MgCl_2$ ), 25  $\mu$ l lysis buffer B (10 mM Tris-HCl, pH 8.3; 2.5 mM  $MgCl_2$ ; 1.5% Tween-20), and 3  $\mu$ l of a 10 mg/ml proteinase K solution (Roche, Penzburg, Germany) was added. Each sample was incubated at 60°C for 1 h, and thereafter at 95°C for 10 min. Following lysis of the cells, DNA extraction was then performed.

#### **3.2.4.2. DNA Isolation**

To each sample, an equal volume of phenol was added in order to remove all proteins. The mixture was then centrifuged for 10 min (Beckman Microfuge E) at 14 000 rpm. The top layer was transferred to a clean Eppendorf tube and to remove all traces of phenol, an equal volume of chloroform:isoamyl (24:1) was added. This was followed by centrifugation at 14 000 rpm for 10 min. The top layer was retained once again and to precipitate the DNA, 0.1 volumes of ice cold 3M sodium acetate and 2.5 volumes of ice cold absolute ethanol was added to it. The samples were then placed at -20°C overnight. After removal from -20°C, the samples were centrifuged at 14 000 rpm for 20 min. The pellets were then washed by adding 70% ethanol and centrifuging for 5 min at 14 000 rpm. The pellets were allowed to air dry, resuspended in  $H_2O$  and placed at -20°C.

**3.2.4.3. PCR to confirm the presence or deletion of the gene encoding IMP in CPV WT or CPV IMP<sup>-</sup>, respectively**

To confirm the presence or absence of the gene encoding IMP in CPV WT and CPV IMP<sup>-</sup>, respectively, primers were designed so that the forward primer would bind upstream of the transcription start site, and the reverse primer would bind downstream of the stop codon. The forward primer IMP PCR FWD (5' ATC TAT TGT GTC GGT AGA CGA 3') bound 201 bp upstream of the start codon, and the reverse primer IMP PCR REV (5' GCT GTA GAG TAC GAC GGT G 3') bound 404 bp downstream of the stop codon (see figure 3.1). Using these primers, products of 1.4 kbp and 3.4 kbp were expected using CPV WT and CPV IMP<sup>-</sup> DNA as a template, respectively. IMP PCR FWD and IMP PCR REV each have a  $T_m$  of 60°C, calculated using the formula  $T_m = 4(G+C) + 2(A+T)$ , and an annealing temperature of 55°C was chosen (5°C below the  $T_m$ ).

The workbench was wiped with 70% ethanol before setting up the PCR reactions. Plugged tips were used to add all reagents to the reaction tubes. In addition, the extracted DNA was added to the specific reaction tube at a separated location.

For each reaction, 50 pmol/μl of each primer, 2.5U of *Taq*DNA polymerase, 1x PCR buffer, 1.5 mM MgCl<sub>2</sub> and 0.2 mM dNTP mixture (Promega, Wisconsin, USA) were used. The PCR conditions were as follows: 94°C for 2 min; 30 cycles of 94°C for 1 min, 55°C for 1 min and 72°C for 2 min; and 72°C for 10 min. In addition, as a positive control the primers VCP PCR FWD (5' GAA TTC TGC TGT ACT ATT CCG TCA C 3') and VCP PCR REV (5' GCG GCC GCT TAG CGT ACA CAT TTT GGA AG 3') (both primers were designed by Dr. Tayo Odunuga) were used. The VCP PCR primers bind within the IMP gene, and thus an absence of that gene would result in the absence of a PCR product (See figure 3.4). CPV WT DNA was used as a positive control. As a negative control, a reaction without template DNA was set up.

#### 3.2.4.4. Agarose gel electrophoresis

All PCR products were subjected to agarose gel electrophoresis on a horizontal submerged agarose gel system, using the protocol outlined in Ausubel, *et al* (1988). The agarose was made up in 1x TAE buffer (40 mM Tris base; glacial acetic acid 0.014% v/v; 1mM EDTA, pH8) to give a 1% gel. This concentration ensured that the pore size in the meshwork formed upon polymerization of the agarose was adequate to allow efficient passage of the DNA of interest through the gel. Ethidium bromide was also added to the gel to a final concentration of 0.5 µg/ml, to allow for visualization of the DNA.

The PCR products were prepared for loading in an area separated from that in which the PCR reactions were set up. To 15 µl of PCR product, 1x loading dye (bromophenol blue [0.25% w/v]; sucrose [40% w/v]; EDTA [20mM, pH 8]) was added.

PCR product was subjected to agarose gel electrophoresis at 90 V for 1.25 h. The gel was visually captured using the computer software UViproplatinum 1.1.

```

34801 atcatctggt agagtagtat cattaaatct attatatttt
34841 atgaaagaṭa tatcactgct cacctctata tttcgtacat
34881 ttttaaactg tttgtataat atctctctga tacaatcaga
34921 tatatctatt gtgtcggtag acgataccgt tacatttgaa
34961 ttaatgggtg tccattttac aacttttaac aagttgacca
35001 attcattttct aatagtatca aactctccat gattaaatat
35041 tttaatagta tccattttta tatcactacg gatacaaagt
35081 agctgacata aaaaccattg tataattttt atgttttatg
35121 tttattagcg tacacatttt ggaagtccg gctgccatgt
35161 atttcctgga gagcaagtag atgatgagga accagatagt
35201 ttatatccgt gtctgcactt aaagtctaca ttgtcgttgt
35241 gtgagtatga tcttttaaac ccgctagaca agtatccgtt
35281 tgttattgaa ggatgtgggc atttaacgat ctgacacgtg
35321 ggtggatcgg accattctcc tctgaacac acgatgccag
35361 agttaccaat caacgaatat ccaactattgc aactatacgt
35401 tacaacgctt ccatcgggat aaaaatcctc gtatccgtta
35441 tgccttccat tggttacaga tggaggggat gggcatttaa
35481 cagattcaca aatgggtgcc tcgggattcc acaccataga
35521 tccagtatat cctagttcac aatacgattt agattctcct
35561 atcaactgat atccgctatt gcaagagtac gttatactag
35601 agccaaactc tactccacca atatcaattt gaccattatc
35641 aatatctcga ggtgatggac atttccgttt aatacattga
35681 ttaaagagtg tccatccagt acctgtacat ttagcatata
35721 taggtcccat tttttgcttt ctgtatccag gtagacatag
35761 atattctata gtgtctccta tgttgtaatt agcattagca
35801 tcagtcccca cactattctt aaatttcata ttaatgggac
35841 gtgacggaat agtacagcat gatagcacgc atcctattcc
35881 caacaatgtc aggaacgtca cgctctccac cttcatattt
35921 atttatccgt aaaaatgtta tctatgcat tgtccaataa
35961 taaaaagtca tgctattgta ggaattgttt ttcacagttg
36001 ctcaaaaacg atggtagtga cttacgagtt acgttacact
36041 ttggagtctc atcttttagta aacatatcat aatattcgat
36081 attacgagtt gacatatcga acaaattcca agtatttgat
36121 tttggataat attcgtattt tgcactgtct ataattaaga
36161 tataatcacc gcaagaacac acgaacatct ttctacatg
36201 gttaaagtac atgtacaatt ctatccattt gtcttctta
36241 actatatatt tgtatagata attacgagtc tcatgagtaa
36281 ttccagtaat tacatagatg taccgctcgt actctacagc
36321 ataaactata ctatgatgtc taggcatggg agactttttt
36361 atccaacgat ttttagtgaa acattccaca tcgtttaata
36401 ctacatattt ctcatcagtg gtataaactc caccattac
36441 atatatatca tcgtttacga ataccgatgc gcctgaatat
36481 ctaggagtaa ttaagtttgg aagtcttatc catttcgaag
36521 tgtcgtgttt caaatattct gctacaccgg ttgaaataga
36561 aaattctaat cctcctatta catataactt tccatcgta

```

Figure 3.1: Figure showing a segment of the CPV genome. The start and stop codons of the IMP gene are highlighted in yellow. The IMP PCR FWD and IMP PCR REV primer binding sites are highlighted in magenta.

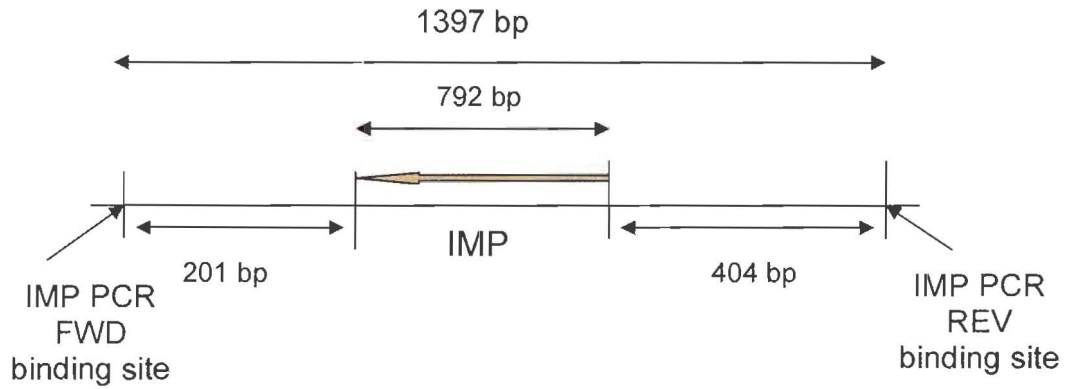


Fig 3.2: Schematic diagram of the IMP PCR FWD and IMP PCR REV primer binding sites, showing the location of the IMP gene within the CPV WT genome. Primers were designed to amplify a fragment of 1397 bp.

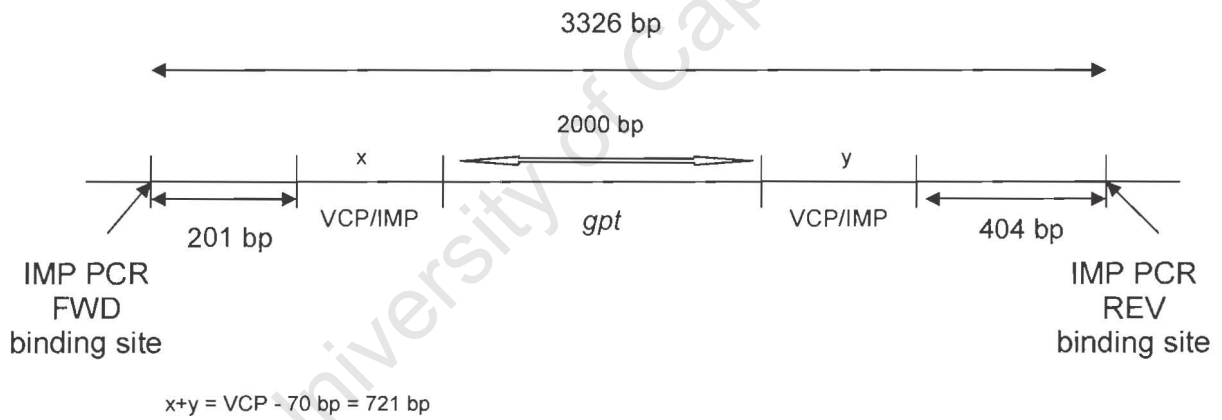


Fig 3.3: Schematic diagram of the IMP PCR FWD and IMP PCR REV primer binding sites, showing the location of the inserted *gpt* cassette within the VCP ORF. The disruption of the gene results in a PCR product that is 3326 bp in size.

```

1   tttttattat ttgtacgatg tccaggataa catttttacg
41  gataaataaa tatgaagggtg gagagcgtga cgttcctgac
81  attgttggga ataggatgcg ttctatcatg ctgtactatt
121 cggtcacgac ccattaatat gaaatttaag aatagtgtgg
161 agactgatgc taatgctaata tacaacatag gagacactat
201 agaatatcta tgtctacctg gatacagaaa gcaaaaaatg
241 ggacctatat atgctaaatg tacagggtact ggatggacac
281 tctttaatca atgtattaaa cggagatgcc catcgctctg
321 agatatagat aatggccaac ttgatattgg tggagttagac
361 tttggctcta gtataacgta ctcttgtaat agcggatata
401 atttgatcgg tgaatctaaa tcgtattgtg aattaggatc
441 tactggatct atgggatgga atcccagggc acctatttgt
481 gaatctgtta aatgccaatc ccctccatct atatccaacg
521 gaagacataa cggatacagag gatttttata ccgatgggag
561 cgttgtaact tatagttgca atagtggata ttcgttgatt
601 ggtaactctg gtgtcctgtg ttcaggagga gaatggtcgg
641 atccaccacac gtgtcagatt gttaaagtgc cacatcctac
681 aatatcaaac ggatacttgt ctagcgggtt taaaagatca
721 tactcataca acgacaatgt agactttaag tgcaagtacg
761 gatataaact atctggttcc tcatcatcta cttgctctcc
801 aggaaataca tgggaagccgg aacttccaaa atgtgtacgc

```

Figure 3.4: Figure showing VCP gene sequence. The start codon of the VCP gene is highlighted in yellow. The VCP PCR FWD and VCP PCR REV primer binding sites are highlighted in magenta. The *EcoRV* cleavage sites are highlighted in green.

### 3.3. Results

#### 3.3.1. Growth of virus on the chorioallantoic membranes of 9-11 day old embryonated hens' eggs

CPV WT and CPV IMP<sup>-</sup> were cultured on embryonated hens' eggs CAMs. The method used was a modification of that described by Joklik, W.K. (1962). Each egg was candled to ensure that it was fertilized and that the embryo was at the correct age. The embryos were found to be between 9 and 11 days old. Twelve eggs were used for each virus. Eleven were infected with either CPV WT or CPV IMP<sup>-</sup>, and the twelfth egg was mock-infected with PBS. The 2 viruses were cultured at different times to prevent cross-contamination of stock cultures.

After 72 h incubation at 37°C, the membranes were harvested. On the membranes infected with virus, red pocks were visible and dilation of blood vessels was evident. In contrast, the mock-infected membranes did not have any pocks and there was no visible dilation of the blood vessels.

The virus extracted from the CAMs was stored at -80° or -20°C. The titre of each virus stock was determined by titration on CV-1 monolayers (section 3.3.3.). The average titre per egg for CPV WT was  $1.88 \times 10^8$  pfu/egg, and for CPV IMP<sup>-</sup> was  $5.05 \times 10^8$  pfu/egg.

#### 3.3.2. Comparison of pock morphology of CPV WT and CPV IMP<sup>-</sup> on the chorioallantoic membrane

CPV WT and CPV IMP<sup>-</sup> were propagated on chick egg membranes in order to compare the pock morphology of each virus. Figure 3.5 shows the images captured.

There was no difference in the appearance of the pocks produced by the 2 viruses. In addition, the extent of haemorrhaging from blood vessels appeared to be similar.

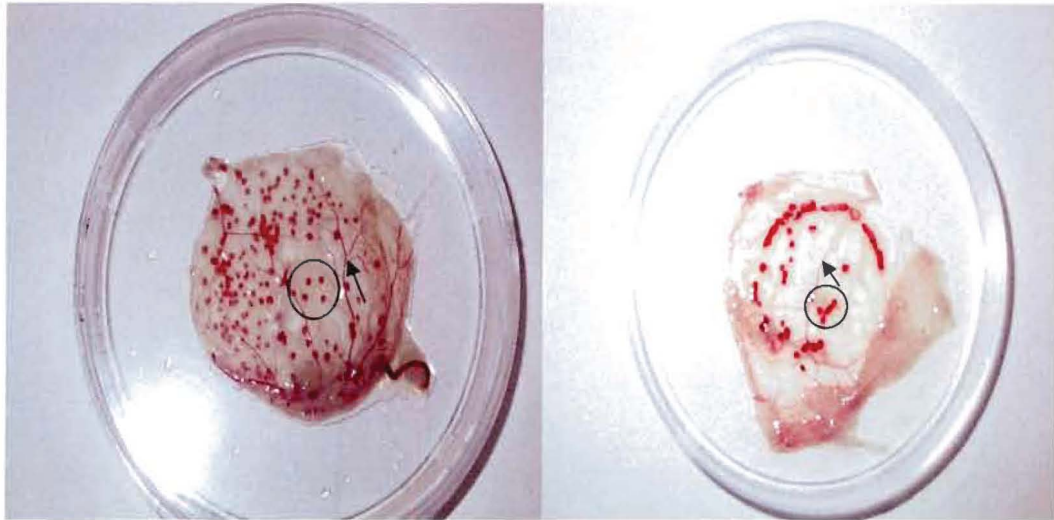


Fig 3.5: Figure showing CAMs of 12-14-day old chick embryos, infected with CPV WT (right) and CPV IMP<sup>-</sup> (left). Membranes were infected with  $1 \times 10^2$  pfu of each virus, and the eggs were incubated at 37°C for 72 h before harvesting of the membranes. A few pocks in each picture are circled. Arrows indicate blood vessels.

### 3.3.3. Titration of virus stocks

The titre was obtained as follows: The group of 3 wells infected with the dilution which yielded 10-100 plaques per well, was chosen for counting. The plaques in each of these three wells were counted, and each number was then multiplied by 5, to determine the number of plaques per ml, and then multiplied by the dilution factor. The 3 titres obtained for each well were averaged. Table 3 shows the average titres obtained for each titration. For CPV WT, a titre of  $2.07 \times 10^9$  pfu/ml was obtained, while for CPV IMP<sup>-</sup>, a titre of  $5.55 \times 10^9$  pfu/ml was obtained.

Table 3: Table showing the number of plaques counted and the calculated titre for each virus.

Virus	#plaques counted (dilution used)	x 5 ¶	X dilution factor	Average titre (pfu/ml)
CPV IMP <sup>-</sup>	117 (1 x 10 <sup>-7</sup> )	585	275 x 10 <sup>7</sup>	5.55 x 10 <sup>9</sup>
	116 (1 x 10 <sup>-7</sup> )	580	255 x 10 <sup>7</sup>	
	100 (1 x 10 <sup>-7</sup> )	500	240 x 10 <sup>7</sup>	
CPV WT	52 (1 x 10 <sup>-7</sup> )	260	260 x 10 <sup>7</sup>	2.07 x 10 <sup>9</sup>
	32 (1 x 10 <sup>-7</sup> )	160	160 x 10 <sup>7</sup>	
	40 (1 x 10 <sup>-7</sup> )	200	200 x 10 <sup>7</sup>	

¶The number of plaques was multiplied by 5 as 200 µl was used as inoculum in each well, and the titre is expressed as pfu/ml.



Fig. 3.6: This is an example of a titration plate. 24-well plates were seeded with CV-1 monolayers, which were then infected with CPV WT, using serial dilutions of the virus. 72 h following infection, the infected monolayers were stained with carbol-fuchsin. Purple regions indicate the presence of cells, whereas the clear regions indicate the formation of plaques on the monolayers. Numbers indicate the dilution of virus used to inoculate a well and the 2 adjacent wells to the right. C indicates 3 adjacent wells inoculated with DMEM as a negative control.

### 3.3.4. Comparison of plaque morphology of CPV WT and CPV IMP<sup>-</sup> on CV-1 monolayers

CPV WT and CPV IMP<sup>-</sup> were used to infect CV-1 monolayers. After 72 h of incubation at 37°C after infection of the monolayers, the cells were stained with carbol-fuchsin. Figure 3.7 shows CV-1 monolayers infected with either CPV WT

or CPV IMP<sup>-</sup>. Purple regions are viable cells that have taken up the stain. Clear dots are plaques formed when virus enters the cells and induces cytopathic effect.

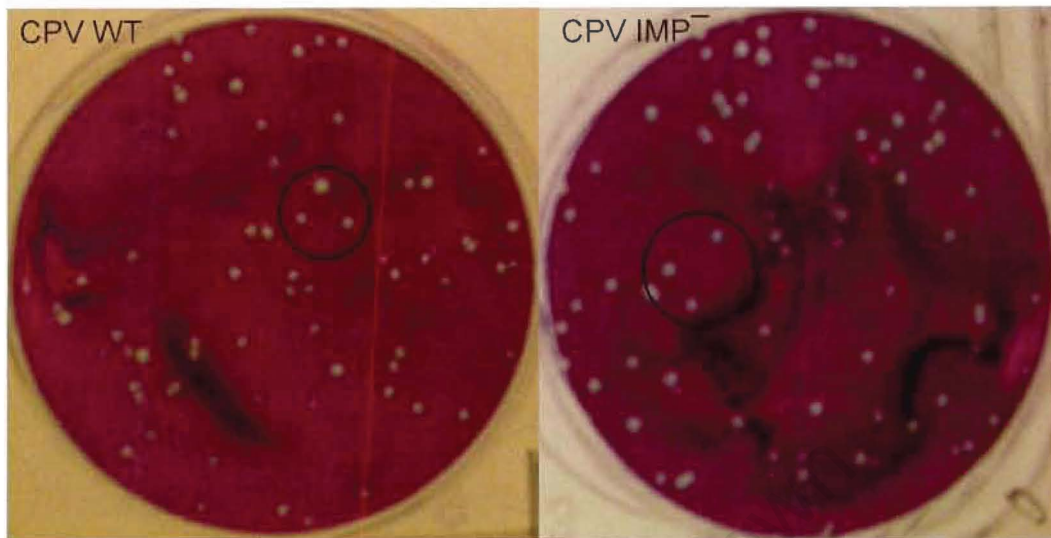


Fig. 3.7: Figure showing CV-1 monolayers infected with CPV WT (left) and CPV IMP<sup>-</sup> (right), and stained with carbol-fuchsin. A few plaques on each plate are circled.

### 3.3.5. PCR analysis of CPV WT and CPV IMP<sup>-</sup> to confirm the presence or absence, respectively, of the gene encoding IMP

Figure 3.8 shows the PCR products which were subjected to agarose gel electrophoresis. The molecular weight marker Roche marker VII (Roche, Penzburg, Germany) was used. In lane 2 is the negative control (i.e. no DNA). In lane 3, a ~1400 bp product was obtained from CPV WT, as expected using the cowpox virus IMP primers (see section 3.2.3.3). Similarly, the expected product of 3400 bp was obtained from CPV IMP<sup>-</sup>, using the cowpox virus IMP primers (lane 4).

In lane 5, a PCR product of ~740 bp was obtained from CPV WT, using the vaccinia virus VCP primers, whereas no PCR product is present in lane 6, from CPV IMP<sup>-</sup>. This is as expected as the vaccinia virus VCP primers bind within the gene encoding IMP, and this is disrupted in CPV IMP<sup>-</sup>.

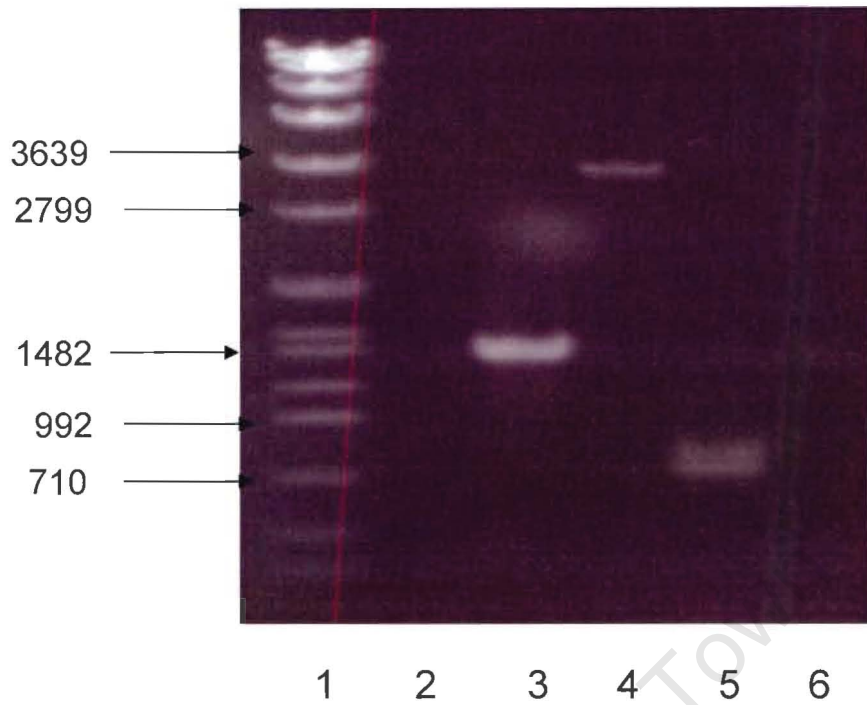


Figure 3.8: Figure showing PCR products following electrophoreses on a 1% agarose gel. Lane 1: molecular weight marker; lane 2: negative control; lane 3: 1396 bp product amplified from CPV WT using IMP PCR primers; lane 4: 3400 bp product amplified from CPV IMP<sup>-</sup> using IMP PCR primers; lane 5: 734 bp product amplified from CPV WT using VCP PCR primers; lane 6: no product amplified from CPV IMP<sup>-</sup> using VCP PCR primers.

### 3.4. Discussion

The chorioallantoic membrane of the chick embryo was chosen as a system for large scale growth of CPV WT and CPV IMP<sup>-</sup>, as it has been shown that high yields of orthopoxviruses can be recovered from it (Joklik, W.K., 1962). For cowpox virus in particular, high yields of viral plaque forming units (pfu) are obtained, with Joklik reporting a titre of  $1 \times 10^9$  pfu per membrane. Here I have shown that the recombinant virus, CPV IMP<sup>-</sup>, is able to grow to as high a titre as the wild type virus, CPV WT. I obtained a titre of  $1.88 \times 10^8$  pfu per egg for CPV WT and  $5.05 \times 10^8$  pfu per egg for CPV IMP<sup>-</sup>.

The CAM was not chosen for determination of viral titres, however. Rather the cell culture system was used. Virus was titrated on CV-1 monolayers. For greater accuracy of the titration, wells were infected in triplicate and an average was obtained from the three wells. For CPV WT, an average titre of  $2.07 \times 10^9$  pfu/ml was obtained from 11 eggs and an average titre of  $5.55 \times 10^9$  pfu/ml was obtained for CPV IMP<sup>-</sup> from 11 eggs.

PCR analysis of the wild type and knockout virus confirmed the presence and absence, respectively, of the gene encoding IMP. PCR products of the appropriate size were obtained for both viruses. For CPV WT, a product of 1396 bp in size was obtained, using the primers IMP PCR FWD and IMP PCR REV. This accounted for the size of the IMP open reading frame (792 bp), the number of bases upstream of the IMP ORF, where IMP PCR FWD binds (201 bp), and the number of bases downstream of the IMP ORF, where IMP PCR REV binds (404 bp). A product of 3326 bp in size was amplified from CPV IMP<sup>-</sup> using these primers. This total was made up of the *gpt* cassette inserted into the VCP ORF (2000 bp), the VCP ORF missing 70 bp (722 bp), plus the 201 bp upstream and 404 bp downstream of the VCP ORF. This confirms that CPV WT has the IMP gene present in its genome, and that CPV IMP<sup>-</sup> has an IMP gene that is disrupted by a deletion of 70 bp and an insertion of 2 kbp. A band of 1396 bp was not amplified from CPV IMP<sup>-</sup> template DNA, showing that the virus preparation is pure and not contaminated with any other orthopoxvirus containing IMP.

No difference was seen between the plaque morphology of CPV WT and CPV IMP<sup>-</sup> in CV-1 cells. As shown in fig. 3.7, the plaques produced were similar and indistinguishable with respect to size and shape. This was not a surprising result as there is no immune system present in cell culture and IMP is presumed to function as a complement binding protein.

The pocks produced on the chorioallantoic membrane of embryonated hens' eggs by wild-type cowpox virus (in this project, the virus termed CPV WT), have been well characterized. Palumbo *et al* (1989) and Fredrickson *et al* (1992) both described pocks that were red in colour due to the dilation of blood vessels and excessive accumulation of blood at the regions of viral replication (i.e. the pocks). The red pock characteristic of CPV WT is due to CrmA, which belongs to the serpin superfamily of proteins (Pickup, D.J., *et al*, 1986). CrmA inhibits caspase 1 (Ray, C.A., *et al*, 1992), a serine protease that converts pro-IL-1 $\beta$  to the mature IL-1 $\beta$  (Thornberry, N.A., *et al*, 1992). IL-1 $\beta$  is a pro-inflammatory cytokine (Dinarello, C.A., 1989). Viruses with a *crmA* deletion have been shown to produce white pocks on the chick CAM, with an influx of inflammatory cells into the pock responsible for this white colour (Palumbo, G.J., *et al*, 1989).

In this experiment, CPV WT and CPV IMP<sup>-</sup> both produced pocks which were bright red in colour and similar in size. Although the morphology appears to be the same, it is not known whether the lack of IMP attenuates viral growth or not. Thus in the next chapter a series of growth curves is described, which aim to determine the effect of deletion of IMP on viral growth.

# **CHAPTER 4**

## **COMPARISON OF GROWTH CHARACTERISTICS OF CPV WT AND CPV IMP<sup>-</sup> IN CV-1 MONOLAYERS AND EMBRYONATED HENS' EGGS**

<b>4.1.</b>	Introduction	<b>53</b>
<b>4.2.</b>	Materials and methods	<b>55</b>
4.2.1.	Quantitation of CV-1 cells on a 25 cm <sup>3</sup> surface area	<b>55</b>
4.2.2.	Viral growth curves generated by growth of CVP WT and CPV IMP <sup>-</sup> in CV-1 monolayers using multiplicities of infection of either 2.9 x 10 <sup>-5</sup> or 2.9 x 10 <sup>-3</sup> pfu/cell	<b>55</b>
4.2.3.	Viral growth curves generated by growth of CPV WT and CPV IMP <sup>-</sup> on chick chorioallantoic membranes using either 1 x 10 <sup>2</sup> or 1 x 10 <sup>4</sup> pfu per egg membrane	<b>57</b>
<b>4.3.</b>	Results	<b>59</b>
4.3.1.	Quantitation of CV-1 cells on a 25 cm <sup>3</sup> surface area	<b>59</b>
4.3.2.	Viral growth curves generated by growth of CPV WT and CPV IMP <sup>-</sup> in CV-1 monolayers	<b>59</b>
4.3.2.1.	Viral growth curve generated using a multiplicity of infection of 2.9 x 10 <sup>-5</sup> pfu/cell in CV-1 monolayers (1 x 10 <sup>2</sup> pfu/flask)	<b>59</b>
4.3.2.2.	Viral growth curve generated using a multiplicity of infection of 2.9 x 10 <sup>-3</sup> pfu/cell in CV-1 monolayers (1 x 10 <sup>4</sup> pfu/flask)	<b>61</b>
4.3.3.	Viral growth curves generated by growth of CPV WT and CPV IMP <sup>-</sup> on chick chorioallantoic membranes	<b>65</b>
4.3.3.1.	Viral growth curve generated using 1 x 10 <sup>2</sup> pfu/egg membrane	<b>65</b>
4.3.3.2.	Viral growth curve generated using 1 x 10 <sup>4</sup> pfu/egg membrane	<b>66</b>
<b>4.4.</b>	Discussion	<b>71</b>

#### 4.1. Introduction

The experiments performed in this chapter were set up to determine whether IMP influences growth of the virus in CV-1 cells and on chick CAMs. To do this, growth curves were generated, which are plots of virus titre against time. Growth curves are useful for examining viral growth under many conditions. For example, they have been used to study the growth of modified vaccinia virus Ankara in different cell lines (Drexler, I., *et al*, 1998); to evaluate the dependence or resistance of vaccinia virus mutants in the presence or absence of a particular compound (Katz, E., *et al*, 1973); to determine the effect of partial gene knockout and replacement with homologous repeats on growth of vaccinia virus (Meng, X. and Xiang, Y., 2006); and to determine the effect of gene knockout and protein complementation on the growth of vaccinia virus (Ramsey-Ewing, A.L. and Moss, B., 1996).

Firstly, viral growth *in vitro* was investigated. For this, CV-1 monolayers were infected with CPV WT or CPV IMP<sup>-</sup>. Previous work has shown that vaccinia virus VCP is not necessary for growth in cell culture (Kotwal, G.J., *et al*, 1990). Since IMP is a homolog of VCP, the hypothesis is that this CPV protein should not be required for growth in cell culture. This has been shown to be true by the construction of the deletion mutant CPV IMP<sup>-</sup>, which form plaques in cell culture. However, IMP is has not yet been characterized with respect to its binding properties and also its role in replication of CPV *in vitro*. Thus until the experiment is performed one cannot make any deductions as to its role in viral growth *in vitro*.

Secondly, growth curves were generated *in ovo*, i.e. in embryonated hens' eggs. The CAM of the chicken egg has been shown to support the growth of all orthopoxviruses (Joklik, W.K., 1962). In addition, experiments have been performed using mutant forms of the wild type orthopoxviruses (Palumbo, G.J., *et al*, 1989), and the characteristics of these mutants with respect to pock morphology and immune properties were determined, relative to the wild type counterparts. Thus this model can serve as a good means of comparing the

growth of the two viruses in an *in vivo* model to determine whether IMP has any influence over viral growth.

University of Cape Town

## 4.2. Materials and Methods

### 4.2.1. Quantitation of CV-1 cells on a 25 cm<sup>2</sup> surface area

Cells were counted to determine the number of cells in a 25 cm<sup>2</sup> flask once the monolayer had reached 100% confluency. The cells were detached from the flask surface by addition of trypsin and incubation at 37°C for 5-10 min. The cell/trypsin mixture was transferred to a sterile tube, and 5 ml DMEM was added to it. To a clean eppendorf tube, 50 µl trypan blue (Sigma-Aldrich, UK) was added. To this 50 µl trypan blue, 50 µl of the cell/trypsin/DMEM mixture was added. A drop of this mixture was placed on a cell counting chamber (Marienfeld). A coverslip was placed over the drops and the slide was viewed using an Olympus CK30 microscope at 4x magnification.

Cells in 2 out of the 9 chambers were counted and the number was averaged. However, to account for the 1:2 dilution of the cells in trypan blue, this average number was then multiplied by 2. The number of cells was calculated using the formula  $c = n/v$ , where  $c$  is the number of cells/ml,  $n$  is the number of cells, and  $v$  is the volume in ml. Since the depth of the chamber is 0.1 mm, and the area of each square is 1 mm<sup>2</sup>, the volume of each square is 0.1 mm<sup>3</sup>, or  $1 \times 10^{-4}$  ml. Thus, the number of cells is calculated using the formula  $c = n \times 10^4$  (Freshney, I.R., 1994).

### 4.2.2. Viral growth curves generated by growth of CPV WT and CPV IMP<sup>r</sup> in CV-1 monolayers using multiplicities of infection of either $2.9 \times 10^{-5}$ or $2.9 \times 10^{-3}$ pfu/cell

Eighteen small flasks with a surface area of 25 cm<sup>2</sup> were seeded with CV-1 cells. The cells were maintained in DMEM supplemented with 10% FCS, until confluent. Once confluent ( $\pm 3.5 \times 10^6$  cells/flask), the medium was removed from each flask. To 9 flasks,  $1 \times 10^2$  pfu of CPV WT, in 1 ml of PBS, was added. To the remaining 9 flasks,  $1 \times 10^2$  pfu of CPV IMP<sup>r</sup>, in 1 ml of PBS, was added. Using this amount of virus, the multiplicity of infection was  $2.87 \times 10^{-5}$  pfu/cell.

The multiplicity of infection is the ratio of the number of virus particles present to the number of CV-1 cells present. In this case for every cell present, there were 0.0000287 virus particles. The flasks were placed in a 37°C and 5% CO<sub>2</sub> incubator, and virus adsorption was allowed for 2 hours. Following adsorption, the flasks were removed from the incubator and the inoculum removed. DMEM supplemented with 4% FCS was then added to each flask. The flasks were again placed in the 37°C incubator.

At various time-points, one flask with a CPV WT-infected monolayer, and one flask with a CPV IMP<sup>-</sup>-infected monolayer were removed from the incubator and placed at -20°C immediately. These time-points were: 0 h (once the inoculum was removed and replaced with DMEM, the flask was placed at -20°C immediately), 6 h, 12 h, 24 h, 30 h, 36 h, 48 h, 60 h and 72 h.

To lyse the CV-1 cells and release the intracellular virus, three cycles of freeze-thawing was carried out at -20°C and 37°C, respectively. The virus-containing medium from each time-point was then titrated on CV-1 cells in 24-well plates, as outlined in chapter 3. Cells were infected in triplicate. The inoculum was allowed to adsorb to the cells for 1.5 h. After removal of the inoculum, 0.5 ml DMEM supplemented with 4% FCS was added to each well. The plates were incubated at 37°C and 5% CO<sub>2</sub> for 72 h. The plates were then removed from the incubator, and the medium was removed from each well. To each well, a few drops of carbol-fuchsin were added, and staining of the cells was allowed for 20-30 sec. The stain was then rinsed off with water and the plates were inverted to allow for drying. Once dry, the plaques in each well were counted and the viral titre at each time-point was calculated.

The same procedure described above was carried out, this time using  $1 \times 10^4$  pfu of CPV WT in 1 ml PBS, or  $1 \times 10^4$  pfu of CPV IMP<sup>-</sup> in 1 ml PBS as an inoculum. This corresponds to an MOI of  $2.87 \times 10^{-3}$  pfu/cell. Thus in this experiment, for every cell present there were 0.00287 virus particles. Titration of virus extract from each time-point was carried out on the same day to ensure that conditions were uniform for each titration.

**4.2.3. Viral growth curves generated by growth of CPV WT and CPV IMP<sup>r</sup> on chick chorioallantoic membranes using either 1 x 10<sup>2</sup> or 1 x 10<sup>4</sup> pfu per egg membrane**

Forty 9-11-day old embryonated hens' eggs were used in this experiment. Using an egg-pricker, holes were made at the air-sac end and on the lateral side of each egg, next to but not directly above any blood vessels. A drop of PBS containing penicillin and streptomycin was placed on top of the hole. A pipette filler bulb was placed over the hole at the air-sac end and gentle pressure was applied using the bulb, thus causing the chorioallantoic membrane (CAM) to collapse at that region. The eggs were placed at 37°C overnight to allow the membranes to stabilize.

After removal of the eggs from 37°C, 100 µl of PBS containing 1 x 10<sup>2</sup> pfu of CPV WT was injected into each of 20 eggs, and 100 µl of PBS containing 1 x 10<sup>2</sup> pfu of CPV IMP<sup>r</sup> was injected into each of the remaining 20 eggs, using 1 ml syringes. The lateral holes were covered with wax to prevent bacterial contamination. Each egg was swirled gently for 10-20 sec, and then placed at 37°C.

At different time points (2, 24, 48 and 72 h), 5 eggs infected with CPV WT and 5 eggs infected with CPV IMP<sup>r</sup> were removed from the incubator. Each egg was cut open and the section of CAM that had dropped from the eggshell was collected. The membranes were placed in autoclaved McCartney bottles tubes containing glass beads. For each membrane in the tube, 1 ml McIlvain's buffer (0.1 M citric acid, 0.2 M disodium hydrogen orthophosphate, pH 7.4) (Stannard *et al*, 1998) was added. The tubes containing the membrane-solvent mixture were shaken vigorously for 2 min, and then placed on ice for 10 min. The tubes were once again shaken vigorously for 2 min. The membrane-solvent mixtures were then placed on ice for 1.5 h.

The tubes were then centrifuged for 10 min at 2 000 rpm in a Sigma 301K centrifuge to remove cell debris. The supernatants containing released virus particles were transferred to 15 ml tubes and placed at -20°C. The titre obtained

from virus extracted from the eggs at 2 h after infection was taken as the zero time-point for the growth curve.

The virus extracted at each time point was immediately placed at  $-20^{\circ}\text{C}$ . Following this, serial dilutions of each virus extract were made, and the titration was performed on CV-1 monolayers in 24-well plates. The titrations were carried out as outlined previously. Briefly: titration of each dilution was performed in triplicate; 200  $\mu\text{l}$  of inoculum was added to each well; adsorption was allowed for 1.5 h at  $37^{\circ}\text{C}$  and 5%  $\text{CO}_2$ , following which the inoculum was removed and replaced with DMEM supplemented with 4% FCS. The plates were placed at  $37^{\circ}\text{C}$  for 72 h, at which point they were removed from the incubator, the inoculum was removed, and the cells stained with carbol-fuchsin. Titration of virus extract from each time-point was carried out on the same day to ensure that conditions were uniform for each titration.

The same procedure described above was carried out, this time using  $1 \times 10^4$  pfu of CPV WT to infect each of 20 eggs, and  $1 \times 10^4$  pfu of CPV IMP<sup>-</sup> to infect each of another 20 eggs.

### 4.3. Results

#### 4.3.1. Quantitation of CV-1 cells on a 25 cm<sup>2</sup> surface area

Cells were counted using a Coulter counter. The number of cells in 2 squares was 58. The number of cells/ml was calculated using the formula  $c=n \times 10^4$  (refer to section 4.2.1). This gave a total of  $58 \times 10^4$  cells/ml. The cells in a flask with a surface area of 25 cm<sup>2</sup> were suspended in 6 ml of DMEM, before counting. Therefore it was calculated that a 25 cm<sup>2</sup> flask, contained approximately  $3.48 \times 10^6$  cells.

#### 4.3.2. Viral growth curves generated by growth of CPV WT and CPV IMP<sup>r</sup> in CV-1 monolayers using multiplicities of infection of either $2.9 \times 10^{-5}$ or $2.9 \times 10^{-3}$ pfu/cell

##### 4.3.2.1. Viral growth curve generated using a multiplicity of infection of $2.9 \times 10^{-5}$ pfu/cell on CV-1 monolayers ( $1 \times 10^2$ pfu/flask)

Each flask containing  $3.48 \times 10^6$  cells was infected with  $10^2$  pfu of virus. This is equivalent to an MOI of  $2.87 \times 10^{-5}$  pfu/cell ( $100/3.48 \times 10^6 = 2.87 \times 10^{-5}$ ). Tables 4.1 (page 60) and 4.2 (page 61) show the average titres obtained at various time-points ranging from 0 h to 72 h, following inoculation of CV-1 monolayers with  $1 \times 10^2$  pfu of either CPV WT or CPV IMP<sup>r</sup>, respectively. Figure 4.1 (page 68) is a graphical display of the viral titres over time.

The growth rates of the two viruses are similar. Initially, fewer CPV IMP<sup>r</sup> particles are recovered, as seen at the first three time-points, but this is probably insignificant as the numbers are small. By 24 hours the titre of CPV IMP<sup>r</sup> is the same as that of CPV. Figure 4.1 shows that the rate of replication of the two viruses is similar. By 48 h both viruses attained titres of more than  $1 \times 10^4$  pfu/ml. Thereafter, there is a plateau in the growth curve.

Table 4.1: Table showing average titres obtained at various time-points following infection of CV-1 monolayers with CPV WT at an MOI of  $2.87 \times 10^{-5}$  pfu/cell ( $1 \times 10^2$  pfu/flask)

Time post-infection (h)	Number of plaques (dilution counted)	Number of plaques multiplied by 5	Titre (pfu/ml)	Average titre (pfu/ml)
0	0 (0)	0	0	5
	2 (0)	10	10	
	1 (0)	5	5	
6	2 (0)	10	10	10
	3(0)	15	15	
	1(0)	5	5	
12	2 (0)	10	10	10
	3 (0)	15	15	
	1 (0)	5	5	
24	116 (0)	580	580	$5.85 \times 10^2$
	118 (0)	590	590	
	117 (0)	585	585	
30	78 ( $1 \times 10^{-1}$ )	390	3900	$3.42 \times 10^3$
	62 ( $1 \times 10^{-1}$ )	310	3100	
	65 ( $1 \times 10^{-1}$ )	325	3250	
36	114 ( $1 \times 10^{-1}$ )	570	5700	$5.27 \times 10^3$
	105 ( $1 \times 10^{-1}$ )	525	5250	
	97 ( $1 \times 10^{-1}$ )	485	4850	
48	86 ( $1 \times 10^{-2}$ )	430	43000	$4.73 \times 10^4$
	94 ( $1 \times 10^{-2}$ )	470	47000	
	104 ( $1 \times 10^{-2}$ )	520	52000	
60	100 ( $1 \times 10^{-2}$ )	500	50000	$5.68 \times 10^4$
	122 ( $1 \times 10^{-2}$ )	610	61000	
	119 ( $1 \times 10^{-2}$ )	595	59500	
72	56 ( $1 \times 10^{-3}$ )	280	280000	$2.92 \times 10^5$
	66 ( $1 \times 10^{-3}$ )	330	330000	
	53 ( $1 \times 10^{-3}$ )	265	265000	

A student's t test was performed using Excel. For all except 2 time-points, the p values returned by the programme were greater than 0.05, indicating that for most of the time-points there was no significant difference between the titres of the two viruses.

Table 4.2: Table showing average titres obtained at various time-points following infection of CV-1 monolayers with CPV IMP<sup>r</sup> at an MOI of  $2.87 \times 10^{-5}$  pfu/cell ( $1 \times 10^2$  pfu/flask).

Time post-infection (h)	Number of plaques (dilution counted)	Number of plaques multiplied by 5	Titre (pfu/ml)	Average titre (pfu/ml)
0	0 (0)	0	0	1.67
	0 (0)	0	0	
	1 (0)	5	5	
6	1 (0)	5	5	3.33
	0 (0)	0	0	
	1 (0)	5	5	
12	0 (0)	0	0	1.67
	1 (0)	5	5	
	0 (0)	0	0	
24	97 (0)	485	485	$4.50 \times 10^2$
	83 (0)	415	415	
	90 (0)	450	450	
30	70 ( $1 \times 10^{-1}$ )	350	3500	$4.02 \times 10^3$
	77 ( $1 \times 10^{-1}$ )	385	3850	
	94 ( $1 \times 10^{-1}$ )	470	4700	
36	24 ( $1 \times 10^{-2}$ )	120	12000	$1.53 \times 10^4$
	28 ( $1 \times 10^{-2}$ )	140	14000	
	40 ( $1 \times 10^{-2}$ )	200	20000	
48	36 ( $1 \times 10^{-2}$ )	180	18000	$2.60 \times 10^4$
	56 ( $1 \times 10^{-2}$ )	280	28000	
	64 ( $1 \times 10^{-2}$ )	320	32000	
60	136 ( $1 \times 10^{-2}$ )	680	68000	$7.42 \times 10^4$
	141 ( $1 \times 10^{-2}$ )	705	70500	
	168 ( $1 \times 10^{-2}$ )	840	84000	
72	69 ( $1 \times 10^{-3}$ )	345	345000	$3.33 \times 10^5$
	61 ( $1 \times 10^{-3}$ )	305	305000	
	70 ( $1 \times 10^{-3}$ )	350	350000	

**4.3.2.2. Viral growth curve generated using a multiplicity of infection of  $2.9 \times 10^{-3}$  pfu/cell on CV-1 monolayers ( $1 \times 10^4$  pfu/flask)**

In this experiment, a higher viral titre was used to inoculate each flask. This was done in order to determine whether using a higher titre influences the rate of replication and whether there are enough cells to support the propagation of the increased number of virus particles. Tables 4.3 (page 62) and 4.4 (page 64) show the average titres obtained at various time-points ranging from 0 h to 72 h, following inoculation of CV-1 monolayers with  $1 \times 10^4$  pfu of either CPV WT

Table 4.3: Table showing average titres obtained at various time-points following infection of CV-1 monolayers with CPV WT at an MOI of  $2.87 \times 10^{-3}$  pfu/cell ( $1 \times 10^4$  pfu/flask).

Time post-infection (h)	Number of plaques (dilution counted)	Number of plaques multiplied by 5	Titre (pfu/ml)	Average titre (pfu/ml)
0	27 (0)	135	135	$1.43 \times 10^2$
	31 (0)	155	155	
	28 (0)	140	140	
6	28 (0)	140	140	$1.52 \times 10^2$
	29 (0)	145	145	
	34 (0)	170	170	
12	49 ( $1 \times 10^{-1}$ )	245	2450	$1.95 \times 10^3$
	31 ( $1 \times 10^{-1}$ )	155	1550	
	37 ( $1 \times 10^{-1}$ )	185	1850	
24	40 ( $1 \times 10^{-3}$ )	200	200000	$2.10 \times 10^5$
	44 ( $1 \times 10^{-3}$ )	220	220000	
30	101 ( $1 \times 10^{-3}$ )	505	505000	$4.83 \times 10^5$
	92 ( $1 \times 10^{-3}$ )	460	460000	
	97 ( $1 \times 10^{-3}$ )	485	485000	
36	107 ( $1 \times 10^{-3}$ )	535	535000	$6.13 \times 10^5$
	144 ( $1 \times 10^{-3}$ )	720	720000	
	117 ( $1 \times 10^{-3}$ )	585	585000	
48	44 ( $1 \times 10^{-4}$ )	220	2200000	$2.85 \times 10^6$
	44 ( $1 \times 10^{-4}$ )	220	2200000	
	83 ( $1 \times 10^{-4}$ )	415	4150000	
60	52 ( $1 \times 10^{-4}$ )	260	2600000	$2.65 \times 10^6$
	47 ( $1 \times 10^{-4}$ )	235	2350000	
	60 ( $1 \times 10^{-4}$ )	300	3000000	
72	55 ( $1 \times 10^{-4}$ )	275	2750000	$2.13 \times 10^6$
	39 ( $1 \times 10^{-4}$ )	195	1950000	
	34 ( $1 \times 10^{-4}$ )	170	1700000	

or CPV IMP<sup>r</sup>, respectively. Figure 4.2 (page 68) is a graphical display of the viral titres over time.

By 48 h there is an increase of approximately  $10^4$ , from  $\pm 10^2$  pfu/ml at 0 h to  $\pm 10^6$  pfu/ml at 48 h. This increase is much the same as that seen when  $1 \times 10^2$  pfu of virus was used to infect the monolayers (fig. 4.1), when an increase from  $1 \times 10^0$  at 0h approximately  $10^4$  at 48 h was seen. For all except 3 time-points, the p values returned by the programme were greater than 0.05, indicating that for most

of the time-points there was no significant difference between the titres of the two viruses.

Using a higher MOI there is an earlier and more definite plateau in the growth curve. This is probably due to all the cells having been infected and no more uninfected cells being available for further replication. Similarly, when a multiplicity of infection of  $2.87 \times 10^{-5}$  pfu/cell was used both the wild type and deletion mutant virus grew at similar rates to each other. Only a 1 log difference at the final time-points was noted using the different multiplicities of infection.

University of Cape Town

Table 4.4: Table showing average titres obtained at various time-points following infection of CV-1 monolayers with CPV IMP<sup>+</sup> at an MOI of  $2.87 \times 10^{-3}$  pfu/cell ( $1 \times 10^4$  pfu/flask).

Time post-infection (h)	Number of plaques (dilution counted)	Number of plaques multiplied by 5	Titre (pfu/ml)	Average titre (pfu/ml)
0	36 (0)	180	180	$1.50 \times 10^2$
	27 (0)	135	135	
	27 (0)	135	135	
6	11 (0)	55	55	$8.61 \times 10^1$
	17 (0)	85	85	
	24 (0)	120	120	
12	45 (0)	225	225	$2.93 \times 10^2$
	66 (0)	330	330	
	65 (0)	325	325	
24	103 ( $1 \times 10^{-2}$ )	515	51500	$5.07 \times 10^4$
	99 ( $1 \times 10^{-2}$ )	495	49500	
	102 ( $1 \times 10^{-2}$ )	510	51000	
30	181 ( $1 \times 10^{-2}$ )	905	90500	$9.07 \times 10^4$
	177 ( $1 \times 10^{-2}$ )	885	88500	
	186 ( $1 \times 10^{-2}$ )	930	93000	
36	106 ( $1 \times 10^{-3}$ )	530	530000	$5.05 \times 10^5$
	100 ( $1 \times 10^{-3}$ )	500	500000	
	97 ( $1 \times 10^{-3}$ )	485	485000	
48	153 ( $1 \times 10^{-3}$ )	765	765000	$7.73 \times 10^5$
	155 ( $1 \times 10^{-3}$ )	775	775000	
	156 ( $1 \times 10^{-3}$ )	780	780000	
60	47 ( $1 \times 10^{-4}$ )	235	2350000	$1.92 \times 10^6$
	44 ( $1 \times 10^{-4}$ )	220	2200000	
	24 ( $1 \times 10^{-4}$ )	120	1200000	
72	31 ( $1 \times 10^{-4}$ )	155	1550000	$1.35 \times 10^6$
	26 ( $1 \times 10^{-4}$ )	130	1300000	
	24 ( $1 \times 10^{-4}$ )	120	1200000	

**4.3.3. Viral growth curves generated by growth of CPV WT and CPV IMP<sup>r</sup> on chick chorioallantoic membranes using either 1 x 10<sup>2</sup> or 1 x 10<sup>4</sup> pfu per egg membrane**

**4.3.3.1. Viral growth curve generated using 1 x 10<sup>2</sup> pfu/ egg membrane**

Tables 4.5 (page 65) and 4.6 (page 66) show the viral titres obtained at 0, 24, 48 and 72 h, after crude extraction of virus from the CAMs of embryonated hens' eggs infected with 1 x 10<sup>2</sup> pfu of either CPV WT or CPV IMP<sup>r</sup>. Figure 4.3 (page 69) is a graphical display of the viral titres over time.

A rapid increase is seen in virus titre over 48 h. For both viruses there is a 7 log increase from 0 h to 48 h. Between 48 and 72 h, the curve tends to plateau. The p value obtained for each time-point using 1 x 10<sup>2</sup> pfu/membrane were greater than 0.05 for all except one time-point. Thus, as with growth in CV-1 monolayers, the growth of the two viruses *in ovo* is not statistically different at most time-points.

Table 4.5: Table showing average titres obtained at 0, 24, 48 and 72 h following infection of embryonated hens' eggs with 1 x 10<sup>2</sup> pfu of CPV WT.

Time post-infection (h)	Number of plaques (dilution counted)	Number of plaques multiplied by 5	Titre (pfu/ml)	Average titre (pfu/ml)
0	0 (0)	0	0	0
	0 (0)	0	0	
	0 (0)	0	0	
24	63 (1 x 10 <sup>-2</sup> )	315	31500	2.92 x 10 <sup>4</sup>
	58 (1 x 10 <sup>-2</sup> )	290	29000	
	54 (1 x 10 <sup>-2</sup> )	270	27000	
48	55 (1 x 10 <sup>-5</sup> )	275	27500000	3.03 x 10 <sup>7</sup>
	62 (1 x 10 <sup>-5</sup> )	310	31000000	
	65 (1 x 10 <sup>-5</sup> )	325	32500000	
72	94 (1 x 10 <sup>-5</sup> )	470	47000000	5.00 x 10 <sup>7</sup>
	96 (1 x 10 <sup>-5</sup> )	480	48000000	
	110 (1 x 10 <sup>-5</sup> )	550	55000000	

Table 4.6: Table showing average titres obtained at 0, 24, 48 and 72 h following infection of embryonated hens' eggs with  $1 \times 10^2$  pfu of CPV IMP<sup>-</sup>.

Time post-infection (h)	Number of plaques (dilution counted)	Number of plaques multiplied by 5	Titre (pfu/ml)	Average titre (pfu/ml)
0	0 (0)	0	0	0
	0 (0)	0	0	
	0 (0)	0	0	
24	72 ( $1 \times 10^{-2}$ )	360	36000	$3.33 \times 10^4$
	63 ( $1 \times 10^{-2}$ )	315	31500	
	65 ( $1 \times 10^{-2}$ )	325	32500	
48	48 ( $1 \times 10^{-5}$ )	240	24000000	$2.82 \times 10^7$
	67 ( $1 \times 10^{-5}$ )	335	33500000	
	54 ( $1 \times 10^{-5}$ )	270	27000000	
72	50 ( $1 \times 10^{-5}$ )	250	25000000	$2.42 \times 10^7$
	50 ( $1 \times 10^{-5}$ )	250	25000000	
	45 ( $1 \times 10^{-5}$ )	225	22500000	

#### 4.3.3.2. Viral growth curve generated using $1 \times 10^4$ pfu/egg membrane

Tables 4.7 (page 67) and 4.8 (page 67) show the viral titres obtained at 0, 24, 48 and 72 h, after crude extraction of virus from the CAMs of embryonated hens' eggs infected with  $1 \times 10^4$  pfu of either CPV WT or CPV IMP<sup>-</sup>. Figure 4.4 (page 69) is a graphical display of the viral titres over time.

As when the CAMs were infected with  $1 \times 10^2$  pfu of virus, there is a rapid increase in viral titre over the first 48 h, after which the curve plateaus. However, this plateau is not as marked as that seen when eggs were infected with  $1 \times 10^2$  pfu of virus. The p values obtained for  $1 \times 10^4$  pfu/membrane at all time-points were less than 0.05, which is inconsistent with the experiments using  $1 \times 10^2$  pfu/membrane.

The titres observed at the final time-point were much the same whether  $1 \times 10^2$  or  $1 \times 10^4$  pfu was used to infect each membrane.

Table 4.7: Table showing average titres obtained at 0, 24, 48 and 72 h following infection of embryonated hens' eggs with  $1 \times 10^4$  pfu of CPV WT.

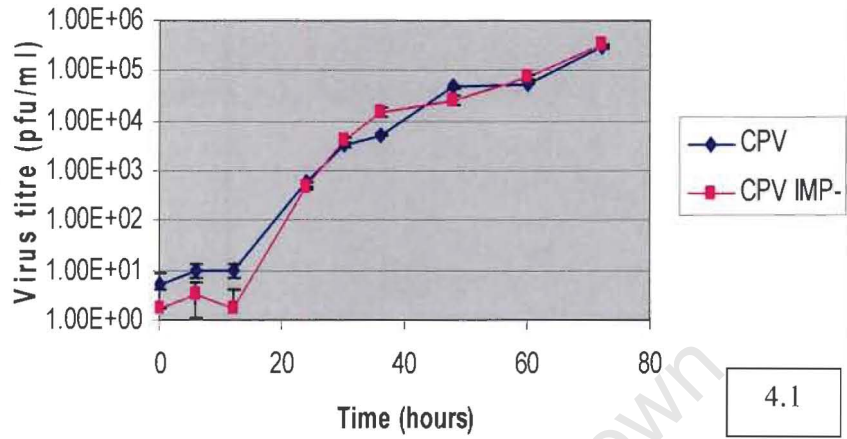
Time post-infection (h)	Number of plaques (dilution counted)	Number of plaques multiplied by 5	Titre (pfu/ml)	Average titre (pfu/ml)
0	0 (0)	0	0	0
	0 (0)	0	0	
	0 (0)	0	0	
24	17 ( $1 \times 10^{-2}$ )	85	8500	$9.50 \times 10^3$
	15 ( $1 \times 10^{-2}$ )	75	7500	
	25 ( $1 \times 10^{-2}$ )	125	12500	
48	102 ( $1 \times 10^{-4}$ )	510	5100000	$5.12 \times 10^6$
	104 ( $1 \times 10^{-4}$ )	520	5200000	
	101 ( $1 \times 10^{-4}$ )	505	5050000	
72	34 ( $1 \times 10^{-5}$ )	170	17000000	$2.08 \times 10^7$
	42 ( $1 \times 10^{-5}$ )	210	21000000	
	49 ( $1 \times 10^{-5}$ )	245	24500000	

Table 4.8: Table showing average titres obtained at 0, 24, 48 and 72 h following infection of embryonated hens' eggs with  $1 \times 10^4$  pfu of CPV IMP<sup>r</sup>.

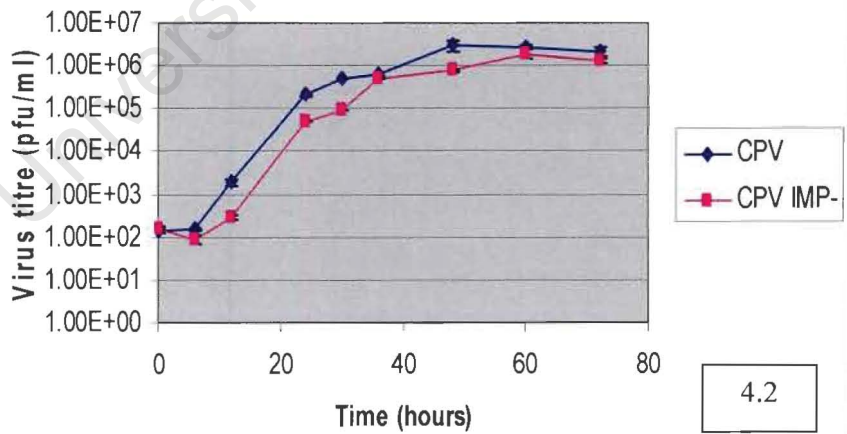
Time post-infection (h)	Number of plaques (dilution counted)	Number of plaques multiplied by 5	Titre (pfu/ml)	Average titre (pfu/ml)
0	0 (0)	0	0	0
	0 (0)	0	0	
	0 (0)	0	0	
24	72 ( $1 \times 10^{-1}$ )	360	3600	$3.47 \times 10^5$
	57 ( $1 \times 10^{-1}$ )	285	2850	
	79 ( $1 \times 10^{-1}$ )	395	3950	
48	124 ( $1 \times 10^{-3}$ )	620	620000	$6.28 \times 10^5$
	129 ( $1 \times 10^{-3}$ )	645	645000	
	124 ( $1 \times 10^{-3}$ )	620	620000	
72	64 ( $1 \times 10^{-5}$ )	320	32000000	$3.33 \times 10^7$
	62 ( $1 \times 10^{-5}$ )	310	31000000	
	74 ( $1 \times 10^{-5}$ )	370	37000000	

Fig 4.1-4.4: 4.1: Figure showing the viral titres of CPV WT and CPV IMP<sup>r</sup> against time in CV-1 monolayers, using a MOI of  $2.9 \times 10^{-5}$  pfu/cell. Fig 4.2: Figure showing the change in viral titres of CPV WT and CPV IMP<sup>r</sup> against time in CV-1 monolayers, using a MOI of  $2.9 \times 10^{-3}$  pfu/cell. Fig 4.3: Figure showing the change in viral titres of CPV WT and CPV IMP<sup>r</sup> against time on the chick CAM, using  $1 \times 10^2$  pfu to infect each membrane. Fig 4.4: Figure showing the change in viral titres of CPV WT and CPV IMP<sup>r</sup> against time on the chick CAM, using  $1 \times 10^4$  pfu to infect each membrane.

Growth curve of CPV WT and CPV IMP- in CV-1 monolayers infected with  $10^2$  pfu of virus



Growth curve of CPV WT and CPV IMP- in CV-1 monolayers infected with  $10^4$  pfu of virus



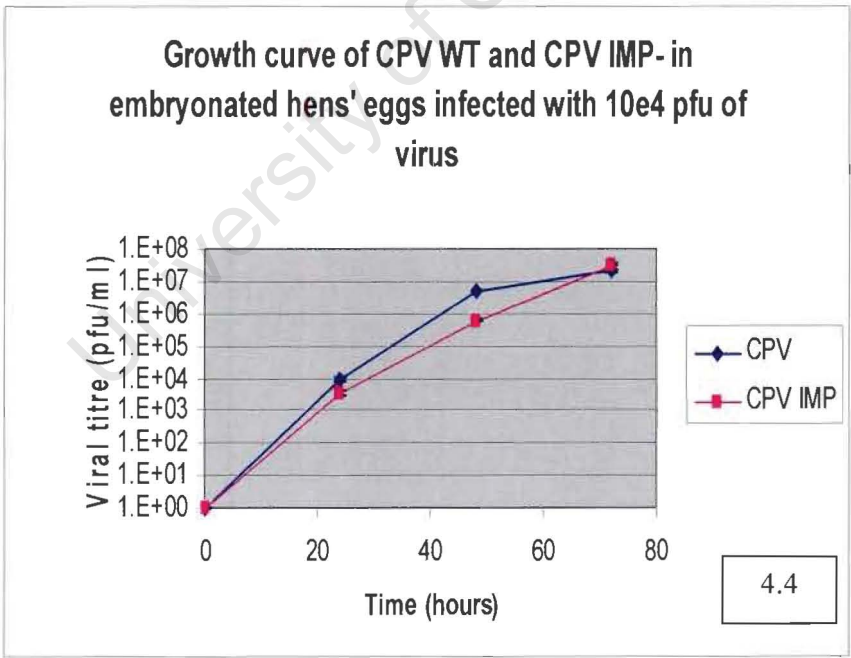
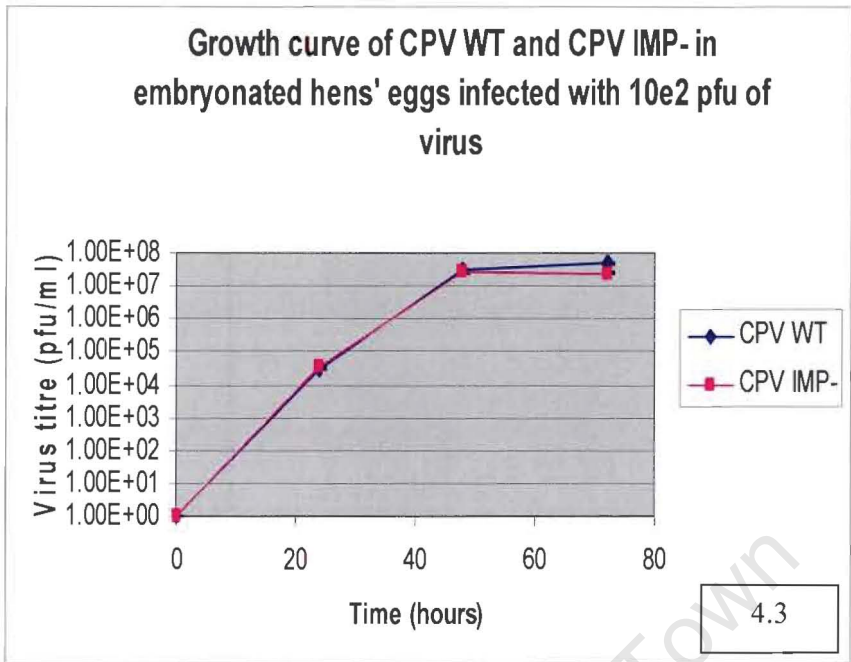


Table 4.9: Table summarizing the average titres obtained at each time point when CPV WT and CPV IMP<sup>r</sup> were propagated in CV-1 cell monolayers or in chorioallantoic membranes, using  $1 \times 10^2$  and  $1 \times 10^4$  pfu of virus to infect.

Time post-infection (hours)	CV-1 monolayers infected with $1 \times 10^2$ pfu CPV WT (titre in pfu/ml)	CV-1 monolayers infected with $1 \times 10^2$ pfu CPV IMP <sup>r</sup> (titre in pfu/ml)	CV-1 monolayers infected with $1 \times 10^4$ pfu CPV WT (titre in pfu/ml)	CV-1 monolayers infected with $1 \times 10^4$ pfu CPV IMP <sup>r</sup> (titre in pfu/ml)	Chorioallantoic membranes infected with $1 \times 10^2$ pfu CPV WT (titre in pfu/ml)	Chorioallantoic membranes infected with $1 \times 10^2$ pfu CPV IMP <sup>r</sup> (titre in pfu/ml)	Chorioallantoic membranes infected with $1 \times 10^4$ pfu CPV WT (titre in pfu/ml)	Chorioallantoic membranes infected with $1 \times 10^4$ pfu CPV IMP <sup>r</sup> (titre in pfu/ml)
0	5	1.67	$1.43 \times 10^2$	$1.50 \times 10^2$	0	0	0	0
6	10	3.33	$1.52 \times 10^2$	$8.61 \times 10^1$				
12	10	1.67	$1.95 \times 10^3$	$2.93 \times 10^2$				
24	$5.85 \times 10^2$	$4.50 \times 10^2$	$2.10 \times 10^5$	$5.07 \times 10^4$	$2.92 \times 10^4$	$3.33 \times 10^4$	$9.50 \times 10^3$	$3.47 \times 10^3$
30	$3.42 \times 10^3$	$4.02 \times 10^3$	$4.83 \times 10^5$	$9.07 \times 10^4$				
36	$5.27 \times 10^3$	$1.53 \times 10^4$	$6.13 \times 10^5$	$5.05 \times 10^5$				
48	$4.73 \times 10^4$	$2.60 \times 10^4$	$2.85 \times 10^6$	$7.73 \times 10^5$	$3.03 \times 10^7$	$2.82 \times 10^7$	$5.12 \times 10^6$	$6.28 \times 10^5$
60	$5.68 \times 10^4$	$7.42 \times 10^4$	$2.65 \times 10^6$	$1.92 \times 10^6$				
72	$2.92 \times 10^5$	$3.33 \times 10^5$	$2.13 \times 10^6$	$1.35 \times 10^6$	$5.00 \times 10^7$	$2.42 \times 10^7$	$2.08 \times 10^7$	$3.33 \times 10^7$

#### 4.4. Discussion

Figures 4.1 and 4.2 show the growth curves for both CPV WT and CPV IMP<sup>r</sup> using  $1 \times 10^2$  and  $1 \times 10^4$  pfu, respectively, of each virus to infect CV-1 monolayers. The growth rates of the two viruses were similar in both cases, with both viruses showing a steady increase in titre with increasing time up to 48 h. A student's t test was performed using Excel. Most of the p values returned by the programme were greater than 0.05. Thus at a confidence interval of 95%, one can say that at the time-points that yielded p values greater than 0.05, the growth of CPV and CPV IMP<sup>r</sup> are not statistically different. However, in order to get a more precise statistical result (since each of the other growth curves did not yield consistent p values at each time point) the growth curves should be repeated. In addition, the dilution series should be repeated for greater statistical accuracy.

The final titres obtained when infecting the monolayers with  $1 \times 10^2$  pfu of CPV WT or CPV IMP<sup>r</sup> were  $2.92 \times 10^5$  and  $3.33 \times 10^5$ , respectively. When infecting with  $1 \times 10^4$  of CPV WT or CPV IMP<sup>r</sup>, titres of  $2.13 \times 10^6$  and  $1.35 \times 10^6$  were obtained, respectively. Thus only a 1 log difference in the final titre was seen between using  $1 \times 10^2$  and  $1 \times 10^4$  pfu of virus to infect (which is a 2 log difference).

In cell culture, there is no immune system present. The IMP of CPV is postulated to bind to C3 and C4 of the complement system (since it is a homolog of VCP, which binds to these complement components [Kotwal, G.J., *et al*, 1990; McKenzie, *et al*, 1992]), thereby inhibiting both the alternative and classical pathways of complement activation. The complement system forms part of the innate immune system (Parham, P., 2005). As such it is absent from cell culture. Therefore, there is no target for IMP in the CV-1 monolayers. Thus the fact that there is no difference in the growth curves of the two viruses is not surprising. Furthermore, it has been shown that VCP is not a requirement for viral growth *in vitro*, since vaccinia virus mutants that are partially or

completely VCP-deficient are able to replicate in cell culture (Kotwal, G.J., *et al*, 1990).

Similarly, growth curves for each virus were generated in embryonated hens' eggs. The CAM of each egg was infected with  $1 \times 10^2$  or  $1 \times 10^4$  pfu of either CPV WT or CPV IMP<sup>r</sup>. Figures 4.3 and 4.4 show the growth curves for both the wild type and recombinant virus, respectively, at time points ranging from 0 to 72 h. The majority of p values obtained at each time-point for  $1 \times 10^2$  pfu/membrane were greater than 0.05, indicating that at these time-points the growth of the two viruses are not statistically different. Using  $1 \times 10^4$  pfu/membrane the p values were less than 0.05, suggesting that the growth curves may not be the same. However, these experiments should be repeated to get statistically significant comparisons. The final titres obtained when infecting the membranes with  $1 \times 10^2$  pfu of CPV WT or CPV IMP<sup>r</sup> were  $5.00 \times 10^7$  and  $2.42 \times 10^7$ , respectively. When infecting  $1 \times 10^4$  pfu of CPV WT or CPV IMP<sup>r</sup>, titres of  $2.08 \times 10^7$  and  $3.33 \times 10^7$  were obtained, respectively. Thus, the amount of virus used to infect initially did not influence the final titre observed in this experiment.

For both the wild type and the knockout viruses, virus was not detected at 0 h post infection of chick CAMs. This phenomenon has been described previously. Hahon and Friel (1961) found that when harvesting the chick CAMs 30 minutes after infection, up to 90% of the virus was present in the fluid used to wash the membranes. In this experiment, each membrane was rinsed twice in PBS before extraction of virus. Virus present in this rinsing fluid was not titrated. This probably accounts for the apparent decrease in viral titre at 0 h after infection. This is in contrast with the results seen by Esteban and Metz (1973), with vaccinia virus infection in cell culture. After a period of only 15 min, viral polypeptides were detected as early as 20 min later. In my experiment in cell culture a 2 log difference was observed in the amount of virus particles used to infect compared to the amount recovered. Perhaps this is due to the fact that following adsorption the inoculum is removed from the flask. Thus any virus that has not yet entered a cell is lost, and at 0 h, at which point the flask contents were snap frozen immediately after the inoculum was removed, only the virus

particles that have gained entry to the cell are detected upon titration. In addition, the virus is uncoated upon entry and no longer infectious. This probably accounts for the decrease in viral titre immediately following infection. When titrating the virus, the inoculum was removed after 1.5 h adsorption. This could account for a further reduction in titre.

In cell culture a  $1 \times 10^4$ -fold increase in viral titre was seen over 48 h, whereas in eggs a  $1 \times 10^7$ -fold increase was seen over the same time period. This was observed when cell monolayers and CAMs were infected with both  $1 \times 10^2$  and  $1 \times 10^4$  pfu of virus. This indicates that the egg CAM system is a much more efficient system for culturing large stocks of virus than the CV-1 monolayer system is.

In the CAM system, it was not known whether there would be a difference between the wild type and recombinant viruses in viral growth as the chick immune system is only a developing immune system. Here I have shown that there does not seem to be a difference between the growth curve of wild type cowpox virus and that of the recombinant lacking the IMP. VCP has been shown to bind to C4b (Kotwal, G.J, *et al*, 1990), thus inhibiting the classical pathway of complement, and also to C3b (McKenzie, *et al*, 1992), thus inhibiting the alternative pathway of complement. The complement system is implicated in inflammation through the production of the chemoattractant by-products, C3a, C4a and C5a (Parham, P., 2005). These bind to receptors on mast cells, resulting in the release of vasoactive substances. However, in the chick embryo, mast cells are first detected at 15 days after fertilization (Crivellato, E., *et al*, 2005). In this experiment the chicks were infected at the age of 9-11 days, and the membranes were thus harvested at 12-14 days. In addition to this, the complement system has been found to be present in the chick embryo by day 13, however, it is present in low levels (Gabrielsen, A., *et al*, 1973). Complement levels slowly increase and continue to do so slowly until there is a sharp increase in complement activity only 21 days after hatching. Since IMP is postulated to bind to C3b and C4b (being a homolog of VCP), it would inhibit the formation of the chemotactic by-products, and therefore eliminate the effects of the vasoactive substances released by the mast cells.

However, one of these systems (mast cell release of vasoactive products) is not yet present and the other (the complement system) is only present at low levels in the developing chick. This may explain why IMP has not conferred any advantage in the chick CAM system.

Previous studies have been conducted in which the expression of certain vaccinia virus genes have been under the control of different expression systems, or where stretches of coding sequences have been deleted from the gene of interest. Other studies have attempted to isolate mutant viruses in which an open reading frame of interest has been inactivated through the insertion of a *gpt* selection marker. These have revealed proteins that are important in viral growth and replication. Examples of these are the I7L gene product (Byrd, C.M., and Hruby, D.E., 2005) and the G1L gene product (Ansarah-Sorbrinho, C. and Moss, B., 2004). These two proteins are involved in the cleavage of core protein precursors and core condensation and the morphogenesis of infectious virions. Other proteins that are essential to viral growth are those involved in DNA replication, such as the products of A20R, D4R and D5R (Ishii, K and Moss, B, 2001; Upton, C., *et al*, 1993; Stuart, D.T., *et al*, 1993; Ellison, K.S., *et al*, 1996; Evans, E., *et al*, 1995). These three proteins form part of a DNA replication complex, with D4R functioning as a uracil DNA glycosylase.

Thus it may be that a protein that is not directly involved in the propagation of infectious progeny may not be essential for viral growth in cell culture or *in ovo*. However, in the presence of a mature immune system the presence of this gene product could confer a growth advantage on the virus. Examples of these proteins are listed in table 1 (chapter 1, section 2). The next chapter describes the mouse model used to investigate the role of IMP in viral replication *in vivo*.

# CHAPTER 5

## COMPARISON OF GROWTH CHARACTERISTICS OF CPV WT AND CPV IMP USING THE AIR POUCH MODEL IN BALB/c MICE

5.1.	Introduction	76
5.2.	Materials and methods	78
5.2.1.	Evaluation of viral titres using the connective tissue air pouch Method	78
5.2.2.	Extraction of DNA from connective tissue samples	79
5.2.3.	PCR to confirm the presence of BALB/c mouse DNA in the connective tissue samples	80
5.2.4.	PCR to confirm the presence of viral DNA in the connective tissue samples	80
5.2.5.	PCR to confirm the presence of the <i>gpt</i> insert in the connective tissue samples infected with CPV IMP	81
5.3.	Results	83
5.3.1.	Evaluation of viral titres using the connective tissue air pouch method	83
5.3.2.	PCR to confirm the presence of viral and cellular DNA in the connective tissue samples	83
5.3.2.1.	PCR to detect BALB/c mouse DNA	83
5.3.2.2.	PCR to detect viral DNA	83
5.3.3.	PCR to confirm the presence of the <i>gpt</i> insert in the connective tissue samples infected with CPV IMP	88
5.4.	Discussion	90

## 5.1 Introduction

The aim of the experiments discussed in this chapter is to determine the effect of IMP on the replication of cowpox virus in a mammalian *in vivo* model. While cowpox virus has been shown to have a broad host range (Baxby, D., *et al*, 1994), the true reservoirs of this virus are rodents (Chantrey, J., *et al*, 1999). Thus, studies using cowpox virus in mice would represent a matched virus:host interaction, and the data generated could be extrapolated to other poxvirus:host systems.

Previous studies have only looked at the effects of IMP on cellular infiltration and host tissue at the site of infection (Miller, C.G., *et al*, 1997). The authors found that infection with the virus lacking the IMP resulted in increased tissue damage relative to infection with the wild type virus. In addition, they found greater haemorrhage of blood vessels and hardening/thickening of tissue (induration) at the site of infection. Injection in the footpads of mice with recombinant virus resulted in a greater swelling response than that seen in mice infected with wild type virus (Miller, C.G., *et al*, 1997).

Kotwal, G.J., *et al* (1998) used the connective tissue air pouch model, described by Edwards, J.C., *et al* (1981), to evaluate the difference between the wild type and knockout viruses. They found that a lack of IMP resulted in a significant influx of mononuclear cells into the site of infection and into the immediately surrounding skin.

Furthermore, Kotwal, G.J., *et al* (1998) found that infection of C3 knockout mice with wild type cowpox virus in the footpads resulted in an increased specific swelling response, relative to infection of mice homozygous for C3 production. This suggests that C3 is important in the pathogenesis of cowpox virus. BALB/c mice have low levels of C3. Thus a more rapid disease progression would be expected with this particular strain. This strain of mice was chosen for my experiments and a difference in growth characteristics was expected between the wild type and the knockout cowpox viruses.

Neither Miller, C.G., *et al* (1997) nor Kotwal, G.J., *et al* (1998) investigated the effect of IMP on viral titre. In this study the wild type and knockout virus were used to infect mice in an air pouch created on the dorsum and the viral titres were determined at various time-points. The wild type virus was expected to grow to higher titres than the knockout virus due to its greater ability to evade the immune response via IMP.

University of Cape Town

## 5.2. Materials and Methods

### 5.2.1. Evaluation of viral titres using the connective tissue air-pouch method

Animal ethics approval was obtained from the University of Cape Town Animal Ethics committee before any animal experimentation was performed. A total of 117 BALB/c mice were used in this experiment. The mice were divided into 3 groups of 39. The mice in each group were infected with PBS, CPV WT or CPV IMP<sup>r</sup>. A volume of 1 cm<sup>3</sup> of air was injected subcutaneously on the dorsum of each mouse using a 29-gauge needle, to create the air pouch. Into this air pouch 100 µl of PBS (containing 10<sup>6</sup> pfu of either CPV WT or CPV IMP<sup>r</sup>, or simply PBS) was injected using a 27-gauge needle.

The connective tissue underlying the air pouch was collected every second day for fourteen days, and thereafter every five days for thirty days. From each group (PBS-, CPV WT- and CPV IMP<sup>r</sup>-infected), three mice were used at each time point. The mice were euthanized by CO<sub>2</sub> asphyxiation. The skin on the dorsum was removed by cutting around the air pouch. The connective tissue was then removed using a surgical blade and snap-frozen in liquid nitrogen. The connective tissue was then stored at -80°C.

To release the virus from the cells, each connective tissue sample was removed from -80°C storage and 2.5 ml trypsin and 2.5 ml PBS was added to it. The connective tissue was then homogenized for 10 minutes using an Ultra-Turrax T8 homogenizer (Ika Labortechnik). The sample was then successively frozen and thawed at -80°C and 37°C, respectively, for 3 cycles. The freeze-thaw cycles were followed by sonication (2 cycles of 30 seconds each, with a 30 sec gap period in between), using a Virsonic 100 (VirTis).

The samples were titrated on BS-C-1 cells as follows: 6-well plates were seeded with BS-C-1 cells. The cells were maintained in DMEM supplemented with 10% FCS, at 37°C. Once the monolayers in each well were confluent, the medium was removed from each well. To each well, 1 ml of the same medium

was added. To the first well, 1  $\mu\text{l}$  of the connective tissue homogenate was added. Thus, this was a 1:1000 dilution of the homogenate. A Gilson pipette was used to mix the medium and virus thoroughly. From the first well, 100  $\mu\text{l}$  was transferred to the second well, making a 1:10 000 dilution of the homogenate. This was repeated until 5 wells were inoculated with 1:10<sup>3</sup>, 1:10<sup>4</sup>, 1:10<sup>5</sup>, 1:10<sup>6</sup> and 1:10<sup>7</sup> dilutions of the homogenate. The last well was left uninfected as a control. The plate was then incubated at 37°C for 2 h, after which 1 ml of the medium removed from the plate before infection was added to each well. Thus, the final volume in each well was 2 ml. The plate was then incubated at 37°C for 72 h. Thereafter the plate was removed from the incubator, the medium removed and the cells stained with crystal violet (10% crystal violet solution [v/v], Merck, New Jersey, USA; 10% formaldehyde [v/v]). After 15-20 min the stain was removed and the plates were allowed to dry overnight.

No plaques were visible in any of the wells of the 6-well plate. Thus, following the mechanical homogenization and titration, each sample was then manually homogenized in 5 ml McIlvain's buffer, using Dounce homogenizers. Lysis of the connective tissue was brought about by 80-100 strokes of the homogenizer probe. Each sample was then taken through 3 freeze-thaw cycles, and following this 50  $\mu\text{l}$  trypsin was added. The sample was incubated with the trypsin for 15 minutes at 37°C. The samples were sonicated for 2 cycles of 30 sec each, with a 30 sec gap period in between.

Each sample was titrated again on BS-C-1 cells as outlined above.

### **5.2.2. Extraction of DNA from connective tissue samples**

Total DNA was extracted from the connective tissue samples. To 500  $\mu\text{l}$  of sample, 5  $\mu\text{l}$  of a 10 mg/ml proteinase K solution was added. Each sample was then placed at 56°C for 15 min. To inactivate the proteinase K the samples were incubated at 95°C for 10 min. To precipitate the DNA, 50  $\mu\text{l}$  of ice cold sodium acetate (3M, pH 8) and 500  $\mu\text{l}$  ice cold isopropanol was added to each sample. Each sample was incubated at -80°C for 5 min and then inverted approximately

20 times. Samples were centrifuged at 14 000 rpm (Beckman Microfuge E). The supernatant was removed and the pellets were washed by addition of 10  $\mu$ l of 70% ethanol and centrifugation at 5000 rpm. Following washing the pellets were allowed to air dry and then resuspended in 30  $\mu$ l H<sub>2</sub>O.

### **5.2.3. PCR to confirm the presence of the BALB/c mouse DNA in the connective tissue samples**

To determine whether BALB/c mouse DNA was present in the connective tissue samples, the forward primer exon 7 forward1 (5' TGA CCT ACA AGG AAC CCA GGC 3') and reverse primer exon 8 reverse (5' CTC GGC GCA CTG ACC CAT CT 3') were used. Exon 7 forward binds within exon 7 and exon 8 reverse binds within exon 8 of the gene encoding IL-4R $\alpha$  in BALB/c mice, amplifying a stretch of 600 bp of the gene. The primers were donated by Prof. F. Brombacher's research group (Division of Immunology, Institute of Infectious Diseases and Molecular Medicine, UCT). For each reaction, 0.25  $\mu$ M of each primer, 0.5U *Taq*DNA Polymerase, 1x PCR buffer, 0.2 mM dNTP mixture and 1.5 mM MgCl<sub>2</sub> were used. The PCR conditions used were as follows: 94°C for 1 min; 40 cycles of 94°C for 30 s, 58°C for 20 s, and 72°C for 1 min; and 72°C for 5 min. Purified BALB/c mouse DNA, also obtained from Prof. F. Brombacher's research group, was used as a positive control.

The PCR products were subjected to agarose gel electrophoresis as outlined in chapter 3.

### **5.2.4. PCR to confirm the presence of the viral DNA in the connective tissue samples**

The primers IMP PCR FWD and IMP PCR REV were used to determine whether CPV WT or CPV IMP' DNA was present in the connective tissue samples. For each reaction, 50 pmol/ $\mu$ l of each primer, 2.5U of GoTaq DNA polymerase, 1x PCR buffer, 1.5 mM MgCl<sub>2</sub> and 0.2 mM dNTP mixture (Promega, Wisconsin, USA) were used. The PCR conditions were as follows: 94°C for 3 min; 30 cycles of 94°C for 1 min, 55°C for 1 min and 72°C for 2

min; and 72°C for 10 min. Purified CPV WT and CPV IMP<sup>-</sup> DNA samples were used as positive controls.

Following amplification, the PCR products were subjected to electrophoresis on a 1% agarose gel as outlined in chapter 3.

#### **5.2.5. PCR to confirm the presence of the *gpt* insert in the connective tissue samples infected with CPV IMP<sup>-</sup>**

PCR using the primers IMP PCR FWD and IMP PCR REV did not yield positive results for all the of the samples infected with CPV IMP<sup>-</sup>. The expected fragment was 3.6 kb for CPV IMP<sup>-</sup>, as compared to 1.4 kb for CPV WT. It is possible that this fragment is too large to amplify efficiently and so primers were designed which bind within the coding sequence of *gpt* (which is part of the 3.6 kb fragment). The forward primer GPT FWD (5' CCT GGG ACA TGT TGC AGA TCC 3') and reverse primer GPT REV (5' TAT CCC ACG GCT GTT CAA TCC 3') were used. A product of 398 bp was expected to be amplified using these primers. For each reaction, 50 pmol/μl of each primer, 2.5U of *Taq*DNA polymerase, 1x PCR buffer, 1.5 mM MgCl<sub>2</sub> and 0.2 mM dNTP mixture (Promega, Wisconsin, USA) were used. The PCR conditions were as follows: 94°C for 1 min; 40 cycles of 94°C for 30 s, 59°C for 20 s, and 72°C for 1 min; and 72°C for 5 min. As a positive control, purified DNA from the plasmid pGPT07/14, in which *gpt* is inserted (Boyle, D.B. and Coupar, E.H., 1988), was used. The plasmid was obtained from Dr. Nicola Douglass, donated to Prof. Dumbell by Dr. David Boyle. Fig. 5.1 shows the *E. coli gpt* gene sequence.

```

1   agaataccac tttatcccgc gtcagggaga ggcagtgcgt
41  aaaaagacgc ggactcatgt gaaatactgg tttttagtgc
81  gccagatctc tataatctcg cgcaacctat tttcccctcg
121 aacacttttt aagccgtaga taaacaggct gggacacttc
161 acatgagcga aaaatacatc gtca ctctggg acatglttgc
201 gatccatgca cgtaaactcg caagccgact gatgccttct
241 gaacaatgga aaggcattat tgccgtaagc cgtggcggtc
281 tggtagcggg tgcgttactg gcgctgaac tgggtattcg
321 tcatgtcgat accgtttgta tttccagcta cgatcacgac
361 aaccagcgcg agcttaaagt gctgaaacgc gcagaaggcg
401 atggcgaagg cttcatcgtt attgatgacc tggtaggatac
441 cggtaggtact gcggttgca ttcgtgaaat gtatccaaaa
481 gcgcactttg tcaccatctt cgcaaaaccg gctggtcgtc
521 cgtgggtgta tgactatggt gttgatatcc cgcaagatac
561 ct ggattgaa cagccgtggg atatgggcgt cgtattcgtc
601 ccgccaatct ccggtcgcta a

```

Fig 5.1: Figure showing the coding sequence of *gpt*. The binding sites for the forward primer, GPT FWD, and the reverse primer, GPT REV, are highlighted in magenta.

University of Cape Town

### **5.3. Results**

#### **5.3.1. Evaluation of viral titres using the connective tissue air-pouch method**

Following titration on BS-C-1 cells, no plaques were seen and so the samples were manually homogenized and re-titrated. No plaques were seen after the second round of homogenization and titration. It was decided to perform PCR to investigate whether viral DNA was present in the samples as the virus may have been inactivated during sample preparation.

#### **5.3.2. PCR to confirm the presence of viral and cellular DNA in the connective tissue samples**

##### **5.3.2.1. PCR to detect BALB/c mouse DNA**

As a control to determine whether DNA was present in the samples, a PCR experiment was set up to amplify BALB/c mouse DNA. The DNA purified from the samples was used as template to amplify a 600 bp region in the gene encoding IL-4R $\alpha$ . This was done primarily to ensure that DNA had been extracted successfully from each sample and that PCR inhibitors were not present in the samples. Figures 5.2, 5.3 and 5.4 show the PCR products after subsection to agarose gel electrophoresis.

All the connective tissue samples yielded a product for the IL-4R $\alpha$  gene, except for 1 (fig 5.3, lane 14). This corresponds to the CPV WT-infected connective tissue, harvested 6 days post-infection. CPV WT DNA was recovered from this sample (fig. 5.6, lane 14).

##### **5.3.2.2. PCR to detect viral DNA**

To determine whether or not viral DNA was present, primers were designed to bind to regions flanking the gene encoding IMP. Thus, for samples in which CPV WT was used, a product of 1397 bp was expected. For samples infected

with CPV IMP<sup>-</sup>, a product of 3326 bp was expected (refer to chapter 3, section 3.2.4.3). For control samples (PBS, uninfected), no product was expected.

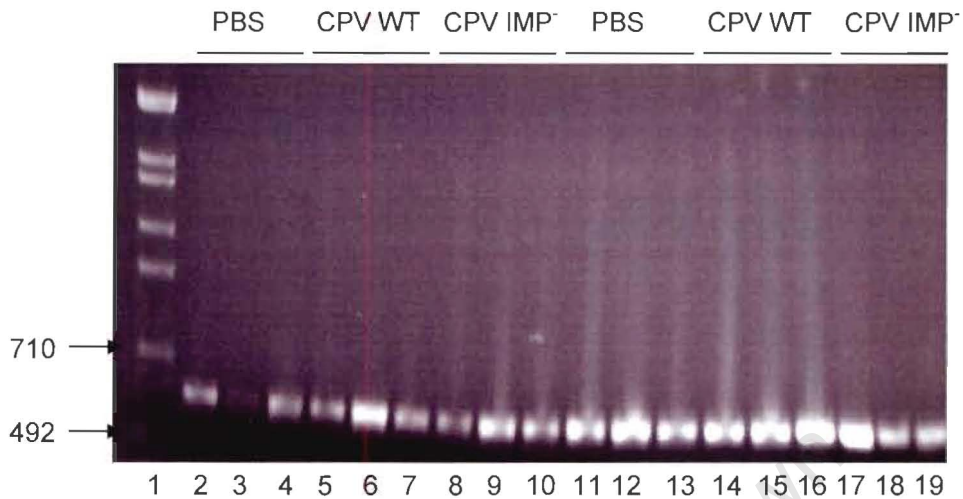


Fig. 5.2: PCR products obtained using primers that amplify 600 bp of the IL-4R $\alpha$  gene, following agarose gel electrophoresis. Lane 1 shows the molecular weight marker. Lanes 2-10 show products from samples harvested 2 days post-infection. Lanes 11-20 show products from samples harvested 10 days post-infection. Product was yielded from all samples.

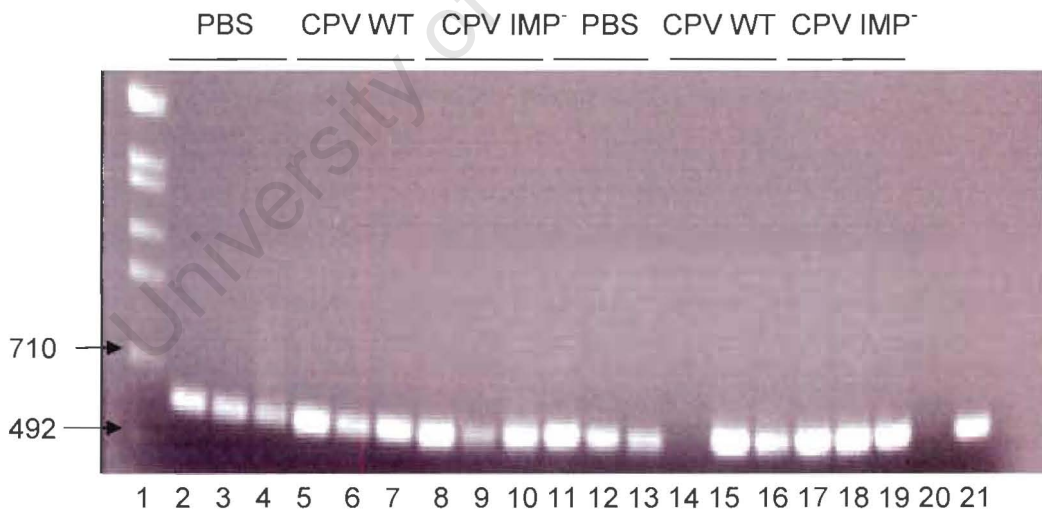


Fig. 5.3: PCR products obtained using primers designed to amplify 600 bp of the IL-4R $\alpha$  gene. Lane 1 shows the molecular weight marker. Lanes 2-10 show product from samples harvested 4 days post-infection. Lanes 11-19 show product from samples harvested 6 days post-infection. Lane 20 shows the negative control. Lane 21 shows the positive control (purified BALB/c mouse DNA used as a template).

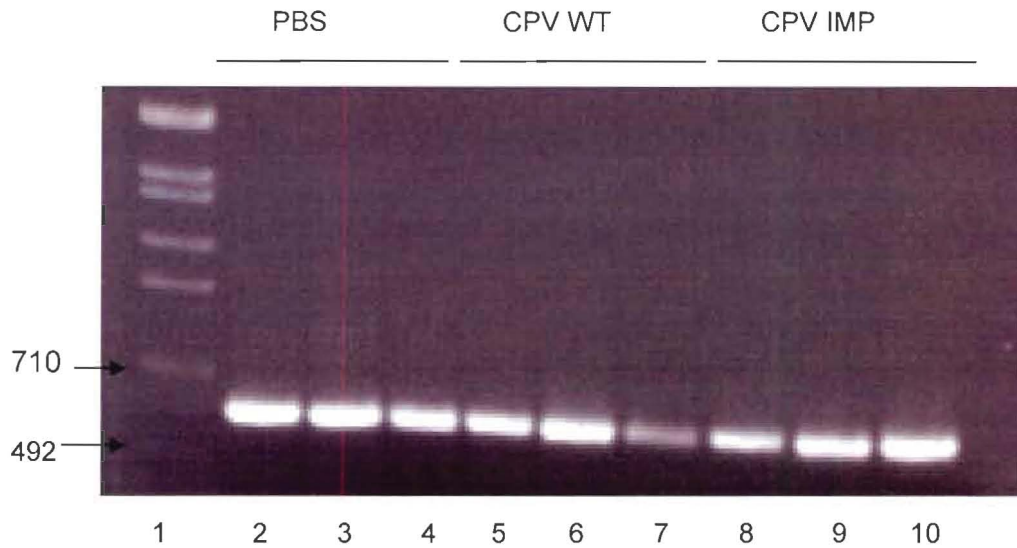


Fig. 5.4: PCR products obtained using primers designed to amplify 600 bp of the IL-4R $\alpha$  gene. Lane 1 shows the molecular weight marker. Lanes 2-10 show product from samples harvested 8 days post-infection.

Figures 5.5, 5.6 and 5.7 show the results of this experiment.

For the first time point (2 days post-infection), only 2 of the 3 wild type samples yielded products of the correct size (fig. 5.5, lanes 7 and 9), while for the knock out samples no products were seen (fig. 5.5, lanes 10-12).

Four days post-infection, 2 of the 3 wild type samples yielded product (fig. 5.6, lanes 5 and 7), and 1 knock out sample yielded product (fig. 5.6, lane 10). At the next time point (6 days post-infection) all the wild type samples yielded a product (fig. 5.6, lanes 14-16). None of the knock out samples yielded products of the correct size. However in lane 18 of fig. 5.6, a band of 1397 bp was seen, indicating possible contamination of this sample, since this band size is expected from the wild type virus. A later experiment (fig. 5.8, lane 11) shows CPV IMP<sup>+</sup> viral DNA is present in this sample.

Eight and 10 days post-infection, all the wild type samples yielded a product (fig. 5.7, lanes 5-7 and 14-16, respectively). One of the 3 (fig. 5.7, lane 9) and 2 of the 3 (fig. 5.7, lanes 18-19) knock out samples, 8 days and 10 days post-

infection, respectively, yielded product of the correct size. Table 5 shows the number of positive PCR products found at the different times when connective tissue was harvested.

Table 5: Table showing the number of samples out of a total of 3 in each test group that yielded a positive PCR result, using the primers IMP PCR FWD and IMP PCR REV.

Days post infection	CPV WT	CPV IMP <sup>-</sup>
2	2	0
4	2	1
6	3	0
8	3	1
10	3	2

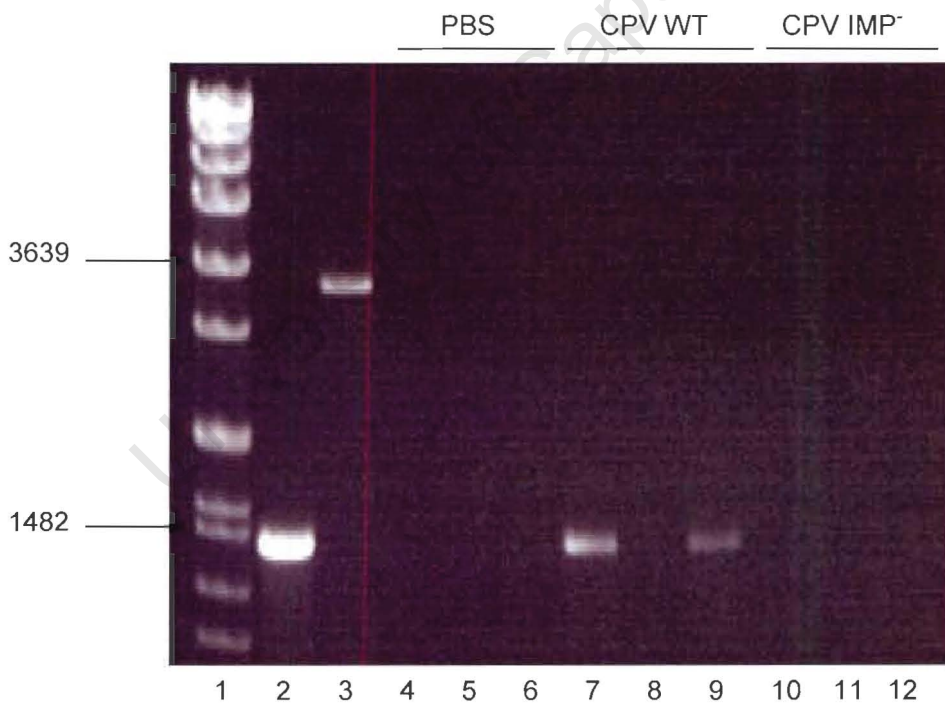


Fig 5.5: PCR products following electrophoresis on a 1% agarose gel. 1: molecular weight marker; 2: Purified CPV WT DNA; 3: Purified CPV IMP<sup>-</sup> DNA; 4-6: PBS samples; 7-9: CPV WT samples; 10-12: CPV IMP<sup>-</sup> samples. Samples in lanes 4-12 were harvested 2 days post-infection

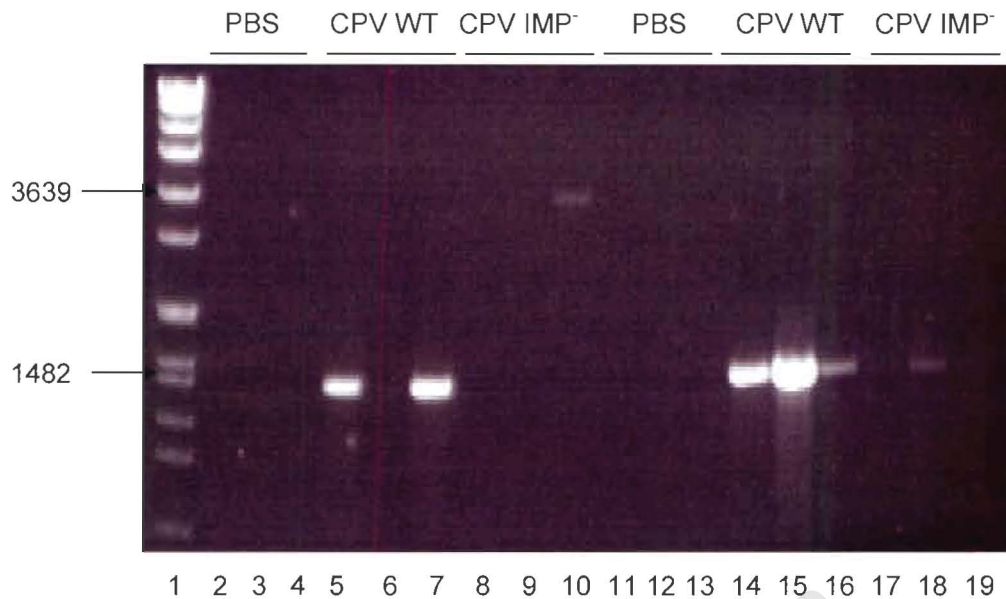


Fig 5.6: PCR products following electrophoresis on a 1% agarose gel. 1: molecular weight marker; 2-4: PBS samples; 5-7: CPV WT samples; 8-10: CPV IMP<sup>-</sup> samples. Samples in lanes 2-10 were harvested 4 days post-infection. 11-13: PBS samples; 14-16: CPV WT samples; 17-19: CPV IMP<sup>-</sup> samples. Samples in lanes 11-19 were harvested 6 days post-infection.

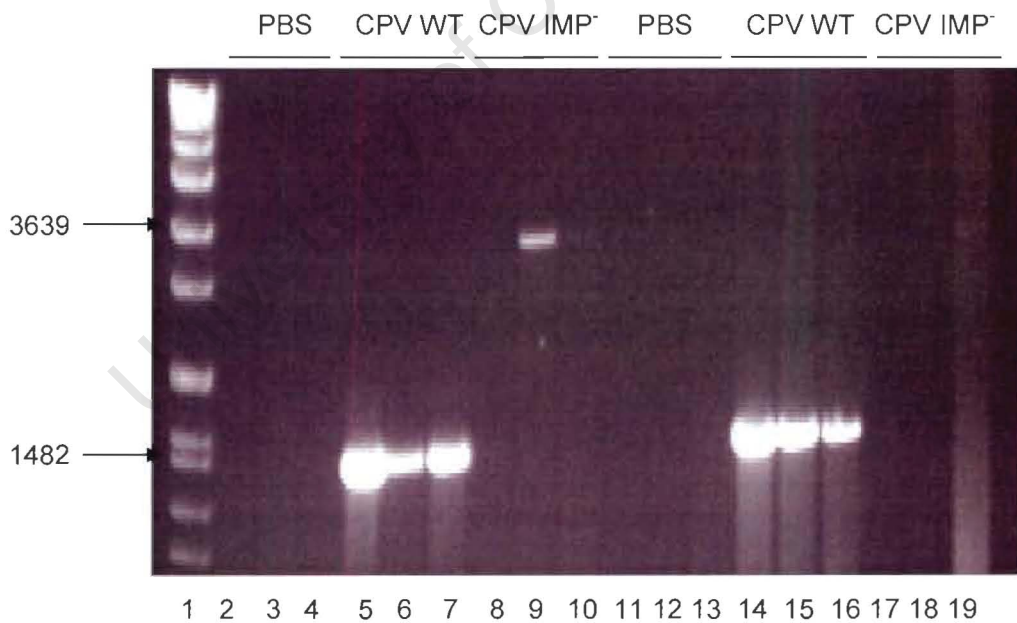


Fig 5.7: PCR products following electrophoresis on a 1% agarose gel. 1: molecular weight marker; 2-4: PBS samples; 5-7: CPV WT samples; 8-10: CPV IMP<sup>-</sup> samples. Samples in lanes 2-10 were harvested 8 days post-infection. 11-13: PBS samples; 14-16: CPV WT samples; 17-19: CPV IMP<sup>-</sup> samples. Samples in lanes 11-19 were harvested 10 days post-infection.

### 5.3.3. PCR to confirm the presence of the *gpt* insert in the connective tissue samples infected with CPV IMP<sup>-</sup>

The IMP primers were designed to amplify a large product (3.639 bp). Therefore a possible reason for the negative results seen for the CPV IMP<sup>-</sup>-infected samples using the IMP primers is that the product size is too large. In PCR, smaller products are amplified more readily than larger ones, and so primers were designed to amplify a smaller DNA sequence.

Fig. 5.8 shows the result of the PCR performed to amplify *gpt* from DNA isolated from samples infected with CPV IMP<sup>-</sup>. Lane 3 shows the positive control. All the other samples, except for those in lanes 13 and 15 (CPV IMP<sup>-</sup>, 8 days post-infection) yielded products. The samples used in lanes 13 and 15 did not yield a product when the primers IMP PCR FWD and IMP PCR REV were used (fig.5.7, lanes 8 and 10).

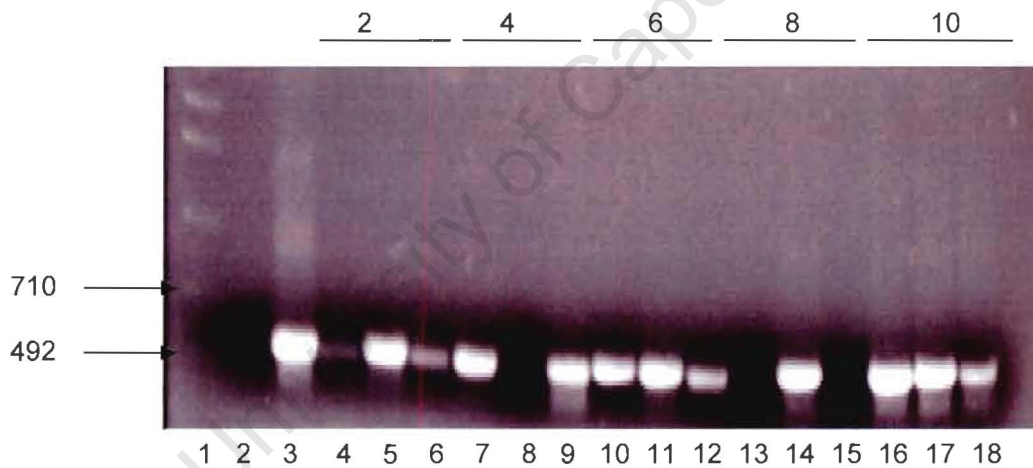


Fig. 5.8: Figure showing PCR products which were subjected to electrophoresis. The primers GPT FWD and GPT REV were used to amplify a 398 bp fragment of the coding sequence. Lane 1: molecular weight marker; lane 2: negative control; lane 3: positive control; lanes 4-6: connective tissue samples harvested 2 days post-infection; lanes 7-9: connective tissue samples harvested 4 days post-infection; lanes 10-12: connective tissue samples harvested 6 days post-infection; lanes 13-15: connective tissue samples harvested 8 days post-infection; lanes 16-18: connective tissue samples harvested 10 days post-infection. All samples were inoculated with CPV IMP<sup>-</sup>. Numbers above gel indicate days post-infection of tissue harvest.

Connective tissue samples which were expected to be negative for *gpt* (PBS- and CPV WT-infected samples) were negative for the 398 bp product after PCR with the GPT FWD and GPT REV primers, shown in fig. 5.9.

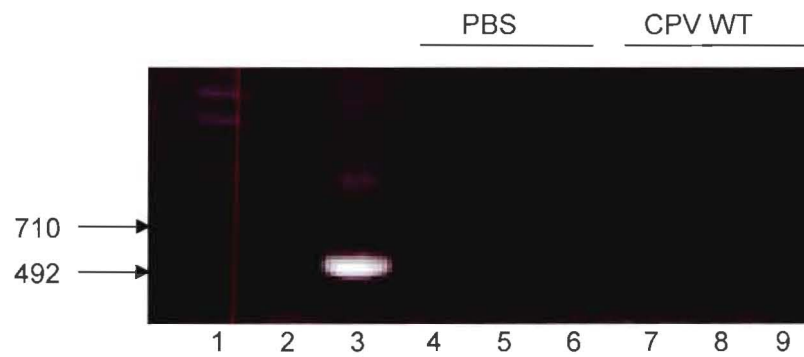


Fig. 5.9: PCR products after electrophoresis on an agarose gel. The GPT FWD and GPT REV primers were used. Lane 1: molecular weight marker; lane 2: negative control; lane 3: positive control; lanes 4-6: PBS samples; lanes 7-9: CPV WT samples. Samples 4-9 were harvested 8 days post-infection.

#### 5.4. Discussion

In order to evaluate the role of IMP in cowpox virus infection in an *in vivo* mammalian model, the air pouch model was used in BALB/c mice. In the air pouch model, 1 cm<sup>3</sup> of air is injected into the dorsum of the animal to create an air pocket. The infectious material is then injected into this air pocket. BALB/c mice were chosen for this experiment as they have low levels of C3, and thus a more rapid disease progression would be expected (Kotwal, G.J., *et al*, 1998).

There were 3 groups of mice, 1 group infected with CPV WT, 1 group with CPV IMP and, and 1 group mock-infected with PBS. At each time-point, 3 mice from each group were sacrificed. The group size was not increased as previous experiments have shown that an increased number of animals per group does not improve the standard deviation (Miller, C.G., *et al*, 1995).

Connective tissue samples collected from BALB/c mice were mechanically homogenized, followed by titration on BS-C-1 cell monolayers. No plaques were seen and so the samples were subjected to a second round of homogenization. Each sample was manually homogenized and then re-titrated. However, this still did not yield any plaques.

This was unexpected as BALB/c mice are known to support the replication of cowpox virus. DNA has been shown to persist at the site of infection following inoculation with a candidate vaccine (Hanke, T. *et al*, 2002), for up to 72 days post-infection. In this project, samples were analysed up to 10 days post-infection. Two possible explanations for the absence of plaques in cell culture are that the virus was eliminated by the mouse immune system, or the virus was lost during the tissue collection/homogenization process. As seen in chapter 4, there was a 2 log difference between the amount of virus used as inoculum and the amount recovered in the titration. Thus the technique may also not have been sensitive enough. To determine whether viral DNA was present in the samples, PCR analysis was performed. The primers IMP PCR FWD and IMP PCR REV were used, designed to bind to regions upstream and downstream, respectively, of the gene encoding IMP.

From table 5 and figs. 5.5, 5.6 and 5.7 (section 5.3.2.2), there appears to be an increase in CPV WT viral DNA as time increases. It cannot be confirmed that CPV WT grows better than CPV IMP<sup>r</sup>, as the smaller band (1.4 kbp) would amplify more readily than the larger band (3.4 kbp). For this reason, primers were designed to amplify a smaller DNA fragment in CPV IMP<sup>r</sup>. Primers designed to amplify a 398 bp region within the *gpt* coding sequence were used.

As seen in fig 5.8, all except 2 samples yielded a PCR product of the correct band size. The 2 negative samples did not yield a product when the primers IMP PCR FWD and IMP PCR REV were used either (fig 5.7, lanes 8 and 10). A likely reason for the absence of product in this sample is a lack of template DNA in the PCR reaction.

Using the GPT FWD and GPT REV primers with CPV IMP<sup>r</sup> DNA as template, it is clear that there is viral DNA present in the samples. However, there is not a clear increase or decrease in the intensities of the bands from the first time point to the last. From the PCR result one cannot say whether or not there is a difference in viral replication between the two viruses.

Since virus was not picked up by the plaque assay, it is possible that virus was inactivated during the collection of tissue or homogenization, and that the DNA detected by PCR is that of killed virus. Alternatively, the plaque assay was not as sensitive an assay as PCR. The sensitivity of the PCR assay was not determined, so the relative amounts of DNA could not be determined.

It was thought that this particular murine model would yield results that indicated whether or not IMP confers any advantage to the virus with regard to viral replication in an animal model. However, it is my opinion that the route of infection employed was not optimal for determination of viral titres, and so the results are inconclusive.

The air pouch model was designed to look at the cellular influx at the site of infection (Smith, S.A. and Kotwal, G.J., 2002), thus it is probably not the ideal model to use when one wants to determine viral titres at various intervals.

Vaccinia virus has been recovered from the meninges when administered intracranially (Morishima, T. and Hayashi, K., 1978) and from the ovaries when administered intravenously (Karupiah, G., *et al*, 1990) or intraperitoneally (N. Douglass, personal communication). One of these models would give a more accurate quantitative result. Due to time constraints, additional animal experimentation could not be performed.

University of Cape Town

### Concluding remarks

Overall, the findings of this project can be summarized in 3 sections. Firstly, the model of IMP that was generated using computer homology was shown to be a highly reliable one. This was indicated by the similarity of the Ramachandran plots generated for both VCP from the known crystal structure and for IMP from the computed structure. This similarity suggests that the functions of IMP and VCP are probably conserved.

Secondly, the CAM model was shown to support the growth of the deletion mutant virus as efficiently as that of the wild type virus. The pocks produced by the two viruses on the chorioallantoic membrane were of equal size and were both bright red in colour. This indicates that IMP is not implicated in the red pock phenotype. The plaques produced by the viruses on CV-1 monolayers were identical in size and morphology.

Thirdly, the growth curves of both the wild type and knockout virus were similar in both cell culture and *in ovo*. In cell culture the growth rates increased steadily up to 48 h, with a 4 log increase followed by a plateau. *In ovo* there was a 6-7 log increase in titre in the first 48 h, followed by a plateau. The CAM system was found to be much more efficient for culturing poxvirus than cell culture, as a  $1 \times 10^7$ -fold increase is seen in eggs in 48 h, compared to a  $1 \times 10^4$ -fold increase seen in cell monolayers over the same time-period.

Although statistical analysis (student's t test) showed that at certain time-points there was a significant difference between the amounts of CPV WT and CPV IMP, in some instances it was the wild type virus that had grown to a higher titre and in others it was the knock out virus. To obtain a more definitive result each growth curve should be repeated, using the same parameters and equipment. Thus, at this stage, one cannot say with certainty whether or not the presence of the IMP gene confers a growth advantage on the virus.

The mouse model employed was not suitable for a quantitative comparison of viral growth *in vivo*. The presence of the IMP gene would be expected to give the virus a growth advantage by inhibition of the complement system. I was therefore expecting to see a reduction in the growth of CPV IMP<sup>-</sup> compared to CPV WT.

A more suitable model for comparison of the growth of CPV WT and CPV IMP<sup>-</sup> should have been used and examples of these have already been mentioned in section 5.4. However, animal ethics approval had not been obtained for enough additional mice to conduct another BALB/c mouse experiment. In addition, my then supervisor, Prof. Kotwal, left suddenly and the animal experiments could not be continued.

To complete this study, the 2 viruses should be compared for growth *in vivo* in a more suitable animal model.

University of Cape Town

**Appendix A: Single-letter and three-letter amino acid abbreviations**

Alanine	Ala	A
Arginine	Arg	R
Asparagine	Asn	N
Aspartic acid	Asp	D
Cysteine	Cys	C
Glutamic acid	Glu	E
Glutamine	Gln	Q
Glycine	Gly	G
Histidine	His	H
Isoleucine	Ile	I
Leucine	Leu	L
Lysine	Lys	K
Methionine	Met	M
Phenylalanine	Phe	F
Proline	Pro	P
Serine	Ser	S
Threonine	Thr	T
Tryptophan	Trp	W
Tyrosine	Tyr	Y
Valine	Val	V

University of Cape Town

## References

- Ahn, B.Y. and Moss, B. (1992). RNA polymerase-associated transcription specificity factor encoded by vaccinia virus. *Proceedings of the National Academy of Sciences* 89:3536-3540.
- Ahn, B.Y., Gershon, P.D. and Moss, B. (1994). RNA-polymerase associated protein Rap94 confers promoter specificity for initiating transcription of vaccinia virus early stage genes. *Journal of Biological Chemistry* 269:7552-7557.
- Alcamí, A. and Smith, G.L. (1995). Vaccinia, cowpox and camelpox viruses encode soluble gamma interferon receptors with novel broad species specificity. *Journal of Virology* 69(8):4633-4639.
- Alcamí, A., and Smith, G.L. (1992). A soluble receptor for interleukin-1 $\beta$  encoded by vaccinia virus: a novel mechanism of virus modulation of the host response to infection. *Cell* 71: 153-167.
- Alcamí, A., Symons, J.A., Collins, P.D., Williams, T.J. and Smith, G.L. (1998). Blockade of chemokine activity by a soluble chemokine binding protein from vaccinia virus. *Journal of Immunology* 160:624-633.
- Ansarah-Sorbrinho, C. and Moss, B. (2004). Vaccinia virus G1 protein, a predicted metalloprotease, is essential for morphogenesis of infectious virions but not cleavage of major core proteins. *Journal of Virology* 78(13):6855-6863.
- Arnold, K., Bordoli, L., Kopp, J., and Schwede, T. (2006). The SWISS-MODEL workspace: a web-based environment for protein structure homology modelling. *Bioinformatics* 22(2):195-201.
- Ausubel, F.M., Brent, R., Kingston, R.E., Moore, D.D., Smith, J.A., Seidman, J.G., and Struhl, K. (1988). *Current Protocols in Molecular Biology*. Greene Publishing Associates and Wiley-Intersciences.
- Baroudy, B.M., Venkatesan, S., and Moss, B. (1982). Incompletely base-paired flip-flop terminal loops link the two DNA strands of the vaccinia virus genome into one uninterrupted polynucleotide chain. *Cell* 28:315-324.

- Baxby, D. (1969). Variability in the characteristics of pocks produced on the chick chorioallantois by white pock mutants of cowpox and other poxviruses. *Journal of Hygiene* 67(4):637-647.
- Baxby, D., Bennett, M., and Getty, B. (1994). Human cowpox 1969-93: a review based on 54 cases. *British Journal of Dermatology* 131:598-607.
- Blackmore, T.K., Hellwage, J., Sadlon, T.A., Higgs, N., Zipfel, P.F., Ward, H.M., and Gordon, D.L. (1998). Identification of the second heparin-binding domain in human complement factor H. *The Journal of Immunology* 160:3342-3348.
- Blangchong, C.A., Chung, E.K., Rupert, K.L., Yang, Y., Yang, Z., Zhou, B., Moulds, J.M., and Yu, C.Y. (2001). Genetic, structural and functional diversities of human complement components C4A and C4B and their mouse homologues, Slp and C4. *International Immunopharmacology* 1:365-392.
- Blomquist, M.C., Hunt, L.T., Barker, W.C. and Barker, W.C. (1984). Vaccinia virus 19-kilodalton protein: relationship to several mammalian proteins, including two growth factors. *Proceedings of the National Academy of Sciences* 81:7363-7367.
- Bowie, A., Kiss-Toth, E., Symons, J.A., Smith, G.L., Dower, S.K., O'Neill, L.A.J. (2000). A46R and A42R from vaccinia virus are antagonists of host IL-1 and toll-like receptor signalling. *Proceedings of the National Academy of Sciences* 97(18):10162-10167.
- Boyle, D.B. and Coupar, E.H. (1988). A dominant selectable marker for the construction of recombinant poxviruses. *Gene* 65:123-128.
- Brown, J.P., Twardzik, D.R., Marquardt, H. and Todaro, G.J. (1985). Vaccinia virus encodes a polypeptide homologous to epidermal growth factor and transforming growth factor. *Nature* 313(6002):491-492.
- Broyles, S.S. and Fesler, B.S. (1990). Vaccinia virus genes encoding a component of the viral early transcription factor. *Journal of Virology* 64:1523-1529.
- Broyles, S.S. and Li, J. (1993). The small subunit of the vaccinia virus early transcription factor contacts the transcription promoter DNA. *Journal of Virology* 67:5677-5680.

- Broyles, S.S. and Moss, B. (1988). DNA-dependent ATPase activity associated with vaccinia virus early transcription factor. *Journal of Biological Chemistry* 263:10761-10765.
- Broyles, S.S., Li, J. and Moss, B. (1991). Promoter DNA contacts made by the vaccine virus early promoter. *Journal of Biological Chemistry* 266:15539-15544.
- Broyles, S.S., Yuen, L., Shuman S. and Moss, B. (1988). Purification of a factor required for vaccinia virus early genes. *Journal of Biological Chemistry* 263:10754-10760.
- Buller, R.M.L., Chakrabarti, S., Moss, B., and Fredrickson, T. (1988b). Cell proliferative response to vaccinia virus is mediated by VGF. *Virology* 164:182-192.
- Byrd, C.M. and Hruby, D.E. (2005). A conditional-lethal vaccinia virus mutant demonstrates that the 17L gene product is required for virion morphogenesis. *Virology Journal*
- Cervoni, F., Fenichel, P., Akhoundi, C., His, B.-L., and Rossi, B. (1993). Characterization of a cDNA clone coding for human testis membrane cofactor protein (MCP, CD46). *Molecular Reproduction and Development* 34:107-113.
- Chang, A. and Metz, D.H. (1976). Further investigations on the mode of entry of vaccinia virus into cells. *Journal of General Virology* 32:275-282.
- Chang, W., Macaulay, C., Hu, S.L., Tam, J.P., McFadden, G. (1990). Tumorigenic poxviruses: characterization of the expression of an epidermal growth factor related gene in Shope fibroma virus. *Virology* 179(2):926-930.
- Chantrey, J., Meyer, H., Baxby, D., Begon, M., Brown, K.J., Hazel, S.M., Jones, T., Montgomery, W.I., and Bennett, M. (1999). Cowpox: reservoir hosts and geographic range. *Epidemiology and Infection* 122:455-460.
- Chen, N., Guiyun, L., Liszewski, M.K., Atkinson, J.P., Jahrling, P.B., Feng, Z., Schriewer, J., Buck, C., Wang, C., Lefkowitz, E.J., Esposito, J.J., Harms, T., Damon, I.K., Roper, R.L., Upton, C., and Buller, R.M.L. (2005). Virulence differences between monkeypox virus isolates from West Africa and the Congo Basin. *Virology* 340:46-63.

- Chen, N., Li, G., Liszewski, M.K., Atkinson, J.P., Jahrling, P.B., Feng, Z., Schriewer, J., Buck, C., Wang, C., Lefkowitz, E.J., Esposito, J.J., Harms, T., Damon, I.K., Roper, R.L., Upton, C. and Buller, R.M.L. (2005). Virulence differences between monkeypox virus isolates from West Africa and the Congo Basin. *Virology* 340:46-63.
- Crivellato, E., Nico, B., Battistig, M., Beltrami, C.A. and Ribatti, D. (2005). The thymus is a site of mast cell development in chick embryos. *Anatomy and Embryology* 209:243-249.
- Dasgupta, A., Hammarland, E., Slifka, M.K. and Früh, K. (2007). Cowpox virus evades CTL recognition and inhibits the intracellular transport of MHC class I molecules. *Journal of Immunology* 178: 1654-1661.
- Davis, I.W., Murray, L.W., Richardson, J.S. and Richardson, D.C. (2004). MolProbity: structure validation and all-atom contact analysis for nucleic acids and their complexes. *Nucleic Acids Research* 32 (web server issue):W615-W619.
- DeLange, A.M. and McFadden, G. (1987). Efficient resolution of replicated poxvirus telomeres to native hairpin structures requires two inverted symmetrical copies of a core target DNA sequence. *Journal of Virology* 61(6):1957-1963.
- Delhon, G., Tulman, E.R., Afonso, C.L., Lu, Z., de la Concha-Bermejillo, A., Lehmkuhl, H.D., Piccone, M.E., Kutish, G.F. and Rock, D.L. (2004). Genomes of the Parapoxviruses orf virus and bovine papular stomatitis virus. *Journal of Virology* 78(1):168-177.
- Dinarello, C.A. (1989). Interleukin-1 and its biologically related cytokines. *Advances in Immunology* 44: 153-205.
- Doms, R.W., Blumenthal, R. and Moss, B. (1990). Fusion of intra- and extracellular forms of vaccinia virus with the cell membrane. *Journal of Virology* 64:4884-4892.
- Drexler, I., Heller, K., Wahren, B., Erfle, V and Sutter, G. (1998). Highly attenuated modified vaccinia virus Ankara replicates in baby hamster kidney cells, a potential host for virus propagation, but not in various human transformed and primary cells. *Journal of General Virology* 79(2):347-352.

- Edwards, J.C., Sedgwick, A.D. and Willoughby, D.A. (1981). The formation of a structure with the features of synovial lining by subcutaneous injection of air: an *in vivo* tissue culture system. *Journal of Pathology* 134(2):147-156.
- Ellison, K.S., Peng, W. and McFadden, G. (1996). Mutations in active-site residues of the uracil-DNA glycosylase encoded by vaccinia virus are compatible with virus viability. *Journal of Virology* 70(11):7965-7973.
- Esteban, M. and Metz, D.H. (1973). Early virus protein synthesis in vaccinia virus-infected cells. *Journal of General Virology* 19:201-216.
- Evans, E., Klemperer, N., Ghosh, R. and Traktman, P. (1995). The vaccinia virus D5R protein, which is required for DNA replication, is a nucleic acid-independent nucleoside triphosphatase. *Journal of Virology* 69(9):5353-5361.
- Falkner, F.G. and Moss, B. (1988). *Escherichia coli gpt* gene provides dominant selection for vaccinia virus open reading frame expression vectors. *Journal of Virology* 62(6):1849-1854.
- Farrar, M.A., and Schreiber, R.D. (1993). The molecular cell biology of interferon- $\gamma$  and its receptor. *Annual Review of Immunology* 11: 571-611.
- Favoreel, H.W., Van de Walle G.R., Nauwynck, H.J., and Pensaert, M.B. (2003). Virus complement evasion strategies. *Journal of General Virology* 84:1-15.
- Fenner, F., Henderson, D.A., Arita, I., Jezek, Z., and Ladnyi, I.D. (1986). Smallpox and its eradication. World Health Organization, Geneva.
- Fiers, W. (1991). Tumour necrosis factor: characterization at the molecular, cellular and *in vivo* level. *FEBS*, 285(2): 199-212.
- Fleming, S.D., Mastellos, D., Karpel-Massler, G., Shea-Donohue, T., Lambris, J.D., and Tsokos, G.C. (2003). C5a causes limited, polymorphonuclear cell-independent, mesenteric ischemia/reperfusion-induced injury. *Clinical Immunology* 108:263-273.
- Fredrickson, T.N., Sechler, J.M., Palumbo, G.J., Albert, J., Khairallah, L.H., and Buller, R.M.L. (1992). Acute inflammatory response to cowpox virus infection of the chorioallantoic membrane of the chick embryo. *Virology* 187:693-704.
- Freshney, I.R. (1994). *Culture of Animal Cells: A Manual of Basic Technique* 3<sup>rd</sup> edition. Wiley-Liss.

- Froggatt, G.C., Smith, G.L. and Beard, P.M. (2007). Vaccinia virus gene F3L encodes an intracellular protein that affects the innate immune response. *Journal of General Virology* 88:1917-1921.
- Gabrielsen, A.E, Pickering, R.J., Linna, T.J. and Good, R.A. (1973). Haemolysis in chicken serum. II. Ontogenic development. *Immunology* 25:179-184.
- Ganesh, V.K., Muthuvel, S.K., Smith, S.A., Kotwal, G.J., and Murthy, K.H.M. (2005). Structural basis for antagonism by suramin of heparin binding to vaccinia complement protein. *Biochemistry* 44(32):10757-10765.
- Ganesh, V.K., Smith, S.A., Kotwal, G.J., and Murthy, K.H.M. (2004). Structure of vaccinia complement protein in complex with heparin and potential implications for complement regulation. *Proceedings of the National Academy of Sciences* 101(24): 8924-8929.
- Garon, C.F., Barbosa, E., and Moss, B. (1978). Visualization of an inverted terminal repetition in vaccinia virus DNA. *Proceedings of the National Academy of Sciences* 75(10):4863-4867.
- Gershon, P.D. and Moss, B. (1990). Early transcription factor subunits are encoded by vaccine virus late genes. *Proceedings of the National Academy of Sciences* 87:4401-4405.
- Gherardi, M.M., Ramírez, J.C. and Esteban, M. (2003). IL-12 and IL-18 act in synergy to clear vaccinia virus infection: involvement of innate and adaptive components of the immune system. *Journal of General Virology* 84:1961-1972.
- Goebel, S.J., Johnson, G.P., Perkus, M.E., Davis, S.W., Winslow, J.P. and Paoletti, E. (1990). The complete DNA sequence of vaccinia virus. *Virology* 179:247-266.
- Götze, O. and Müller-Eberhard, H.J. (1971). The C3-activator system: an alternate pathway of complement activation. *Journal of Experimental Medicine* 134(3):90s-108s.
- Graham, K.A., Lalani, A.S., Macen, J.L., Ness, T.L., Barry, M., Liu, L.-Y., Lucas, A., Clark-Lewis, I., Moyer, R.W., and McFadden, G. (1997). The T1/135kDa family of poxvirus-secreted proteins bind chemokines and modulate leukocyte influx into virus-infected cells. *Virology* 229:12-24.

- Gubser, C., Hue, S., Kellam, P., and Smith, G.L. (2004). Poxvirus genomes: a phylogenetic analysis. *Journal of General Virology* 85:105-117.
- Guex, N., and Peitsch, M.C. (1997). SWISS-MODEL and the Swiss-PdbViewer: an environment for comparative protein modelling. *Electrophoresis* 18:2714-2723.
- Hahon, N., and Friel, J.J. (1961). Comparative studies of the multiplication of antigenically related poxviruses on the chorioallantoic membrane of the chick embryo. *Journal of Bacteriology* 83: 837-843.
- Haig, D.M. (1998). Poxvirus interference with the host cytokine response. *Veterinary Immunology and Immunopathology* 63:149-156.
- Hanke, T., McMichaelson, A.J., Samuel, R.V., Powell, L.A.J., McLoughlin, L., Crome, S.J. and Edlin, A. (2002). Lack of toxicity and persistence in the mouse associated with the administration of DNA- and modified vaccinia virus Ankara (MVA)-based HIV vaccines for Kenya. *Vaccine* 21:108-114.
- Harris, N., Rosales, R. and Moss, B. (1993). Transcription initiation factor activity of vaccinia virus capping enzyme is independent of mRNA guanylylation. *Proceedings of the National Academy of Sciences* 90:2860-2864.
- Herbert, A., O'Leary, J., Krych-Goldberg, M., Atkinson, J.P., and Barlow, P.N. (2002). Three-dimensional structure and flexibility of proteins of the RCA family – a progress report. *Biochemical Society Transactions* 30(6):990-996.
- Hensing, M., Vlooswijk, R.A.A., Hackeng, T.M., Kanters, D., and Bouma, B.N. (1990). The localization of heparin-binding fragments on human C4b-binding protein. *The Journal of Immunology* 144:204-208.
- Hollinshead, M., Vanderplasschen, A., Smith, G.L. and Vaux, D.J. (1999). Vaccinia virus intracellular mature virions contain only one lipid membrane. *Journal of Virology* 73(2):1503-1517.
- Howard, J., Justus, D.E., Totmenin, A.V., Shchelkunov, S. and Kotwal, G.J. (1998). Molecular mimicry of the inflammation modulatory proteins (IMPs) of poxviruses: evasion of the inflammatory response to preserve viral habitat. *Journal of Leukocyte Biology* 64(1):68-71.

- Hu, F.-Q., Smith, C.A., and Pickup, D.J. (1994). Cowpox virus contains two copies of an early gene encoding a soluble secreted form of the type II TNF receptor. *Virology* 204:343-356.
- Hubbs, A.E and Wright, C.F. (1996). The A2L intermediate gene product is required for *in vitro* transcription from a vaccinia virus late promoter. *Journal of Virology* 70:327-331.
- Hughes, A.L., and Friedman, R. (2005). Poxvirus genome evolution by gene gain and loss. *Molecular Phylogenetics and Evolution* 35(2005):186-195.
- Hutin, Y.J.F., Williams, R.J., Malfait, P., Pebody, R., Loparev, V.N., Ropp, S.L., Rodriguez, M., Knight, J.C., Tshioko, F.K., Khan, A.S., Szczeniowski, and Esposito, J.J. (2001). Outbreak of human monkeypox, Democratic Republic of Congo, 1996-1997. *Emerging Infectious Diseases* 7(3):434-438.
- Isaacs, S.N., Kotwal, G.J. and Moss, B. (1992). Vaccinia virus complement-control protein prevents antibody-dependent complement-enhanced neutralization of infectivity and contributes to virulence. *Proceedings of the National Academy of Sciences* 89:628-632.
- Ishii, K. and Moss, B. (2001). Role of vaccinia virus A20R protein in DNA replication: Construction and characterization of temperature-sensitive mutants. *Journal of Virology* 75(4):1656-1663.
- Jensen, F.C., Girardi, A.J., Gilden, R.V., and Koprowski, H. (1964). Infection of human and simian tissue cultures with Rous sarcoma virus. *Proceedings of the National Academy of Sciences* 52:53-59.
- Joklik, W.K. (1962). The purification of four strains of poxvirus. *Virology* 18:9-18.
- Joklik, W.K. and Becker, Y. (1964). The replication and coating of vaccinia DNA. *Journal of Molecular Biology* 10:452-474.
- Karupiah, G., Coupar, B., Ramshaw, I., Boyle, D, Blanden, R. and Andrew, M. (1990). Vaccinia virus-mediated damage of murine ovaries and protection by virus-expressed interleukin-2. *Immunology and Cell Biology* 68:325-333.
- Katz, E., Winer, B., Margalith, E. and Goldblum, N. (1973). Isolation and characterization of an IBT-dependent mutant of vaccinia virus. *Journal of General Virology* 19:161-164.

- Keck, J.G., Feigenbaum, F. and Moss, B. (1993a). Mutational analysis of a predicted zinc-binding motif in the 26-kilodalton protein encoded by the vaccinia virus A2L gene: correlation of zinc binding with late transcriptional transactivation activity. *Journal of Virology* 67:5740-5748.
- Keck, J.G., Kovacs, G.R. and Moss, B. (1993b). Overexpression, purification and late transcription factor activity of the 17-kilodalton protein encoded by the vaccinia virus A1L gene. *Journal of Virology* 67:7264-7270.
- Kellogg, D.E. and Kwok, S (1990). Detection of Human Immunodeficiency virus. In *PCR Protocols: A Guide to Methods and Applications* 337-347.
- King, C.S., Cooper, J.A., Moss, B. and Twardzik, D.R. (1986). Vaccinia virus growth factor stimulates tyrosine protein kinase activity of A431 cell epidermal growth factor receptors. *Molecular and Cellular Biology* 6(1):332-336.
- Kit, S. and Dubbs, D.R. (1962). Biochemistry of vaccinia-infected mouse fibroblasts (strain L-M). I. Effects on nucleic acid and protein synthesis. *Virology* 18:274-285.
- Kolb, W.P. and Müller-Eberhard, H.J. (1973). The membrane attack mechanism of complement. Verification of a stable C5-9 complex in free solution. *Journal of Experimental Medicine* 138:438-451.
- Kopp, J., and Schwede, T. (2006). The SWISS-MODEL repository: new features and functionalities. *Nucleic Acids Research* 34:315-318.
- Kotwal, G.J., (1997). Microorganisms and their interaction with the immune system. *Journal of Leukocyte Biology* 62:415-429.
- Kotwal, G.J., and Moss, B. (1988). Vaccinia virus encodes a secretory polypeptide structurally related to complement control proteins. *Nature* 335(6186): 176-178.
- Kotwal, G.J., Isaacs, S.N., McKenzie, R., Frank, M.M., Moss, B. (1990). Inhibition of the complement cascade by the major secretory protein of vaccinia virus. *Science* 250:827-830.
- Kotwal, G.J., Miller, C.G., and Justus, D.E. (1998). The inflammation modulatory protein (IMP) of cowpox virus drastically diminishes the tissue damage by down-regulating cellular infiltration resulting from complement activation. *Molecular and Cellular Biochemistry* 185(1-2):39-46.

- Kovacs, G.R. and Moss, B. (1996). The vaccinia virus H5R gene encodes late gene transcription factor 4: purification, cloning and overexpression. *Journal of Virology* 70:6796-6802.
- Lee, S.-H., Jung, J.U., and Means, R.E. (2003). 'Complementing' viral infection: mechanisms for evading innate immunity. *TRENDS in Microbiology* 11(10): 449-452.
- Li, J., Pennington, M.J. and Broyles, S.S. (1994). Temperature-sensitive mutations in the gene encoding the small subunit of the vaccine virus early transcription factor impair promoter binding, transcription activation, and packaging of multiple virion components. *Journal of Virology* 68:2605-2614.
- Lintin, S.J., Lewin, A.R., and Reid, K.B.M. (1988). Derivation of the sequence of the signal peptide in human C4-binding protein and interspecies cross-hybridisation of the C4bp cDNA sequence. *FEBS Letters* 232(2):328-332.
- Liszewski, M.K., Leung, M., Cui, W., Subramanian, B., Parkinson, J., Barlow, P.N., Manchester, M., and Atkinson, J.P. (2000). Dissecting sites important for complement regulatory activity in membrane cofactor protein (MCP; CD46). *Journal of Biological Chemistry* 275(48):37692-37701.
- Liszewski, M.K., Leung, M.K., Hauhart, R., Buller, R.M.L., Bertram, P., Wang, X., Rosengard, A.M., Kotwal, G.J. and Atkinson, J.P. (2006). Structure and regulatory profile of the monkeypox inhibitor of complement: comparison to homologs in vaccinia and variola and evidence for dimer formation. *Journal of Immunology* 176:3725-2734.
- Loparev, V.N., Parsons, J.M., Knight, J.C., Fanelli Panus, J., Ray, C.A., Buller, R.M.L., Pickup, D.J., and Esposito, J.J. (1998). A third distinct tumor necrosis factor receptor of the orthopoxviruses. *Proceedings of the National Academy of Sciences* 95:3786-3791.
- Marcus, R.L., Shin, H.S. and Mayer, M.M. (1971). An alternate complement pathway: C-3 cleaving activity, not due to C4,2a on endotoxic lipopolysaccharide after treatment with guinea pig serum; relation to properdin. *Proceedings of the National Academy of Sciences* 68(6):1351-1354.

- Martinez-Pomares, L., Stern, R.J. and Moyer, R.W. (1993). The ps/hr (B5R open reading frame homolog) of rabbitpox virus controls pock colour, is a component of extracellular enveloped virus, and is secreted into the medium. *Journal of General Virology* 67(9):5450-5462.
- Martinez-Pomares, L., Thompson, J.P. and Moyer, R.W. (1995). Mapping and investigation of the role in pathogenesis of the major unique secreted 35-kDa protein of rabbitpox virus. *Virology* 206:591-600.
- Massung, R.F., Esposito, J.J., Liu, L., Qi, J., Utterback, T.R., Knight, J.C., Aubin, L., Yuran, T.E., Parsons, J.M., Loparev, V.N., Selivanov, N.A., Cavallaro, K.F., Kerlavage, A.R., Mahy, B.W.J., and Venter, J.C. (1993). Potential virulence determinants in terminal regions of variola smallpox virus genome. *Nature* 336:748-751.
- Massung, R.F., Liu, L.-I., Qi, J., Knight, J.C., Yuran, T.E., Kervlavage, A.R., Parsons, J.M., Venter, J.C. and Esposito, J.J. (1994). Analysis of the complete genome of smallpox variola major virus strain Bangladesh-1975. *Virology* 201:215-240.
- Massung, R.F., Loparev, V.N., Knight, J.C., Totmenin, A.V., Chizhikov, V.E., Parsons, J.M., Safronov, P.F., Gutorov, V.V., Shchelkunov, S.N. and Esposito, J.J. (1996). Terminal region sequence of variola virus DNA. *Virology* 221:291-300.
- McCraith, S., Holtzman, T., Moss, B. and Fields, S. (2000). Genome-wide analysis of vaccinia virus protein-protein interactions. *Proceedings of the National Academy of Sciences* 97:4879-4884.
- McKenzie, R., Kotwal, G.J., Moss, B., Hammer, C.H., and Frank, M.M. (1992). Regulation of complement activity by vaccinia virus complement control protein. *Journal of Infectious Diseases* 166(6): 1245-1250.
- McLysaght, A., Baldi, P.F., and Gaut, B.S. (2003). Extensive gene gain associated with adaptive evolution of poxviruses. *Proceedings of the National Academy of Sciences* 100(26):15655-15660.
- Medzhitov, R., Preston-Hurlburt, P. and Janeway, C.A. (1997). A human homolog of the *Drosophila* toll protein signals activation of adaptive immunity. *Nature* 388:394-397.

- Meng, X. and Xiang, Y. (2006). Vaccinia virus K1L protein supports viral replication in human and rabbit cells through a cell-type-specific set of its ankyrin repeat residues that are distinct from its binding site for ACAP2. *Virology* 353(1):220-233.
- Merchlinsky, M. (1990). Mutational analysis of the resolution sequence of vaccinia virus DNA: essential sequence consists of two separate AT-rich regions highly conserved among poxviruses. *Journal of Virology* 64(10):5029-5035.
- Meri, S. and Pangburn, M.K. (1990). Discrimination between activators and nonactivators of the alternative pathway of complement: regulation via a sialic acid/polyanion binding site on factor H. *Proceedings of the National Academy of Sciences* 87:3982-3986.
- Miller, C.G., Justus, D.E., Jayaraman, S., and Kotwal, G.J. (1995). Severe and prolonged inflammatory response to localized cowpox virus infection in footpads of C5-deficient mice: investigation of the role of host complement in poxvirus pathogenesis. *Cellular Immunology* 162:326-332.
- Miller, C.G., Shchelkunov, S.N., and Kotwal, G.J. (1997). The cowpox virus-encoded homolog of the vaccinia virus complement control protein is an inflammation modulatory protein. *Virology* 229(1): 126-133.
- Morishima, T. and Hayashi, K. (1978). Meningeal exudate cells in vaccinia meningitis of mice: role of local T cells. *Infection and Immunity* 20(3):752-759.
- Moss, B. (2001), *Poxviridae: the viruses and their replication*. In Fields Virology, Volume 2. Editors-in-chief D.M. Knipe and P.M. Howley.
- Mossman, K., Upton, C., Buller, R.M.L., and McFadden, G. (1995). Species specificity of ectromelia virus and vaccinia virus interferon- $\gamma$  binding proteins. *Virology* 208:762-769.
- Müller-Eberhard, H.J., Polley, M.J and Calcott, M.A. (1967). Formation and functional significance of a molecular complex derived from the second and the fourth component of human complement. *Journal of Experimental Medicine* 125:359-380.
- Mulligan, R.C. and Berg, P. (1980). Expression of a bacterial gene in mammalian cells. *Science* 209:1422-1427.

- Mulligan, R.C. and Berg, P. (1981). Factors governing the expression of a bacterial gene in mammalian cells. *Molecular and Cellular Biology* 1(5):449-459.
- Murthy, K., Smith, S.A., Ganesh, V.K., Judge, K.W., Mullin, N., Barlow, P.N., Ogata, C.M., and Kotwal, G.J. (2001). Crystal structure of a complement protein that regulates both pathways of complement activation and binds heparin sulphate proteoglycans. *Cell* 104:301-311.
- Oie, K.L. and Pickup, D.J. (2001). Cowpox virus and other members of the orthopoxvirus genus interfere with the regulation of NF- $\kappa$ B activation. *Virology* 288:175-187.
- Palumbo, G.J., Pickup, D.J., Fredrickson, T.N., McIntyre, L.J., and Buller, R.M.L. (1989). Inhibition of an inflammatory response is mediated by a 38-kDa protein of cowpox virus. *Virology* 172(1):262-273.
- Pangburn, M.K. and Müller-Eberhard, J.H. (1980). Relation of a putative thioester bond in C3 to activation of the alternative pathway and the binding of C3 to biological targets of complement. *Journal of Experimental Medicine* 152:1102-1114.
- Pangburn, M.K., Atkinson, M.A.L., and Meri, S. (1991). Localization of the heparin-binding site on complement factor H. *Journal of Biological Chemistry* 266(25):16847-16853.
- Pangburn, M.K., Pangburn, K.W.L., Koistinen, V., Meri, S., and Sharma, A.K. (2000). Molecular mechanisms of target recognition in an innate immune system: interactions among factor H, C3b, and target in the alternative pathway of human complement. *The Journal of Immunology* 164:4742-4751.
- Pangburn, M.K., Schreiber, R.D. and Müller-Eberhard, J.H. (1981). Formation of the initial C3 convertase of the alternative complement pathway. *Journal of Experimental Medicine* 154:856-867.
- Parham, P. (2005). *The Immune System* 2<sup>nd</sup> Edition Garland Science
- Parker, A.K., Parker, S., Yokoyama, W.M., Corbett, J.A. and Buller, R.M.L. (2007). Induction of natural killer cell responses by ectromelia virus controls infection. *Journal of Virology* 81(8):4070-4079.

- Passarelli, A.L., Kovacs, G.R. and Moss, B. (1996). Transcription of a vaccinia virus late promoter template: requirement of the product of the A2L intermediate stage gene. *Journal of Virology* 70:4444-4450.
- Patel, A.H., Gaffney, D.F., Subak-Sharpe, J.H. and Stow, N.D. (1990). DNA sequence of a gene encoding a major secreted protein of vaccinia virus, strain Lister. *Journal of General Virology* 71:2013-2021.
- Pickup, D.J., Ink, B.S., Hu, W., Ray, C.A., and Joklik, W.K. (1986). Haemorrhage in lesions caused by cowpox virus is induced by a viral protein that is related to plasma protein inhibitors of serine proteases. *Proceedings of the National Academy of Sciences* 83:7698-7702.
- Ramsey-Ewing, A.L. and Moss, B. (1996). Complementation of a vaccinia virus host-range K1L gene deletion by the nonhomologous CP77 gene. *Virology* 222(1):75-86.
- Ray, C.A., Black, R.A., Kronheim, S.R., Greenstreet, T.A., Sleath, P.R., Salvesen, G.S., and Pickup, D.J. (1992). Viral inhibition of inflammation: cowpox virus encodes an inhibitor of the interleukin-1 $\beta$  converting enzyme. *Cell* 69:597-604.
- Rodriguez, J.R., Risco, C., Carrascosa, J.L., Esteban, M. and Rodriguez, D. (1997). Characterization of early stages in vaccinia virus biogenesis: implications of the 21-kilodalton protein and a newly identified 15-kilodalton envelope protein. *Journal of Virology* 71(3):1821-1833.
- Rodriguez, J.R., Risco, C., Carrascosa, J.L., Esteban, M. and Rodriguez, D. (1998). Vaccinia virus 15-kilodalton (A14L) protein is essential for assembly and attachment of viral crescents to virosomes. *Journal of Virology* 72(2):1287-1296.
- Rosengard, A.M., Liu, Y., Nie, Z., and Jimenez, R. (2002). Variola virus immune evasion design: expression of a highly efficient inhibitor of human complement. *Proceedings of the National Academy of Sciences* 99(13):8808-8813.
- Sakala, I.G., Chaudhri, G., Buller, R.M., Nuara, A.A., Bai, H., Chen, N. and Karupiah, G. (2007). Poxvirus-encoded gamma interferon binding protein dampens the host immune response to infection. *Journal of Virology* 81(7):3346-3353.

- Salmons, T., Kuhn, A., Wylie, F., Schleich, S., Rodriguez, J.R., Rodriguez, D., Esteban, M., Griffiths, G. and Locker, J.K. (1997). Vaccinia virus membrane proteins p8 and p16 are cotranslationally inserted into the rough endoplasmic reticulum and retained in the intermediate compartment. *Journal of Virology* 71(10):7404-7420.
- Sanderson, C.M., Hollinshead, M and Smith, G.L. (2000). The vaccinia virus A27L protein is needed for the microtubule-dependent transport of intracellular mature virus particles. *Journal of General Virology* 81:47-58.
- Sanz, P. and Moss, B. (1998). A new vaccinia virus intermediate transcription factor. *Journal of Virology* 72:6880-6883.
- Sanz, P. and Moss, B. (1999). Identification of a transcription factor, encoded by two vaccinia virus early genes, that regulates the intermediate stage of viral gene expression. *Proceedings of the National Academy of Sciences* 96:2692-2697.
- Saraiva, M. and Alcami, A. (2001). CrmE, a novel soluble tumour necrosis factor receptor encoded by poxviruses. *Journal of Virology* 75(1):226-233.
- Schwede, T., Kopp, J., Guex, N., and Peitsch, M.C. (2003). SWISS-MODEL: an automated protein homology-modelling server. *Nucleic Acids Research* 31(13):3381-3385.
- Shchelkunov, S.N., Blinov, V.M., and Sandakhchiev, L.S. (1993). Genes of variola and vaccinia viruses necessary to overcome the host protective mechanisms. *FEBS* 319(1-2): 80-83.
- Shchelkunov, S.N., Safronov, P.F., Totmenin, A.V., Petrov, N.A., Ryazankina, O.I., Gutorov, V.V., and Kotwal, G.J. (1998). The genomic sequence analysis of the left and right species-specific terminal region of a cowpox virus strain reveals unique sequences and a cluster of intact ORFs for immunomodulatory and host range proteins. *Virology* 243:432-460.
- Shchelkunov, S.N., Totmenin, A.V. and Sandakhchiev, L.S. (1996). Analysis of the nucleotide sequence of 23.8 kbp from the left terminus of the genome of variola major virus strain India-1967. *Virus Research* 40:169-183.
- Smith, C.A., Davis Smith, T., Smolak, P.J., Friend, D., Hagen, H., Gerhart, M., Park, L., Pickup, D.J., Torrance, D., Mohler, K., Schooley, K., and Goodwin, R.G. (1997). Poxvirus genomes encode a secreted, soluble protein

- that preferentially inhibits  $\beta$  chemokine activity yet lacks sequence homology to known chemokine receptors. *Virology* 236:316-327.
- Smith, C.A., Hu, F.-Q., Smith, T.D., Richards, C.L., Smolak, P., Goodwin, R.G., and Pickup, D.J. (1996). Cowpox virus genome encodes a second soluble homologue of cellular TNF receptors, distinct from crmB, that binds TNF but not LT $\alpha$ . *Virology* 223:132-147.
  - Smith, S.A. and Kotwal, G.J. (2002). Immune response to poxvirus infections in various animals. *Critical Reviews in Microbiology* 28(3):149-185.
  - Smith, S.A., Mullin, N.P., Parkinson, J., Shchelkunov, S.N., Totmenin, A.V., Loparev, V.N., Srisatjaluk, R., Reynolds, D.N., Keeling, K.L., Justus, D.E., Barlow, P.N., and Kotwal, G.J. (2000). Conserved surface-exposed K/R-X-K/R motifs and net positive charge on poxvirus complement control proteins serve as putative heparin binding sites and contribute to inhibition of molecular interactions with human endothelial cells: a novel mechanism for evasion of host defence. *Journal of Virology* 74(12):5659-5666.
  - Smith, V.P., Bryant, N.A., and Alcamí, A. (2000). Ectromelia, vaccinia and cowpox viruses encode secreted interleukin-18-binding proteins. *Journal of General Virology* 81: 1223-1230.
  - Sodeik, B., Doms, R.W., Ericsson, M., Hiller, G., Machamer, C.E., van't Hof, W., van Meer, G., Moss, B and Griffiths, G. (1993). Assembly of vaccinia virus: role of the intermediate compartment between the endoplasmic reticulum and the Golgi stacks. *Journal of Cell Biology* 121(3):521-541.
  - Spriggs, M.K., Hruby, D.E., Maliszewski, C.R., Pickup, D.J., Sims, J.E., Buller, R.M.L., and van Slyke, J. (1992). Vaccinia and cowpox viruses encode a novel secreted interleukin-1-binding protein. *Cell* 71: 145-152.
  - Stack, J., Haga, I.R., Schröder, M., Bartlett, N.W., Maloney, G., Reading, P.C., Fitzgerald, K.A., Smith, G.L. and Bowie, A.G. (2005). Vaccinia virus protein A46R targets multiple toll-like-interleukin-1 receptor adaptors and contributes to virulence. *Journal of Experimental Medicine* 201(6):1007-1018.
  - Stannard, L.M., Marais, D., Kow, and Dumbell, K.R. (1998). Evidence for incomplete replication of a penguin poxvirus in cells of mammalian origin. *Journal of General Virology* 79:1637-1646.

- Stroobant, P., Rice, A.P., Gullick, W.J., Cheng, D.J., Kerr, I.M., and Waterfield, M.D. (1985). Purification and characterization of vaccinia virus growth factor. *Cell* 42:383-393.
- Struyer, L. (1995). *Biochemistry* 4<sup>th</sup> edition. W.H. Freeman and Company, New York.
- Stuart, D.T., Upton, C., Higman, M.A., Niles, E.G. and McFadden, G. (1993). A poxvirus-encoded uracil DNA glycosylase is essential for virus viability. *Journal of Virology* 67(5):2503-2512.
- Tewari, M. and Dixit, V.M. (1995). Fas- and tumour necrosis factor-induced apoptosis is inhibited by the poxvirus *crmA* gene product. *Journal of Biological Chemistry* 270(7):3256-3260.
- Thiel, S., Vorup-Jensen, T., Stover, C.M., Schwaeble, W., Laursen, S.B., Poulsen, K., Willis, A.C., Eggleton, P., Hansen, S., Holmskov, U., Reid, K.B.M. and Jensenius, J.C. (1997). A second serine protease associated with mannan-binding lectin tat activates complement. *Nature* 386:506-510.
- Thornberry, N.A., Bull, H.B., Calaycay, J.R., Chapman, K.T., Howard, A.D., Kostura, M.J., Miller, D.K., Molineaux, S.M., Weiner, J.R., Aunins, J., Elliston, K.O., Ayala, J.M., Casano, F.J., Chin, J., Ding, G. J.-F., Egger, L.A., Gaffney, E.P., Limjuco, G., Palyha, O.C., Raju, S.M., Rolando, A.M., Salley, J.P., Yamin, T.-T., Lee, T.D., Shively, J.E., MacCross, M., Mumford, R.A., Schmidt, J.A. and Tocci, M.J. (1992). A novel heterodimeric cysteine protease is required for interleukin-1 $\beta$  processing in monocytes. *Nature* 356:768-774
- Tosi, M.J. (2005). Innate immune responses to infection. *Journal of Allergy and Clinical Immunology* 116:241-249.
- Traktman, P., Liu, K., DeMasi, J., Rollins, R., Jesty, S. and Unger, B. (2000). Elucidating the essential role of the A14 phosphoprotein in vaccinia virus morphogenesis: construction and characterization of a tetracycline-inducible recombinant. *Journal of Virology* 74(8):3682-3695.
- Tran, G.T., Hodgkinson, S.J., Carter, N., Killingsworth, M., Spicer, S.T., and Hall, B.M. (2002). Attenuation of experimental allergic encephalomyelitis in complement component 6-deficient rats is associated with reduced complement C9 deposition, P-selectin expression, and cellular infiltrate in spinal cords. *The Journal of Immunology* 168:4293-4300.

- Tulman, E.R., Afonso, C.L., Lu, Z., Zsak, L., Kutish, G.F. and Rock, D.L. (2004). The genome of canarypox virus. *Journal of Virology* 78(1):353-366.
- Tuppo, E.E., and Arias, H.R. (2005). The role of inflammation in Alzheimer's disease. *The International Journal of Biochemistry and Cell Biology* 37(2):289-305.
- Upton, C., Macen, J.L., Schreiber, M., and McFadden, G. (1991). Myxoma virus expresses a secreted protein with homology to the tumour necrosis factor receptor gene family that contributes to viral virulence. *Virology* 184: 370-382.
- Upton, C., Stuart, D.T. and McFadden, G. (1993). Identification of a poxvirus gene encoding a uracil glycosylase. *Proceedings of the National Academy of Sciences* 90:4518-4522.
- Uvarova, E.A. and Shchelkunov, S.N. (2001). Species-specific differences in the structure of orthopoxviruses complement-binding protein. *Virus Research* 81:39-45.
- Viac, J. and Chardonnet, Y. (1990). Immunocompetent cells and epithelial modifications in molluscum contagiosum. *Journal of Cutaneous Pathology* 17:202-205.
- Vos, J.C., Saker, M. and Stunnenberg, H.G. (1991). Vaccinia virus capping enzyme is a transcription initiation factor. *EMBO Journal* 10:2553-2558.
- Willer, D.O., McFadden, G. and Evans, D.H. (1999). The complete genome sequence of Shope (rabbit) fibroma virus. *Virology* 264:319-343.
- Wittek, R. and Moss, B. (1980). Tandem repeats within the inverted terminal repetition of vaccinia virus DNA. *Cell* 21:277-284.
- Wolffe, E.J., Moore, D.M., Peters, P.J. and Moss, B. (1996). Vaccinia virus A17L open reading frame encodes an essential component of nascent viral membranes that is required to initiate morphogenesis. *Journal of Virology* 70(5):2797-2808.
- Wright, C.F. and Coroneos, A.M. (1993). Purification of the late transcription system of vaccinia virus: identification of a novel transcription factor. *Journal of Virology* 67:7264-7270.

- Wright, C.F., Keck, J.G., Tsai, M.M. and Moss, B. (1991). A transcription factor for vaccinia virus late genes is encoded by an intermediate gene. *Journal of Virology* 65:3715-37-20.
- Zarembek, K.A. and Godowski, P.J. (2002). Tissue expression of human toll-like receptors and differential regulation of toll-like receptor mRNAs in leukocytes in response to microbes, their products and cytokines. *Journal of Immunology* 168:554-561.
- Zhang, L. and Morikis, D. (2006). Immunophysical properties and prediction of activities for vaccinia virus complement control protein and smallpox inhibitor of complement enzymes using molecular dynamics and electrostatics. *Biophysical Journal* 90(9):3106-3119.

University of Cape Town